Diversity of lateral habenula neuron roles in negative valence events

Marjorie Rose Levinstein

A dissertation

submitted in partial fulfillment of the

requirements for the degree of

Doctor of Philosophy

University of Washington

2020

Reading Committee:

John F. Neumaier, Chair

Jeansok Kim

Eric Turner

Larry Zweifel

Program Authorized to Offer Degree:

Neuroscience

University of Washington

Abstract

Diversity of lateral habenula neuron roles in negative valence events

Marjorie Rose Levinstein

Chair of the Supervisory Committee:
John F. Neumaier
Departments of Psychiatry and Behavioral Sciences, and Pharmacology

The lateral habenula (LHb) integrates critical information regarding aversive stimuli that shapes decision making and behavioral responses. Three major LHb outputs innervate dorsal raphe nucleus (DRN), ventral tegmental area (VTA), and the rostromedial tegmental nucleus (RMTg). LHb neurons that project to these targets are segregated and nonoverlapping, and this led us to consider whether they have distinct molecular phenotypes and adaptations to stress exposure in chapter 2. In order to capture a time-locked profile of gene expression after repeated forced swim stress, we used intersectional expression of RiboTag in rat LHb neurons and next-gen RNA sequencing to interrogate the RNAs actively undergoing translation from each of these pathways. The "translatome" in the neurons comprising these pathways was similar at baseline, but diverged after stress, especially in the neurons projecting to the RMTg. Using weighted gene co-expression network analysis, we found one module, which had an overrepresentation of genes associated with phosphoinositide 3 kinase (PI3K) signaling,

comprising genes downregulated after stress in the RMTg-projecting LHb neurons. Reduced PI3K signaling in RMTg-projecting LHb neurons may be a compensatory adaptation that alters the functional balance of LHb outputs to GABAergic vs. monoaminergic neurons following repeated stress exposure.

Additionally, while primarily glutamatergic, LHb neurons express numerous neuropeptides, such as pituitary adenylate cyclase-activating polypeptide (PACAP), which itself has been associated with anxiety and stress disorders. In chapter 3, we explored these neurons. Using Cre-dependent viral vector expression, we characterized these neurons based on their anatomical projections and found that they projected to raphe and rostromedial tegmentum but not ventral tegmental area. Using RiboTag to capture ribosomal-associated RNA from these neurons and reanalysis of existing single cell RNA sequencing data, we did not identify a unique molecular phenotype that characterized these PACAP-expressing neurons in LHb.

In order to understand the function of these neurons, we chemogenetically excited PACAP-expressing neurons using virally-mediated gene transfer of DREADDs in PACAP-Cre mice and tested the mice using open field test, contextual fear conditioning, sucrose preference, novelty suppressed feeding, and conditioned place preference. We found that activating these neurons produce behaviors opposite to what is expected from the LHb as a whole – they decreased anxiety-like and fear behavior and produced a conditioned place preference. In conclusion, PACAP-expressing neurons in LHb represents a unique population of cells that oppose the actions of the remainder of LHb neurons by being rewarding or diminishing the negative consequences of aversive events.

Dedication

To my wonderful and supporting husband, Greg. Your love and encouragement helped me fight through the doubt and difficulties. Thank you for keeping my spirits up and pushing me to keep going. This would have been even more challenging without you by my side. There is no one I would rather quarantine with while writing my dissertation. You are the best.

Thank you to my parents, Janna and Irwin. Your intellectual curiosity and drive guided me onto this path. You made me ask the big questions when I was growing up, and here I am still asking big questions. We have not been able to be with each other this year, but your love can be felt across the country. Additionally, thank you to my brother, Ben. Even with a newborn, you found time to read articles on the lateral habenula to prepare for my defense.

Table of Contents

List of Figures

Chapter 1

Chapter 2

Chapter 3

List of Tables

Chapter 2

Chapter 1: Introduction

Marjorie R Levinstein

1. The Lateral Habenula

The lateral habenula (LHb) is a small nucleus in the epithalamus. It is well known as a negative reward prediction error nucleus [1, 2]. However, this brain region has more complexity behaviorally and anatomically than this one facet. Figure 1 (as published in Baker, et al. (2015) [3]) depicts the location and some of the projections to and from this nucleus in the rat brain. The LHb receives inputs from several forebrain regions and projects to monoaminergic and GABAergic midbrain nuclei including the medial and dorsal raphe nuclei (MRN and DRN), the ventral tegmental area (VTA), and the rostral medial tegmental nucleus (RMTg). Interestingly, the MRN, DRN, and VTA send reciprocal projections back to the LHb. Both serotonin (produced in the raphe nuclei) and dopamine (produced in the VTA) modify firing rates in the LHb [4–9]. The RMTg sends GABAergic projections to both the VTA and DRN [10]. Thus, the circuitry of the LHb and its targets is quite complex.

2. Phylogeny of habenula

The habenular nuclei are phylogenetically conserved throughout all vertebrate animals from the lamprey to humans [11, 12]. The habenulae are divided into medial (MHb) and lateral (LHb) in mammalian and lizard brains, with homologs being dorsal and ventral respectively in zebrafish [11]. Figure 2 (as published in Namboodiri, et al (2016) [13]) displays images of the habenula in human, monkey,

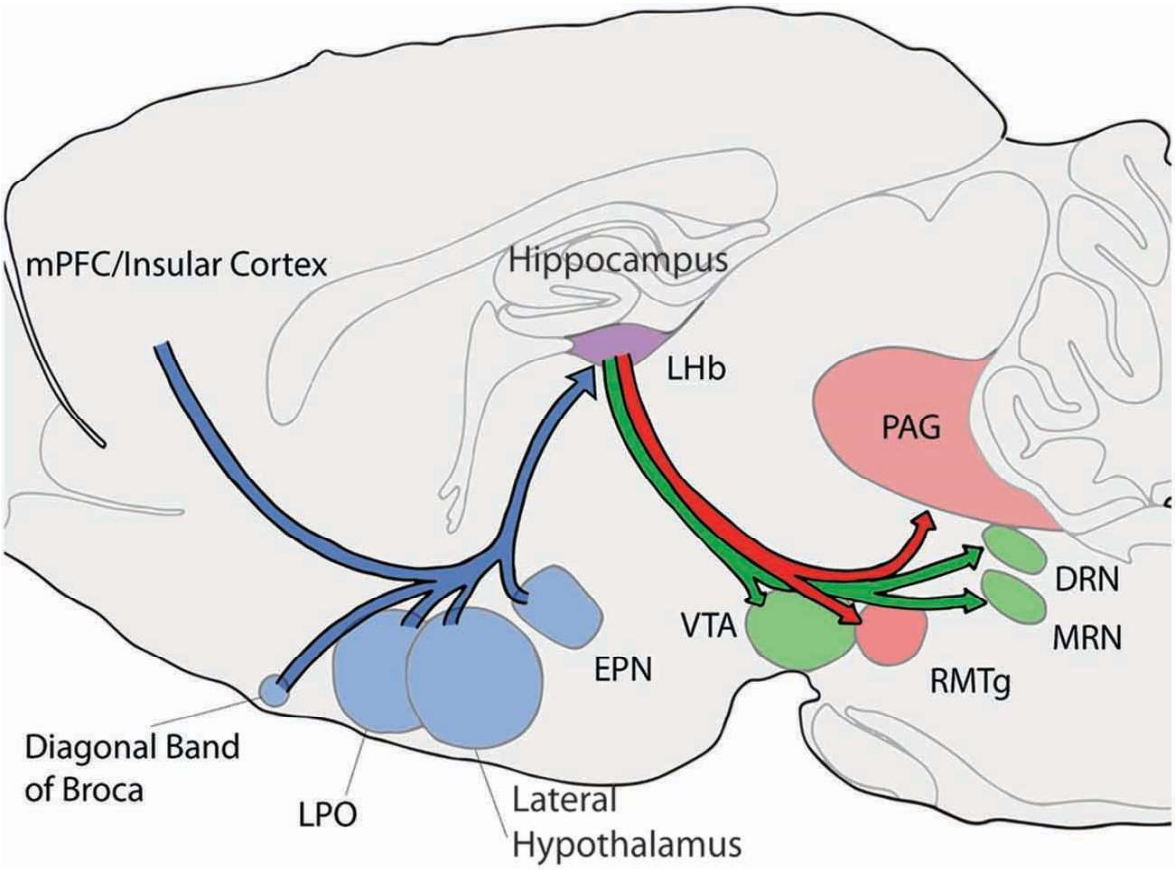

Figure 1: Schematic of selected afferent and efferent connections of the lateral habenula (LHb; shown in purple). Afferent connections/structures are shown in blue, efferent connections are shown in red, and bidirectional connections are in green. LHb, lateral habenula; PAG, periaqueductal gray;DRN, dorsal rahpe; MRN, median raphe; RMTg, rostromedial tegmental nucleus; VTA, ventral tegmental area; LPO, lateral preoptic area; EPN, entopeduncular nucleus; and mPFC, medial prefrontal cortex. From Baker, et al. (2015) [3]

mouse and zebrafish. The medial/dorsal habenula project through the fasciculus retroflexus to the interpeduncular nucleus, this pathway has been conserved in vertebrate animals [11]. In contrast, the lateral/ventral habenula connect to several brain regions. The mammalian LHb also sends its axons through the FR; however, they terminate in the at the VTA, the RMTg, the DRN and MRN (as mentioned above), as well as the lateral hypothalamus, the central pontine gray, the nucleus incertus, and the dorsal tegmental nucleus [11, 14]. The first three of these pathways

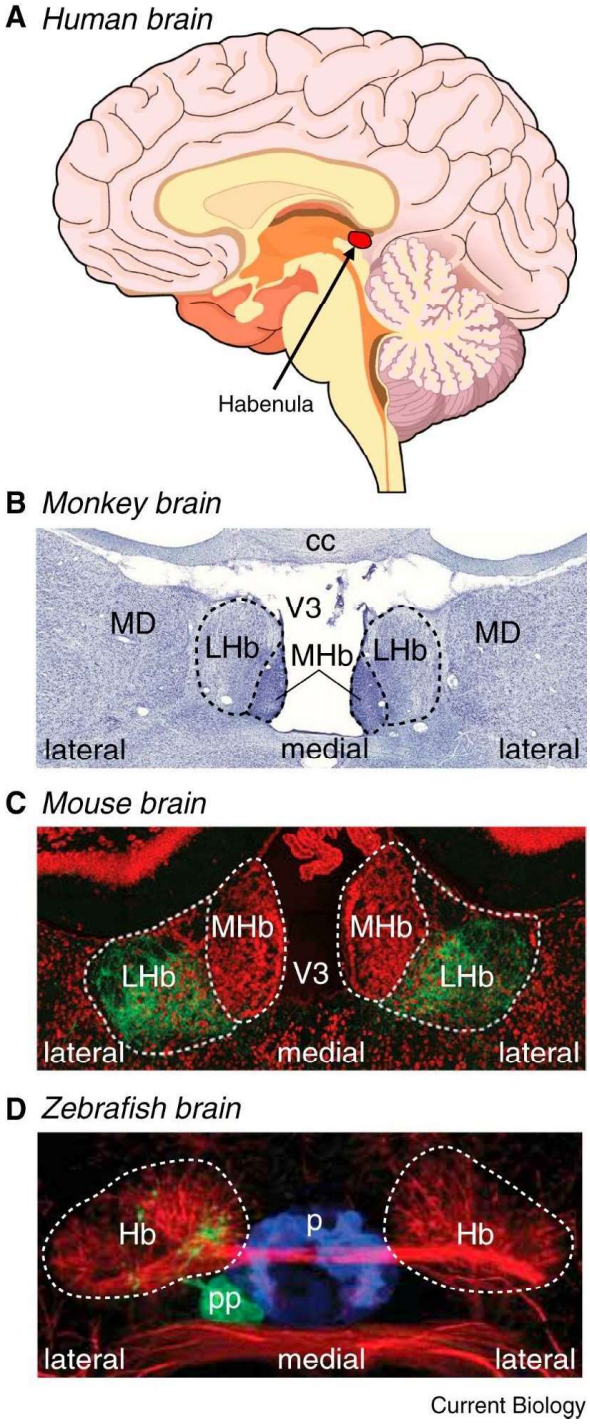

Figure 2: Habenulae in vertebrates. (A) Human brain, sagittal view, indicating the location of the habenula. (B) Rhesus macaque brain, coronal view: Nissl stained sections show the division between lateral habenula (LHb) and medial habenula (MHb) below the corpus callosum (cc) and next to the mediodorsal thalamus (MD). V3, third ventricle. (The NIH Blueprint Non-Human Primate Atlas, NIH Contract HHSN-271-2008-00047-C to the Allen Institute for Brain Science, Seattle, WA.) (C) C57 mouse brain, coronal view: section showing ventral tegmental area terminals (green) in the lateral habenula, not medial habenula (red). (Adapted from Stamatakis et al., 2013.) (D) Zebrafish brain, coronal view: section showing the habenula (Hb, red), pineal (p, blue), and the asymmetric projection from the parapineal (pp, green). (From Namboodiri, et al. (2016) [13])

will be explored in more depth later. The LHb can be thought of as a control of the modulatory system due to these efferent pathways as it exerts direct and indirect control over major dopaminergic and serotonergic regions [12]. In the lamprey, separate neurons in the analogous LHb target dopamine neurons and GABAergic neurons [12], a similar pattern was recently found using single cell RNAseq (scRNAseq) [15]. Phylogenic conservation of the habenula is not limited to the efferent connections either. In lamprey and mammals, the globus pallidus give direct, tonically active projections to the lateral habenula [16].

3. Gene expression in the habenulae

The mammalian habenulae are divided into two nuclei – the lateral habenula and medial habenula. While these two small nuclei are predominantly glutamatergic and project through the FR, there is a clear distinction between these two brain regions. The MHb, while quite heterogeneous, can be divided into three main subdivisions - solely glutamatergic, substance P-ergic and glutamatergic, or cholinergic and glutamatergic [17].

Similarly to the MHb, LHb neurons are overwhelmingly glutamatergic. Furthermore, the LHb also expresses several cell-type markers which can segregate different regions of the LHb [15, 18, 19]. Interestingly, while topographically separate, these cell-types do not appear to segregate into different pathways. All of the cell-type markers investigated project to the DRN [15]. LHb Gpr151+ neurons, a marker for the lateral LHb, avoid VTA dopaminergic neurons, preferentially synapsing onto GABAergic VTA neurons [15] and heavily innervating the RMTg and MRN [20]. The majority of neurons which innervated VTA dopamine neurons are Chrm3+, a marker

for the oval nucleus of the LHb [15]. Figure 3 (as published in Namboodiri, et al. (2016) [13]) gives an overview of genetic markers for both the MHb and LHb, as well as their afferent and efferent projections.

Recently, a surge in transcriptomic data emphasizes the heterogeneity of LHb neurons. More than a decade ago Quina, et al. (2009) [19] reported regional specificity of several transcripts to habenular subnuclei. They identified MHb and LHb neurons which express Brn3a and Nurr1 both project similarly through the FR to the interpeduncular nucleus. Additionally, they describe transcripts such as Gpr151, Pou4f1, and Efcpb2 all are expressed on the lateral part of the LHb. Wagner, et al. (2016) [21] added to this using in situ hybridization images from the Allen Brain Atlas to map transcript expression throughout the LHb and its subregions, finding ten distinct anatomical patterns of expression. Recent scRNAseq profiles of the habenular nuclei identified several types of distinct neurons [15, 18], although none of these appeared to be pathway-specific. However, these studies did not explicitly examine gene expression among all three of the pathways to the DRN, VTA and RMTg. Cerniauskas, et al. (2019) [22] identified a depression-like phenotype which gave rise to differential gene expression in mouse LHb neurons projecting to the VTA. Given the heterogeneity of the LHb transcriptome and the functional differences between its anatomically segregated output pathways, it seems plausible that gene expression in these pathways respond differentially to stress.

4. Circuitry

LHb neurons are mainly glutamatergic, contributing excitatory synapses onto both GABAergic and monoaminergic neurons in the DRN and the VTA at roughly equivalent rates [23–28]. LHb afferents to RMTg are also excitatory, and in turn RMTg inhibits both the DRN and VTA through GABAergic projection neurons. Both the DRN and VTA send reciprocal projections to each other and back to the LHb, and

serotonin and dopamine presumably released from these projections modulate LHb excitability [4–9, 29]. Interestingly, norepinephrine from the VTA may also activate D4 receptors in the LHb [30]. Thus, there is a complex interplay of excitation and inhibition of DRN and VTA that is controlled by the relative activation of these LHb output pathways.

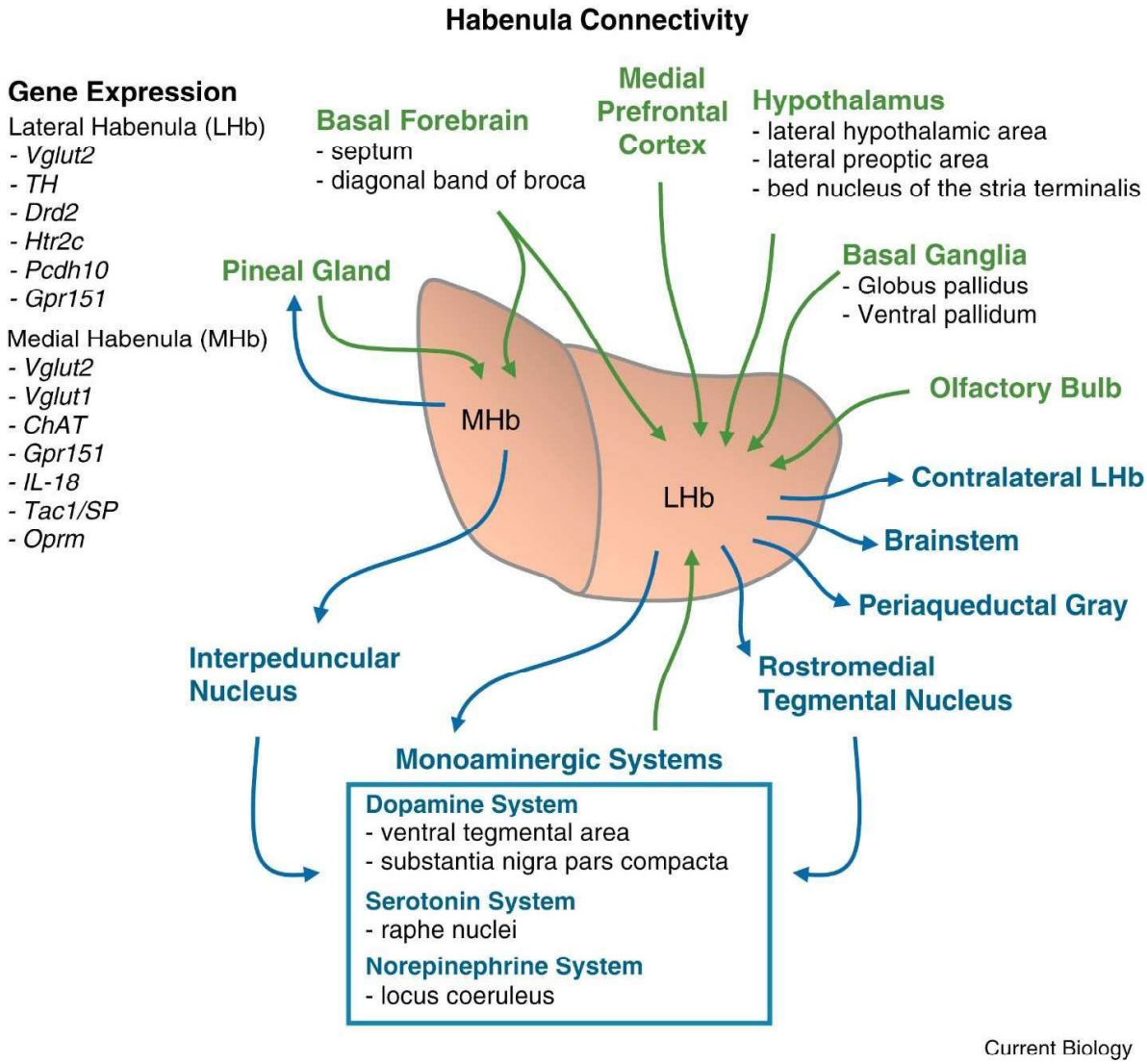

Figure 3: Anatomical organization of the habenula. Inputs (green) and outputs (blue) to and from the lateral habenula (LHb) and medial habenula (MHb) subnuclei. Left inset: gene expression in medial and lateral habenula [17]. (From Namboodiri, et al (2016) [13]).

5. Behavioral implications of the habenulae

The MHb and LHb both project through the fasciculus retroflexus but terminate in different locales leading to divergent behavioral impact. The MHb primarily terminates on the interpeduncular nucleus. Activation of the dorsal medial MHb is rewarding and mice will nosepoke for optogenetic stimulation [31]. This region also appears to influence circadian rhythm activity [32]. Additionally, inhibition of MHb to interpeduncular nucleus neurons diminishes somatic nicotine withdrawal symptoms [33, 34]. However, the mechanism for this is unclear [35]. Further, disruption of MHb signaling decreases fear, anxiety, and depression-like behavior [33]. Lesions of the MHb in rats which underwent chronic unpredictable mild stress had a significantly higher preference for sucrose, but did not differ in time spent immobile in the forced swim test than CUMS rats which did not have MHb lesions [36]. This indicates that the MHb is involved in hedonic state but not behavioral despair aspects of depression-like behavior.

The LHb may be an important target for treating stress disorders [37–39]. Stress exposure activates LHb neurons intensely and induces c-Fos, a marker of neuronal activity [40]. Stimulation of LHb neurons promotes passive avoidance [27, 41] while inhibition of the LHb, and its connection to both serotonergic and dopaminergic regions, reduces anxiety- and depression-like behaviors [42–44]. Inhibition of the LHb via the inhibitory DREADD receptor hM_4Di decreases passive coping in the forced swim test, a measure of behavioral despair [45]. LHb projections to the DRN are thought to mediate this effect [46].

Lateral habenular hyperactivity is common in depression and animal models of depression. Interestingly, ketamine blocks this bursting activity as part of it rapid antidepressant effects [47, 48]. The astroglial receptor Kir4.1 modulates LHb activity and

affects depression-like behavior bidirectionally [49]. Increased expression of Kir4.1 in the LHb produced mice with severe depression-like behavior; whereas, loss-of-function experiments led to a dramatic decrease in depression-like behavior. Interestingly, overexpression of Kir4.1 in the astrocytes of the LHb lead to a decreased resting membrane potential and increased burst firing of LHb neurons; moreover, loss-of-function of this receptor eliminated burst-firing [49, 50].

The LHb has also been implicated in other psychiatric disorders, most notably addiction. The LHb has become known for generating reward-prediction errors [51]. The LHb begins to fire rapidly when a predicted reward does not occur. This in turn inhibits VTA dopaminergic neurons and modifies reward motivated behavior [51–53].

Additionally, the LHb has been found to be involved in fear learning and memory [54]. Rats which had their LHb chemogenetically inhibited during conditioning displayed less freezing to the context, but more freezing to the tone associated with the footshocks [54]. The LHb has more recently been found to be integral to decision making. The LHb has been shown to be involved with behavioral flexibility [53]. Inhibition of the LHb prevents adaptive learning and decision making in a tone-directed maze task [55]. Lesions to the LHb significantly decreased a win-stay strategy but did not affect lose-shift strategy in a competitive choice task [56].

6. Questions to answer

Recently, our lab showed that inhibition of the pathway to the DRN decreases immobility in the forced swim test and perseveration in a reward omission test; however, the inhibition of the pathways to the VTA or RMTg did not affect either behavior [46]. Additionally, activation of the pathway to the DRN increased perseveration during reward omission, but it did not alter forced swim behavior. Conversely, Proulx, et al. (2018) [57] found that activating the pathway to the RMTg

increased immobility in the forced swim test and was aversive. Activation of the pathway to the VTA is also aversive [24]. It is important to note that Proulx, et al. (2018) [57] and [24] each investigated one pathway, so it is difficult to know how the pathways of interest differ from each other in these behaviors. However, in our recent report we demonstrated a clear difference in two behavioral tests between the pathway to the DRN and the pathways to the VTA or RMTg. What is the reason for the differences in these outputs? One possibility is that these distinct pathways from the LHb to the DRN, VTA, and RMTg are molecularly distinct. In the second chapter, I test this hypothesis. I use an intersectional viral vector strategy wherein a Cre-dependent RiboTag adeno-associated virus is injected into the LHb and a retrogradely transported canine adenovirus containing Cre is injected into one of the three output pathways of Sprague-Dawley rats. I stress half of the rats using a forced swim stress protocol and later extract the pathway-specific ribosome-associated RNAs actively undergoing translation [58]. I use next-gen sequencing to analyze the molecular profiles of the pathways at baseline and after stress. We expected the pathway to the DRN to the be the most changed with stress given our prior behavioral results; however, we found that the pathway to the RMTg was the most altered after stress. In fact, the genes in this pathway were predominantly downregulated, particularly those associated with phosphoinositide 3-kinase signaling.

Molecularly profiling several of the pathways from the LHb is a useful approach but may not encompass the heterogeneity of the neurons within the LHb. Subpopulations of neurons within the LHb may also contribute to the differences in behavioral control. For example, a sparsely distributed population of neurons located in the rostromedial region of the LHb expresses pituitary adenylate cyclase-activating polypeptide (PACAP, encoded by the Adycap1 gene), which is expressed in several brain regions and is particularly abundant in stress-associated nuclei [21, 59]. PACAP

has been implicated in both stress and addiction [60, 61]. It regulates cellular signaling, protects from oxidative stress, and has organism-wide effects, such as activating the hypothalamic-pituitary-adrenal hormone system in response to stress [62] although previous studies have focused on other brain areas, such as the extended amygdala. Chronic stress increases PACAP expression in the bed nucleus of the stria terminalis, a brain region associated with anxiety [63]. Moreover, PACAP infusion increases freezing and other anxiety-like behaviors [64, 65]. A single nucleotide polymorphism of the *ADCYAP1R1* receptor is associated with increased likelihood of developing PTSD in adult women and female children [66, 67]. However, the effect of PACAP in LHb on stress-related behaviors has not been investigated. Thus, in the third chapter, I focus on the neurons in the LHb which express PACAP by employing PACAP-Cre mice. I use Cre-dependent viruses to 1) anterogradely trace these neurons to their targets, 2) compare the genetic expression of RiboTag-purified RNAs from these neurons to scRNAseq data, 3) chemogenetically excite these neurons and test anxiety, fear, and appetitive behaviors. We found that these neurons project to the raphe and the RMTg, but not to the VTA. They also do not map onto one cluster of neurons. While we had initially hypothesized that activating these neurons would be anxiogenic and aversive, we found that it was anxiolytic, reduced fear learning, and was somewhat rewarding.

References

[1] S. Hong, T. C. Jhou, M. Smith, K. S. Saleem, O. Hikosaka, Negative Reward Signals from the Lateral Habenula to Dopamine Neurons Are Mediated by Rostromedial Tegmental Nucleus in Primates, Journal of Neuroscience 31 (32) (2011) 11457–11471. doi:10.1523/jneurosci.1384- 11.2011.

[2] M. Ullsperger, D. Y. von Cramon, Error Monitoring Using External Feedback: Specific Roles of the Habenular Complex, the Reward System, and the Cingulate Motor Area Revealed by Functional Magnetic Resonance Imaging, The Journal of Neuroscience 23 (10) (2003) 4308– 4314. doi:10.1523/jneurosci.23-10-04308.2003.

[3] P. M. Baker, S. E. Oh, K. S. Kidder, S. J. Y. Mizumori, Ongoing behavioral state information signaled in the lateral habenula guides choice flexibility in freely moving rats, Frontiers in Behavioral Neuroscience 9 (2015). doi:10.3389/fnbeh.2015.00295.

[4] C. Gruber, A. Kahl, L. Lebenheim, A. Kowski, A. Dittgen, R. W. Veh, Dopaminergic projections from the VTA substantially contribute to the mesohabenular pathway in the rat, Neuroscience Letters 427 (3) (2007) 165–170. doi:10.1016/j.neulet.2007.09.016.

[5] L. N. Han, L. Zhang, L. B. Li, Y. N. Sun, Y. Wang, L. Chen, Y. Guo, Y. M. Zhang, Q. J. Zhang, J. Liu, Activation of serotonin(2c) receptors in the lateral habenular nucleus increases the expression of depression-related behaviors in the hemiparkinsonian rat, Neuropharmacology 93 (2015) 68–79.

[6] A. B. Kowski, R. W. Veh, T. Weiss, Dopaminergic activation excites rat lateral habenular neurons in vivo, Neuroscience 161 (4) (2009) 1154–1165. doi:10.1016/j.neuroscience.2009.04.026.

[7] X. Shen, X. Ruan, H. Zhao, Stimulation of midbrain dopaminergic structures modifies firing rates of rat lateral habenula neurons, PLoS One 7 (2012).

[8] G. Xie, W. Zuo, L. Wu, W. Li, W. Wu, A. Bekker, J. H. Ye, Serotonin modulates glutamatergic transmission to neurons in the lateral habenula, Scientific Reports 6 (2016). doi:10.1038/srep23798.

[9] H. Zhang, K. Li, H. S. Chen, S. Q. Gao, Z. X. Xia, J. T. Zhang, F. Wang, J. G. Chen, Dorsal raphe projection inhibits the excitatory inputs on lateral habenula and alleviates depressive behaviors in rats, Brain Struct Funct 223 (2018) 2243–2258.

[10] Y. Yang, H. Wang, J. Hu, H. Hu, Lateral habenula in the pathophysiology of depression, Curr Opin Neurobiol 48 (2018) 90–96.

[11] H. Aizawa, Habenula and the asymmetric development of the vertebrate brain, Anat Sci Int 88 (2013) 1–9.

[12] S. Grillner, A. von Twickel, B. Robertson, The blueprint of the vertebrate forebrain – With special reference to the habenulae, Seminars in Cell & Developmental Biology 78 (2018) 103– 106. doi:10.1016/j.semcdb.2017.10.023.

[13] V. M. K. Namboodiri, J. Rodriguez-Romaguera, G. D. Stuber, The habenula, Current Biology 26 (19) (2016) R873–R877. doi:10.1016/j.cub.2016.08.051.

[14] L. A. Quina, L. Tempest, L. Ng, J. A. Harris, S. Ferguson, T. C. Jhou, E. E. Turner, Efferent Pathways of the Mouse Lateral Habenula, Journal of Comparative Neurology 523 (1) (2015) 32–60. doi:10.1002/cne.23662.

[15] M. L. Wallace, K. W. Huang, D. Hochbaum, M. Hyun, G. Radeljic, B. L. Sabatini, Anatomical and single-cell transcriptional profiling of the murine habenular complex, eLife 9 (2020). doi:10.7554/elife.51271.

[16] L. Freudenmacher, A. Twickel, W. Walkowiak, The habenula as an evolutionary con-

served link between basal ganglia, limbic, and sensory systems—A phylogenetic comparison based on anuran amphibians, Journal of Comparative Neurology 528 (5) (2020) 705–728. doi:10.1002/cne.24777.

[17] H. Aizawa, M. Kobayashi, S. Tanaka, T. Fukai, H. Okamoto, Molecular characterization of the subnuclei in rat habenula, The Journal of Comparative Neurology 520 (18) (2012) 4051–4066. doi:10.1002/cne.23167.

[18] Y. Hashikawa, K. Hashikawa, M. A. Rossi, M. L. Basiri, Y. Liu, N. L. Johnston, O. R. Ahmad, G. D. Stuber, Transcriptional and Spatial Resolution of Cell Types in the Mammalian Habenula, Neuron 106 (5) (2020) 743–758.e5. doi:10.1016/j.neuron.2020.03.011.

[19] L. A. Quina, S. Wang, L. Ng, E. E. Turner, Brn3a and Nurr1 Mediate a Gene Regulatory Pathway for Habenula Development, Journal of Neuroscience 29 (45) (2009) 14309–14322. doi:10.1523/jneurosci.2430-09.2009.

[20] J. Broms, B. Antolin-Fontes, A. Tingström, I. Ibañez-Tallon, Conserved expression of the GPR151 receptor in habenular axonal projections of vertebrates, Journal of Comparative Neurology 523 (3) (2015) 359–380. doi:10.1002/cne.23664.

[21] F. Wagner, L. French, R. W. Veh, Transcriptomic-anatomic analysis of the mouse habenula uncovers a high molecular heterogeneity among neurons in the lateral complex, while gene expression in the medial complex largely obeys subnuclear boundaries, Brain Struct Funct 221 (2016) 39–58.

[22] I. Cerniauskas, J. Winterer, J. W. de Jong, D. Lukacsovich, H. Yang, F. Khan, J. R. Peck, S. K. Obayashi, V. Lilascharoen, B. K. Lim, C. Földy, S. Lammel, Chronic Stress Induces Activity, Synaptic, and Transcriptional Remodeling of the Lateral Habenula Associated with Deficits in Motivated Behaviors, Neuron 104 (5) (2019) 899–915.e8. doi:10.1016/j.neuron.2019.09.005.

[23] P. L. Brown, P. D. Shepard, Functional evidence for a direct excitatory projection from the lateral habenula to the ventral tegmental area in the rat, Journal of Neurophysiology 116 (3) (2016) 1161–1174. doi:10.1152/jn.00305.2016.

[24] S. Lammel, B. K. Lim, C. Ran, K. W. Huang, M. J. Betley, K. M. Tye, K. Deisseroth, R. C. Malenka, Input-specific control of reward and aversion in the ventral tegmental area, Nature 491 (7423) (2012) 212–217. doi:10.1038/nature11527.

[25] S. K. Ogawa, J. Y. Cohen, D. Hwang, N. Uchida, M. Watabe-Uchida, Organization of Monosynaptic Inputs to the Serotonin and Dopamine Neuromodulatory Systems, Cell Reports 8 (4) (2014) 1105–1118. doi:10.1016/j.celrep.2014.06.042.

[26] N. Omelchenko, R. Bell, S. R. Sesack, Lateral habenula projections to dopamine and gaba neurons in the rat ventral tegmental area, Eur J Neurosci 30 (2009) 1239–1250.

[27] A. M. Stamatakis, G. D. Stuber, Activation of lateral habenula inputs to the ventral midbrain promotes behavioral avoidance, Nature Neuroscience 15 (8) (2012) 1105–1107. doi:10.1038/nn.3145.

[28] B. Weissbourd, J. Ren, K. E. DeLoach, C. J. Guenthner, K. Miyamichi, L. Luo, Presynaptic Partners of Dorsal Raphe Serotonergic and GABAergic Neurons, Neuron 83 (3) (2014) 645– 662. doi:10.1016/j.neuron.2014.06.024.

[29] Y.-Q. Li, M. Takada, Y. Shinonaga, N. Mizuno, The sites of origin of dopaminergic afferent fibers to the lateral habenular nucleus in the rat, The Journal of Comparative Neurology 333 (1) (1993) 118–133. doi:10.1002/cne.903330110.

[30] D. H. Root, A. F. Hoffman, C. H. Good, S. Zhang, E. Gigante, C. R. Lupica, M. Morales, Norepinephrine Activates Dopamine D4 Receptors in the Rat Lateral

Habenula, Journal of Neuroscience 35 (8) (2015) 3460–3469. doi:10.1523/jneurosci.4525-13.2015.

[31] Y. W. Hsu, G. Morton, E. G. Guy, S. D. Wang, E. E. Turner, Dorsal medial habenula regulation of mood-related behaviors and primary reinforcement by tachykinin-expressing habenula neurons, eNeuro 3 (2016). doi:10.1523/ENEURO.0109-16.2016.

[32] Y. W. A. Hsu, J. J. Gile, J. G. Perez, G. Morton, M. Ben-Hamo, E. E. Turner, H. O. de la Iglesia, The Dorsal Medial Habenula Minimally Impacts Circadian Regulation of Locomotor Activity and Sleep, Journal of Biological Rhythms 32 (5) (2017) 444–455. doi:10.1177/0748730417730169.

[33] H. W. Lee, S. H. Yang, J. Y. Kim, H. Kim, The role of the medial habenula cholinergic system in addiction and emotion-associated behaviors, Front Psychiatry 10 (2019). doi:10.3389/fpsyt.2019.00100.

[34] R. Zhao-Shea, L. Liu, X. Pang, P. D. Gardner, A. R. Tapper, Activation of GABAergic Neurons in the Interpeduncular Nucleus Triggers Physical Nicotine Withdrawal Symptoms, Current Biology 23 (23) (2013) 2327–2335. doi:10.1016/j.cub.2013.09.041.

[35] G. Morton, N. Nasirova, D. W. Sparks, M. Brodsky, S. Sivakumaran, E. K. Lambe, E. E. Turner, Chrna5-Expressing Neurons in the Interpeduncular Nucleus Mediate Aversion Primed by Prior Stimulation or Nicotine Exposure, The Journal of Neuroscience 38 (31) (2018) 6900– 6920. doi:10.1523/jneurosci.0023-18.2018.

[36] C. Xu, Y. Sun, X. Cai, T. You, H. Zhao, Y. Li, H. Zhao, Medial habenula-interpeduncular nucleus circuit contributes to anhedonia-like behavior in a rat model of depression, Front Behav Neurosci 12 (2018).

[37] C. A. Browne, R. Hammack, I. Lucki, Dysregulation of the lateral habenula in major depressive disorder, Front Synaptic Neurosci 10 (2018). doi:10.3389/fnsyn.2018.00046.

[38] S. Geisler, M. Trimble, The Lateral Habenula: No Longer Neglected, CNS Spectrums 13 (6) (2008) 484–489. doi:10.1017/s1092852900016710.

[39] E. H. Lee, S. L. Huang, Role of lateral habenula in the regulation of exploratory behavior and its relationship to stress in rats, Behav Brain Res 30 (1988) 90169–90175.

[40] D. Wirtshafter, K. E. Asin, M. R. Pitzer, Dopamine agonists and stress produce different patterns of Fos-like immunoreactivity in the lateral habenula, Brain Research 633 (1-2) (1994) 21–26. doi:10.1016/0006-8993(94)91517-2.

[41] Y. Ootsuka, M. Mohammed, Activation of the habenula complex evokes autonomic physiological responses similar to those associated with emotional stress, Physiological Reports 3 (2) (2015). doi:10.14814/phy2.12297.

[42] M. J. Gill, S. M. Ghee, S. M. Harper, R. E. See, Inactivation of the lateral habenula reduces anxiogenic behavior and cocaine seeking under conditions of heightened stress, Pharmacology Biochemistry and Behavior 111 (2013) 24–29. doi:10.1016/j.pbb.2013.08.002.

[43] X. F. Luo, B. L. Zhang, J. C. Li, Y. Y. Yang, Y. F. Sun, H. Zhao, Lateral habenula as a link between dopaminergic and serotonergic systems contributes to depressive symptoms in parkinson's disease, Brain Res Bull 110 (2015) 40–46.

[44] Q. Zhang, J. J. Feng, S. Yang, X. F. Liu, J. C. Li, H. Zhao, Lateral habenula as a link between thyroid and serotoninergic system modiates depressive symptoms in hypothyroidism rats, Brain Res Bull 124 (2016) 198–205.

[45] S. G. Nair, N. S. Strand, J. F. Neumaier, DREADDing the lateral habenula: A review of

methodological approaches for studying lateral habenula function, Brain Research 1511 (2013) 93–101. doi:10.1016/j.brainres.2012.10.011.

[46] K. R. Coffey, R. G. Marx, E. K. Vo, S. G. Nair, J. F. Neumaier, Chemogenetic inhibition of lateral habenula projections to the dorsal raphe nucleus reduces passive coping and perseverative reward seeking in rats, Neuropsychopharmacology 45 (7) (2020). doi:10.1038/s41386-020-0616- 0.

[47] R. D. Shepard, L. D. Langlois, C. A. Browne, A. Berenji, I. Lucki, F. S. Nugent, Ketamine reverses lateral habenula neuronal dysfunction and behavioral immobility in the forced swim test following maternal deprivation in late adolescent rats, Front Synaptic Neurosci 10 (2018). doi:10.3389/fnsyn.2018.00039.

[48] Y. Yang, Y. Cui, K. Sang, Y. Dong, Z. Ni, S. Ma, H. Hu, Ketamine blocks bursting in the lateral habenula to rapidly relieve depression, Nature 554 (2018) 317–322.

[49] Y. Cui, Y. Yang, Y. Dong, H. Hu, Decoding depression: Insights from glial and ketamine regulation of neuronal burst firing in lateral habenula, Cold Spring Harb Symp Quant Biol 83 (2018) 141–150.

[50] Y. Cui, Y. Yang, Z. Ni, Y. Dong, G. Cai, A. Foncelle, S. Ma, K. Sang, S. Tang, Y. Li, Y. Shen, H. Berry, S. Wu, H. Hu, Astroglial kir4.1 in the lateral habenula drives neuronal bursts in depression, Nature 554 (2018) 323–327.

[51] M. Matsumoto, O. Hikosaka, Lateral habenula as a source of negative reward signals in dopamine neurons, Nature 447 (7148) (2007) 1111–1115. doi:10.1038/nature05860.

[52] M. Matsumoto, O. Hikosaka, Two types of dopamine neuron distinctly convey positive and negative motivational signals, Nature 459 (7248) (2009) 837–841. doi:10.1038/nature08028.

[53] P. M. Baker, T. Jhou, B. Li, M. Matsumoto, S. J. Mizumori, M. Stephenson-Jones, A. Vicentic, The Lateral Habenula Circuitry: Reward Processing and Cognitive Control, The Journal of Neuroscience 36 (45) (2016) 11482–11488. doi:10.1523/jneurosci.2350-16.2016.

[54] L. Durieux, V. Mathis, K. Herbeaux, M. Muller, A. Barbelivien, C. Mathis, R. Schlichter, S. Hugel, M. Majchrzak, L. Lecourtier, Involvement of the lateral habenula in fear memory, Brain Structure and Function 225 (7) (2020) 2029–2044. doi:10.1007/s00429-020-02107-5.

[55] S. J. Mizumori, P. M. Baker, The Lateral Habenula and Adaptive Behaviors, Trends in Neurosciences 40 (8) (2017) 481–493. doi:10.1016/j.tins.2017.06.001.

[56] R. Thapa, C. H. Donovan, S. A. Wong, R. J. Sutherland, A. J. Gruber, Lesions of lateral habenula attenuate win-stay but not lose-shift responses in a competitive choice task, Neuroscience Letters 692 (2019) 159–166. doi:10.1016/j.neulet.2018.10.056.

[57] C. D. Proulx, S. Aronson, D. Milivojevic, C. Molina, A. Loi, B. Monk, S. J. Shabel, R. Malinow, A neural pathway controlling motivation to exert effort, Proceedings of the National Academy of Sciences 115 (22) (2018) 5792–5797. doi:10.1073/pnas.1801837115.

[58] E. Sanz, L. Yang, T. Su, D. R. Morris, G. S. McKnight, P. S. Amieux, Cell-type-specific isolation of ribosome-associated mRNA from complex tissues, Proceedings of the National Academy of Sciences 106 (33) (2009) 13939–13944. doi:10.1073/pnas.0907143106.

[59] J. Hannibal, Pituitary adenylate cyclase-activating peptide in the rat central nervous system: An immunohistochemical and in situ hybridization study, The Journal of Comparative Neurology 453 (4) (2002) 389–417. doi:10.1002/cne.10418.

[60] H. Hashimoto, N. Shintani, M. Tanida, A. Hayata, R. Hashimoto, A. Baba, PACAP is Implicated in the Stress Axes, Current Pharmaceutical Design 17 (10) (2011) 985–989. doi:10.2174/138161211795589382.

[61] P. Marquez, D. Bebawy, V. Lelièvre, A.-C. Coûté, C. J. Evans, J. A. Waschek, K. Lutfy, The role of endogenous PACAP in motor stimulation and conditioned place preference induced by morphine in mice, Psychopharmacology 204 (3) (2009) 457–463. doi:10.1007/s00213-009-1476- 9.

[62] N. Stroth, Y. Holighaus, D. Ait-Ali, L. E. Eiden, PACAP: a master regulator of neuroendocrine stress circuits and the cellular stress response, Annals of the New York Academy of Sciences 1220 (1) (2011) 49–59. doi:10.1111/j.1749-6632.2011.05904.x.

[63] S. E. Hammack, J. Cheung, K. M. Rhodes, K. C. Schutz, W. A. Falls, K. M. Braas, V. May, Chronic stress increases pituitary adenylate cyclase-activating peptide (pacap) and brain-derived neurotrophic factor (bdnf) mrna expression in the bed nucleus of the stria terminalis (bnst): Roles for pacap in anxiety-like behavior, Psychoneuroendocrinology 34 (2009)833–843.

[64] E. G. Meloni, A. Venkataraman, R. J. Donahue, W. A. Carlezon, Bi-directional effects of pituitary adenylate cyclase-activating polypeptide (PACAP) on fear-related behavior and c-Fos expression after fear conditioning in rats, Psychoneuroendocrinology 64 (2016) 12–21. doi:10.1016/j.psyneuen.2015.11.003.

[65] G. Telegdy, A. Adamik, Neurotransmitter-mediated anxiogenic action of PACAP-38 in rats, Behavioural Brain Research 281 (2015) 333–338. doi:10.1016/j.bbr.2014.12.039.

[66] T. Jovanovic, A. F. Stenson, N. Thompson, A. Clifford, A. Compton, S. Minton, S. J. F. V. Rooij, J. S. Stevens, A. Lori, N. Nugent, C. F. Gillespie, B. Bradley, K. J. Ressler, Impact of adcyap1r1 genotype on longitudinal fear conditioning in children: Interaction with trauma and sex, Neuropsychopharmacology 45 (2020) 1603–1608.

[67] K. J. Ressler, K. B. Mercer, B. Bradley, T. Jovanovic, A. Mahan, K. Kerley, S. D. Norrholm, V. Kilaru, A. K. Smith, A. J. Myers, M. Ramirez, A. Engel, S. E. Hammack, D. Toufexis, K. M. Braas, E. B. Binder, V. May, Post-traumatic stress disorder is associated with PACAP and the PAC1 receptor, Nature 470 (7335) (2011) 492–497. doi:10.1038/nature09856.

Chapter 2: Stress induces divergent gene expression among lateral habenula efferent pathways

Marjorie R Levinstein[a,b], Kevin R Coffey[a], Russell G Marx[a,b], Atom J Lesiak[a,c], John F Neumaier[a,b,d,*]

[a]*Department of Psychiatry and Behavioral Sciences, University of Washington, Seattle, WA, USA*
[b]*Graduate Program in Neuroscience, University of Washington, Seattle, WA, USA*
[c]*Department of Genome Sciences, University of Washington, Seattle, WA, USA*
[d]*Department of Pharmacology, University of Washington, Seattle, WA, USA*

Abstract

The lateral habenula (LHb) integrates critical information regarding aversive stimuli that shapes decision making and behavioral responses. The three major LHb outputs innervate dorsal raphe nucleus (DRN), ventral tegmental area (VTA), and the rostromedial tegmental nucleus (RMTg). LHb neurons that project to these targets are segregated and nonoverlapping, and this led us to consider whether they have distinct molecular phenotypes and adaptations to stress exposure. In order to capture a time-locked profile of gene expression after repeated forced swim stress, we used intersectional expression of RiboTag in rat LHb neurons and next-gen RNA sequencing to interrogate the RNAs actively undergoing translation from each of these pathways. The "translatome" in the neurons comprising these pathways was similar at baseline, but diverged after stress, especially in the neurons projecting to the RMTg. Using weighted gene co-expression network analysis, we found one module, which had an overrepresentation of genes associated with phosphoinositide 3 kinase (PI3K) signaling, comprising genes downregulated after stress in the RMTg-projecting LHb neurons. Reduced PI3K signaling in RMTg-projecting LHb neurons may be a compensatory adaptation that alters the functional balance of LHb outputs to GABAergic vs. monoaminergic neurons following repeated stress exposure.

1. Introduction

Stress disorders, anxiety, and depression are associated with altered functional connectivity of key brain regions and are critical determinants of associated symptoms [1], including the lateral habenula (LHb), a small nucleus in the epithalamus that acts as an anti-reward nucleus. While it receives inputs from diverse regions throughout the brain, it has three main efferent pathways – to the ventral tegmental area (VTA), the rostromedial tegmental nucleus (RMTg), and the dorsal raphe nucleus (DRN) [2, 3]—these three outputs contribute to different elements of adaptive responses to stress [2, 4]. The neurons comprising these three main output pathways appear to be quite segregated as they do not send collaterals to more than one of these targets [5–8]. LHb neurons are mainly glutamatergic, contributing excitatory synapses onto both GABAergic and monoaminergic neurons in the DRN and the VTA at roughly equivalent rates [9–14]. LHb afferents to RMTg are also excitatory, and in turn RMTg inhibits both the DRN and VTA through GABAergic projection neurons. Both the DRN and VTA send reciprocal projections to each other and back to the LHb, and serotonin and dopamine presumably released from these projections modulate LHb excitability [15–21]. Interestingly, norepinephrine from the VTA may also activate D4 receptors in the LHb [22]. Thus, there is a complex interplay of excitation and inhibition of DRN and VTA that is controlled by the relative activation of these LHb output pathways. The LHb may be an important target for treating stress disorders [3, 23, 24]. Stress exposure activates LHb neurons intensely and induces c-Fos, a marker of neuronal activity [25]. Stimulation of LHb neurons promotes passive avoidance [13, 26] while inhibition of the LHb, and its connection to both serotonergic and dopaminergic regions, reduces anxiety- and depression-like behaviors [27–29]. Inhibition of the LHb via the inhibitory DREADD receptor hM_4Di decreases

passive coping in the forced swim test (FST), a measure of behavioral despair [30]. LHb projections to the DRN are thought to mediate this effect [4].

Recently, a surge in transcriptomic data emphasizes the heterogeneity of LHb neurons. Wagner, et al. (2016) [31] used in situ hybridization images from the Allen Brain Atlas to map transcript expression throughout the LHb and its subregions, finding ten distinct anatomical patterns of expression. Recent single cell RNA-seq profiles of the habenular nuclei identified several types of distinct neurons [32, 33], although none of these appeared to be pathway-specific. However, these studies did not explicitly examine gene expression between the three major LHb outputs. Cerniauskas, et al. (2019) [34] identified a depression-like phenotype which gave rise to differential gene expression in mouse LHb neurons projecting to the VTA. Given the heterogeneity of the LHb transcriptome and the functional differences between its anatomically segregated output pathways, it seems plausible that gene expression in these pathways respond differentially to stress. Additionally, while Hashikawa, et al. (2020) [32], Wallace, et al. (2020) [33] and Cerniauskas, et al. (2019) [34] studied the mouse habenula, this is the first study examining the genetic profile of LHb neurons in the rat.

To investigate this, we used next-gen sequencing after intersectional expression of RiboTag in neurons from each of these pathways to isolate ribosome-associated RNAs actively undergoing translation [35], a method that reveals evolving changes in gene expression in response to stress [36]. This is the first such application of intersectional translatome analysis in rat neurons and by capturing ribosome-associated RNA from the soma and dendrites, may be sensitive to rapid changes in translation following stress. We found that LHb neurons projecting to RMTg are differentially regulated by stress in comparison to those projecting to DRN or VTA.

2. Materials and Methods

2.1 Animals

For all experiments, male Sprague-Dawley rats (n=43, Charles River, Raleigh, NC) weighing 251-275 g were used. Rats were double-housed in a temperature- and humidity-controlled vivarium with a 14-10 light-dark cycle and allowed to acclimate to the facility for two weeks prior to surgery. All experiments were carried out during the light period. Food and water were freely available at all times. All experimental procedures were approved by the University of Washington Institutional Animal Care and Use Committee and were conducted in accordance to the guidelines of the 'Principles of Laboratory Animal Care' (NIH publication no. 86-23, 1996). 9 animals were excluded because viral-mediated gene expression of RiboTag was below the threshold. A second cohort of 13 rats was used for a replication of differentially expressed genes in the RMTg-projected LHb neurons using the same procedures as the RNAsequencing cohort.

2.2 Experimental design

Our overarching experimental strategy was to use an intersectional viral vector approach to express RiboTag [35] in LHb neurons selectively projecting to VTA, RMTg or DRN based using our recently published procedures [4] . This was achieved through injection of Cre-dependent adeno-associated viral vectors (AAV8-hSyn-DIO-RiboTag) into LHb and a retrogradely transported canine adenovirus-2 expressing Cre (CAV2-Cre) into one of the three output regions. Separate groups of animals were used for each pathway to evaluate the effect of repeated swim stress on gene expression. All experimental procedures were approved by the University of Washington Institutional Animal Care and Use Committee and were conducted in

accordance with National Institutes of Health (NIH) guidelines.

2.3 *Surgical Methods*

For intersectional surgeries, anesthesia was induced with 5% isoflurane/95% oxygen and maintained at 1–3% isoflurane during the surgical procedure. Using a custom robotic stereotaxic instrument [37], 27 animals received AAV8-hSyn-DIO-RiboTag injected into LHb. Blunt 28g needles were inserted bilaterally at a 10° angle terminating at A/P -3.2, M/L ±0.7, and D/V −5.25 and 1 μl of AAV8-hSyn-DIO-RiboTag was injected at a rate of 0.2 μl/min. Nine animals received bilateral 1 μl injections of CAV2-Cre into the DRN at a 15° angle terminating at A/P -7.8, M/L ±0.23, and D/V −6.85. Nine animals received bilateral 1 μl injections of CAV2-Cre into the VTA at a 10° angle terminating at A/P -5.8, M/L ±0.6 and D/V -8.6. Nine animals received bilateral 1 μl injections of CAV2-Cre into the RMTg at a 10° angle terminating at A/P -7.6, M/L ±0.62 and D/V -8.5. For the replication experiment, an additional 13 rats received bilateral injections of AAV8-hSyn-DIO-RiboTag into the LHb and CAV2-Cre into the RMTg. After surgeries, rats were given meloxicam (0.2 mg/kg, s.c.) for pain management and monitored for at least 3 days. Accuracy of injection coordinates was confirmed by RTqPCR detection of RiboTag and Cre RNAs from LHb homogenate; these injection volumes and coordinates were optimized to produce selective transduction of LHb neurons with minimal expression adjacent regions. Rats recovered for three weeks post-surgery to give time for viral expression to occur. For "sham" control samples, rats were anesthetized and placed in the robotic stereotaxic instrument; however, no needle was inserted, nor any virus injected.

2.4 *Behavioral Methods*

After three weeks of handling post-surgery, rats in the stressed grouping

underwent a two-day forced swim protocol. Rats were placed in an inescapable 40cm tall x 20cm diameter Plexiglas cylinder filled with water (23±2C) to 30cm, a level deep enough to prevent them from standing on the bottom [38]. Rats were stressed for 15 minutes on day one; 24 hours later, they were placed into the same chamber for five minutes. Rats in the unstressed group were handled as normal. Decapitation and tissue extraction occurred 3 hours following this protocol.

2.5 RiboTag Extraction

RiboTag-associated RNA extraction as previously described [36, 39].The LHb was extracted using a 4mm punch and homogenized in 2mL of supplemented homogenizing buffer [S-HB, 50 mM Tris-HCl, 100 mM KCl, 12 mM MgCl2, 1% NP40, 1 mM DTT, 1× Protease inhibitor cocktail (Sigma-Aldrich), 200 U/mL RNasin (Promega, Madison, WI), 100 μg/mL cyclohexamide (Sigma-Aldrich), 1 mg/mL heparin (APP Pharmaceuticals, Lake Zurich, IL)]. Samples were centrifuged at 4°C at 11,934 × g for 10 min, and supernatant was collected, reserving 50 μL (10%) as an input fraction. Mouse monoclonal HA-specific antibody (2.5 μL) (HA.11, ascites fluid; Covance, Princeton, NJ) was added to the remaining supernatant, and RiboTag-IP fractions were rotated at 4°C for 4 h. Protein A/G magnetic beads (200 μL) (Pierce) were washed with Homogenizing Buffer (HB 50 mM Tris-HCl, 100 mM KCl, 12 mM MgCl2, 1% NP40) prior to addition to the RiboTag-IP fraction and were rotated at 4°C overnight. The next day, RiboTag-IP fractions were placed on DynaMag-2 magnet (Life Technologies), and the bead pellet was washed 3 times for 15 min with high salt buffer (HSB; 50 mM Tris, 300 mM KCl, 12 mM MgCl2, 1% NP40, 1 mM DTT, and 100 μg/mL cyclohexamide) and placed on a rotator. After the final wash, HSB was removed and beads were re-suspended in 400 μL supplemented RLT buffer (10 μL β-

mercaptoethanol/10 mL RLT Buffer) from the RNeasy Plus Micro Kit (Qiagen, Hilden, Germany) and vortexed vigorously. These samples were then placed back on the magnet and the RLT buffer was removed from the magnetic beads prior to RNA extraction. 350 μL supplemented RLT buffer was added to the Input Fraction prior to RNA extraction. RNA was extracted using Qiagen RNeasy Plus Micro kit according to package directions. RNA from both IP and input fractions were isolated using RNeasy Plus Micro Kit and eluted with 14-16μl of water. RNA concentration was measured using Quant-iT RiboGreen RNA Assay (ThermoFisher Cat. R11490, Waltham, MA). Total RNA yield for the RiboTag-IP fraction 36 ng (sham controls 12ng) and for the input fraction 196ng (sham controls 188ng).

2.6 RNAseq Library Preparation

RNAseq libraries were prepared using SMARTer Stranded Total RNA-Seq Kit v2 – Pico Input Mammalian (Takara Bio USA, Inc. Cat. 635007, Mountain View, CA). 10ng of RNA or average equivalent volumes of "sham" control samples were used to generate the negative control samples. RNAseq libraries were submitted to Northwest Genomics Center at University of Washington (Seattle, WA) where library quality control was measured using a BioAnalyzer, library concentrations were measured using Qubit dsDNA HS Assay Kit (ThermoFisher), and then samples were normalized and pooled prior to cluster generation on HiSeq High Output for Paired-end reads. RNAseq libraries were sequenced on the HiSeq4000, Paired-end 75bp to sufficient read depth with PhiX spike-in controls (7%) (Illumina San Diego, CA).

2.7 RT-qPCR Analysis

The remaining RNA was reverse transcribed to create cDNA libraries for qPCR using Superscript VILO Master Mix (ThermoFisher Cat. 11754050, Waltham, MA), and then cDNA libraries were diluted to a standard concentration before running the

qPCR assay using Power Sybr Green on ViiA7 Real-Time PCR System (Thermo Fisher) or QuantStudio 5 Real-Time PCR System (Thermo Fisher). The normalized relative starting quantities (NRStQ) was determined by qPCR analysis conducted using the standard curve method and normalized to four housekeeping genes (*Gapdh*, *Ppia*, *Hprt*, and *Actinb*) [40]. NRStQ data was analyzed using ANOVA with Bonferroni Post-Hoc.

For the replication experiment, several RNA transcripts identified in the WGCNA analysis were quantified on QuantStudio 7 Pro Real-Time PCR System (Thermo Fisher); RiboTag expression was checked for surgical misses. NRStQ data of *Kdr*, *Tek*, and *Ptpn13* was analyzed using unpaired t-tests.

2.8 Bioinformatics

RNA sequencing was analyzed as previously described [36, 41] with modification as noted below.

2.8.1 Transcript Quantification and Quality Control

Raw fastq files were processed using multiple tools through the Galaxy platform26. Fastq files were inspected for quality using FastQC (Galaxy Version 0.7.0), and then passed to Salmon27 (Galaxy Version 0.8.2) for quantification of transcripts. The Salmon index was built using the protein coding transcriptome GRCm38-mm10.

2.8.2 Non-Specific Immunoprecipitated RNA Subtraction

Due to the inherent issue of non-specific precipitation of immunoprecipitation (IP) procedures, we used a novel computational method for subtraction of non-specific RNA counts from the pathway specific RiboTag sample [41]. Briefly, an IP was performed on an equivalent tissue sample from animals that did not receive the RiboTag virus ("sham" controls). RNA quantity from these samples was then quantified (mean ~12ng)

along with the RiboTag-expressing experimental IP samples (mean ~36ng). Non-specific RNA contamination is considered to be a random sampling of the Input RNA, and the proportion of the IP sample that is contaminated is calculated from the true RNA quantity calculated for each sample. We capped the contamination level at 30% to prevent over-correction. All IP data presented in main manuscript have undergone this adjustment, but we also performed all bioinformatics on the raw IP files as well, which are available in the data archive. The adjusted bioinformatics are labeled "IP Minus Noise" while the raw files are labeled "IP".

2.8.3 Differential Expression Analysis

Differential gene expression was calculated using DESeq228 (Galaxy Version 2.11.39). All Salmon and DESeq2 settings were left default and our analysis pipeline is archived on our Galaxy server. Differential expression analysis was performed on the IP and Input samples. To determine pathway specific gene enrichment, all IP samples were compared to pooled Input samples. For all other test of differential expression, IP samples were compared to IP samples. To determine the pathway expression at baseline, the unstressed DRN pathway was compared to the unstressed RMTg or VTA pathways and the unstressed RMTg pathway was compared to the unstressed VTA pathway. To determine the effects of stress between each pathway, the stressed DRN pathway was compared to the stressed RMTg or VTA pathways and the stressed RMTg pathway was compared to the stressed VTA pathway. To determine the effects of stress within each pathway, the stressed DRN pathway was compared to the unstressed DRN pathway, stressed RMTg to unstressed RMTg, and stressed VTA to unstressed VTA. For all comparisons, a positive Wald statistic means that a gene is expressed more in the first group as compared to the second group. An FDR of q = 0.10 was used as the threshold for differential expression throughout the manuscript.

2.8.4 Gene Set Enrichment Analysis (GSEA)

Wald statics generated by DESeq2 were used as the ranking variable for gene set enrichment analysis (GSEA). The Wald statistic has a benefit over log2(fold change) as it incorporates an estimate of variance, and ultimately is used to determine significance in differential expression analysis. All genes with reliable statistical comparisons (those not filtered by DeSeq2) were entered into WebGestalt 201929 [42] and we performed GSEA on all pertinent comparisons (Stressed vs Unstressed for each pathway, pairwise comparisons between the three stressed pathways, and pairwise comparisons between the three unstressed pathways). Gene sets used include three Gene Ontology (GO) classes: Biological Process, Molecular Function, and Cellular Component, as well as Kyoto Encyclopedia of Genes and Genomes (KEGG) pathways, Panther, Transcription Factor Targets, and MicroRNA Targets. All advanced parameters were left default except for significance level, which was set to FDR = 0.1.

2.8.5 Weighted Gene Co-expression Network Analysis (WGCNA)

Topological overlap matrix for IP samples were generated, and module clustering was accomplished using the WGCNA [43] package for R [44]. Briefly, the TPM matrix for each group was filtered to remove zero-variance genes, and a signed adjacency matrix was generated using “bicor” as the correlation function. From this a signed topological overlap matrix was generated, followed by a dissimilarity topological overlap matrix. Finally, module membership was assigned using a dynamic tree cut. The complete code used to run WGCNA are available in the data archive. Post processing of the topological overlap matrix was completed with a custom object based Matlab class structure that we released previously [41]. The WGCNA class structure can be accessed on https://github.com/levinsmr/WGCNA and the code

used to generate all of the WGCNA figures in this manuscript is available in the Supplementary Code and Data for use as an example. When the average Wald score of a module was >2.0, we performed a secondary overrepresentation analysis of the component genes to evaluate for overrepresentation of genes associated with particular biological functions with WebGestalt.

3. Results

3.1 Read Depth

Three weeks after viral vector injections, we compared handled but unstressed rats to rats subjected to a two-day forced swim stress and then all animals were sacrificed 3 hrs after completion of the stress procedure. This differs from the conventional Porsolt Forced Swim Test, where the behavior is measured during the second swim session. RNA was purified, sequencing libraries were prepared, and samples were sequenced as described in the Materials and Methods section (Figure 1). The IP samples were sequenced to a depth of 7.4 ±0.4 $x10^6$ double stranded reads whereas the Input RNA samples were sequenced to a read depth of 1.1 ± 0.1 $x10^7$ double stranded reads (Table 1). We sequenced Input RNA from pooled samples including each animal from that treatment group rather than each individual; this allowed us to estimate and subtract the small amount of contaminating input RNA that is carried forward during RiboTag immunoprecipitation [41].

3.2 Stress Induced Divergent Gene Expression in LHb Output Pathways

Initially, we compared differential gene expression in the three pathways using pairwise comparisons among the unstressed conditions (usDRN, usVTA, usRMTg), then the stressed conditions (sDRN, sVTA, sRMTg), and then between stressed and

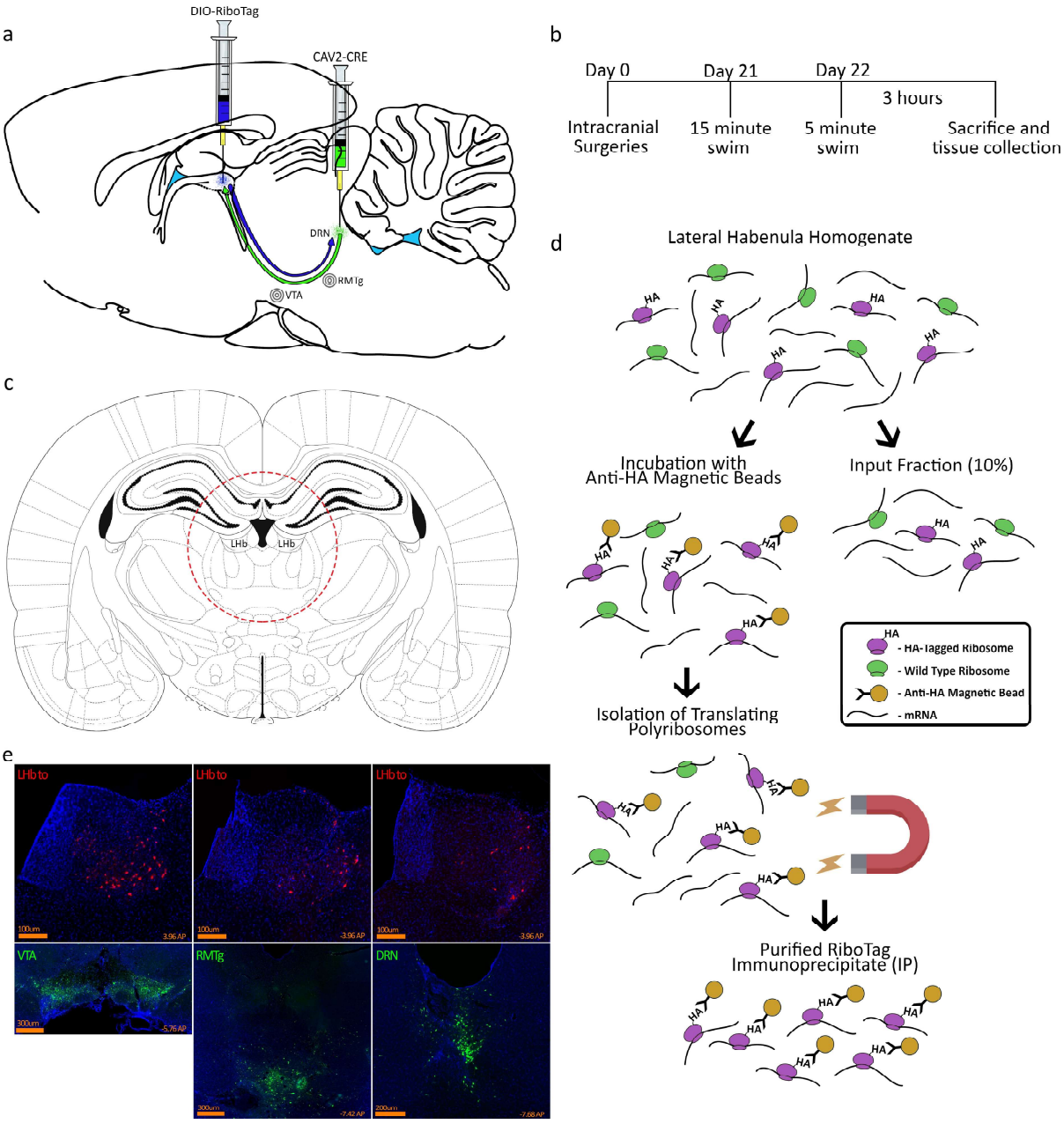

Figure 1: Intersectional viral mediated gene transfer and RiboTag strategy. a) Rats were injected with AAV8-DIO-RiboTag into the LHb and CAV2-Cre injected into one of the three target regions, either the DRN, RMTg or VTA. b) Experimental timeline. c) Location of tissue punch for LHb extraction. d) RiboTag immunoprecipitation protocol. e) Representative images from animals injected with the same AAV8-DIO vector expressing hM4Di-mCherry (injected into LHb) and CAV2-Cre mixed with 5% CAV2-ZsGreen (injected into VTA, DRN, or RMTg). Of note, ZsGreen expression marks the target area that was injected very brightly whereas mCherry is only expressed in neurons that project from LHb to the site of the target where CAV2-Cre was injected and retrogradely infected the LHb neurons.

Table 1: Read Depth

Sample Type	Pathway	Stress Condition	n	Read Depth (mean ±SEM)
IP	DRN	Stressed	3	6.624×106 (± 1.742×106)
IP	DRN	Unstressed	3	8.601×106 (± 0.958×106)
IP	RMTg	Stressed	3	7.957×106 (± 0.077×106)
IP	RMTg	Unstressed	3	7.001×106 (± 0.079× 105)
IP	VTA	Stressed	3	7.055×106 (± 0.077×106)
IP	VTA	Unstressed	3	7.217×106 (± 0.202×106)
Input	DRN, RMTg, VTA	Stressed	3 (pooled each pathway)	11.84×106 (± 1.667×106)
Input	DRN, RMTg, VTA	Unstressed	3 (pooled each pathway)	10.01×107 (± 1.371×106)
IP	Sham	Unstressed	3	5.299×106 (± 0.773×106)
Input	Sham	Unstressed	3	8.05×106 (± 0.813×106)

unstressed conditions within each pathway using DESeq2 (Figure 2). In all cases, if the gene was more highly expressed in the first group, the Wald score is positive (upregulated) and if it was more highly expressed in the second group, the Wald score is negative (downregulated). We used an FDR of q= 0.1 for these initial pair-wise comparisons between pathways. Gene expression profiles in the LHb projection neurons were relatively similar among the three pathways under the basal, unstressed condition (Figure 2a-c). Thirty-one genes were differentially expressed between the unstressed DRN pathway and unstressed RMTg pathway (Figure 2a). Of these, 21 genes were more highly expressed in the DRN pathway. Eleven genes were differentially expressed between DRN and VTA-projecting LHb neurons (Figure 2b). The VTA and RMTg pathways showed the greatest difference at baseline, with 236 Differentially Expressed Genes (DEGs) (Figure 2c). Most of these genes (141) were expressed at greater levels in the VTA pathway compared to the RMTg pathway.

Interestingly, gene expression in stressed rats showed striking differences between the pathways (Figure 2d-f). 125 genes were differentially expressed between the stressed DRN and RMTg pathways, and 95 of those genes were more highly expressed in the DRN pathway (Figure 2d). As with the unstressed comparisons, the stressed DRN and VTA pathways remained similar – only 11 genes were differentially expressed (Figure 2e). Further, 1,078 genes were differentially expressed between the stressed VTA and RMTg pathways (Figure 2f). The majority of these genes (657) were expressed at greater levels in the VTA pathway.

We next determined the effects of stress within the neurons of each pathway (Figure 2g-i). Stress had the smallest impact on gene expression within the DRN-projecting LHb neurons–only 14 genes were different with 5 being upregulated and 9 being downregulated following stress (Figure 2g). In the RMTg-projecting neurons, 204

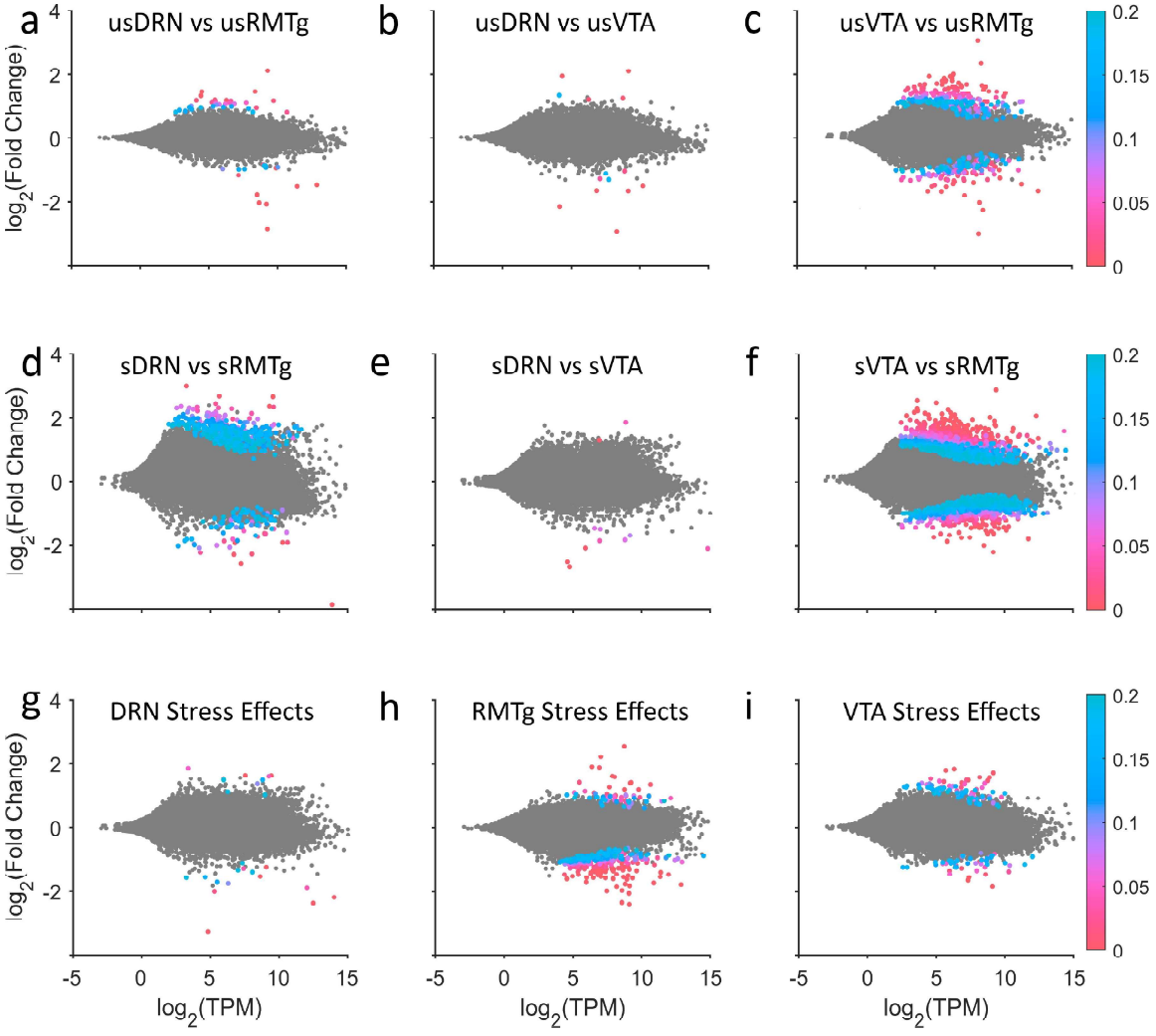

Figure 2: Pairwise DESeq2 comparisons. The top row shows comparisons between the unstressed pathways (a-c); there were few differences between LHb neurons projecting to the DRN and neurons projecting to the RMTg or VTA, although several hundred genes differed between the RMTg and VTA pathways at baseline. The middle row shows comparisons between the stressed pathways (d-f). There were only a few differences between the DRN and the VTA pathway, but stress exposure caused dramatic gene expression changes in the RMTg-projecting neurons relative to either the DRN or VTA pathways. The bottom row shows stress effects within each pathway (g-i). As is evident, the neurons projecting to the RMTg had the most differentially expressed genes, and most of those were downregulated.

genes were changed by stress; with 38 being upregulated and 166 being downregulated (Figure 2h). 63 genes were changed by stress in the VTA pathway – 40 were upregulated and 23 were downregulated (Figure 2i).

Figure 3 illustrates overlapping DEGs between and within the pathways. When comparing the effects of stress on each pathway, there were only a small number of gene expression differences that overlapped across pathways. Sema4d was consistently downregulated with stress in all three pathways (Wald scores =-5.2 to -8, q score <0.001). Several other genes (*Plekha7*, *Zfp467*, and *Slfn5*) were significantly differentially expressed in some but not all cases (q<0.001-0.09) (Figure 3a). All specific genes mentioned throughout this manuscript can be located in Table 3. When comparing the unstressed pathways, only a few genes overlapped. Compared to usDRN, no genes were more heavily expressed in both the usRMTg and usVTA (Figure 3b). When compared to the usRMTg pathway, 6 were more highly expressed in both the usDRN and usVTA (Figure 3c). When comparing to the usVTA pathway, *Trpc4* was more highly expressed in both usDRN and usRMTg pathways (usDRN vs usVTA Wald= 4.7, q=0.006; usVTA vs usRMTg Wald=-3.4, q=0.06) (Figure 3d). Oxytocin was positively differentially expressed in the DRN in both of these comparisons (usDRN vs usRMTg Wald=4.93, q=0.0011; usDRN vs usVTA Wald=5.63, q<0.0001) (Figure 3c-d). We confirmed the oxytocin expression results with RTqPCR on RiboTag RNA samples from the same brains (Supplemental Figures 2 and 4). Compared to the sDRN pathway, Hcfc1 (sDRN vs sRMTg Wald=-8.4, q<0.0001; sDRN vs sVTA Wald=-4.4, q=0.04) and AABR07037536.1 (sDRN vs sRMTg Wald=-3.4, q=0.09; sDRN vs sVTA Wald=-5.7, q=0.0002) were more heavily expressed in the sRMTg and sVTA pathways (Figure 3e). While there were only a handful of overlapping DEGs between the pairwise comparisons within stressed and unstressed

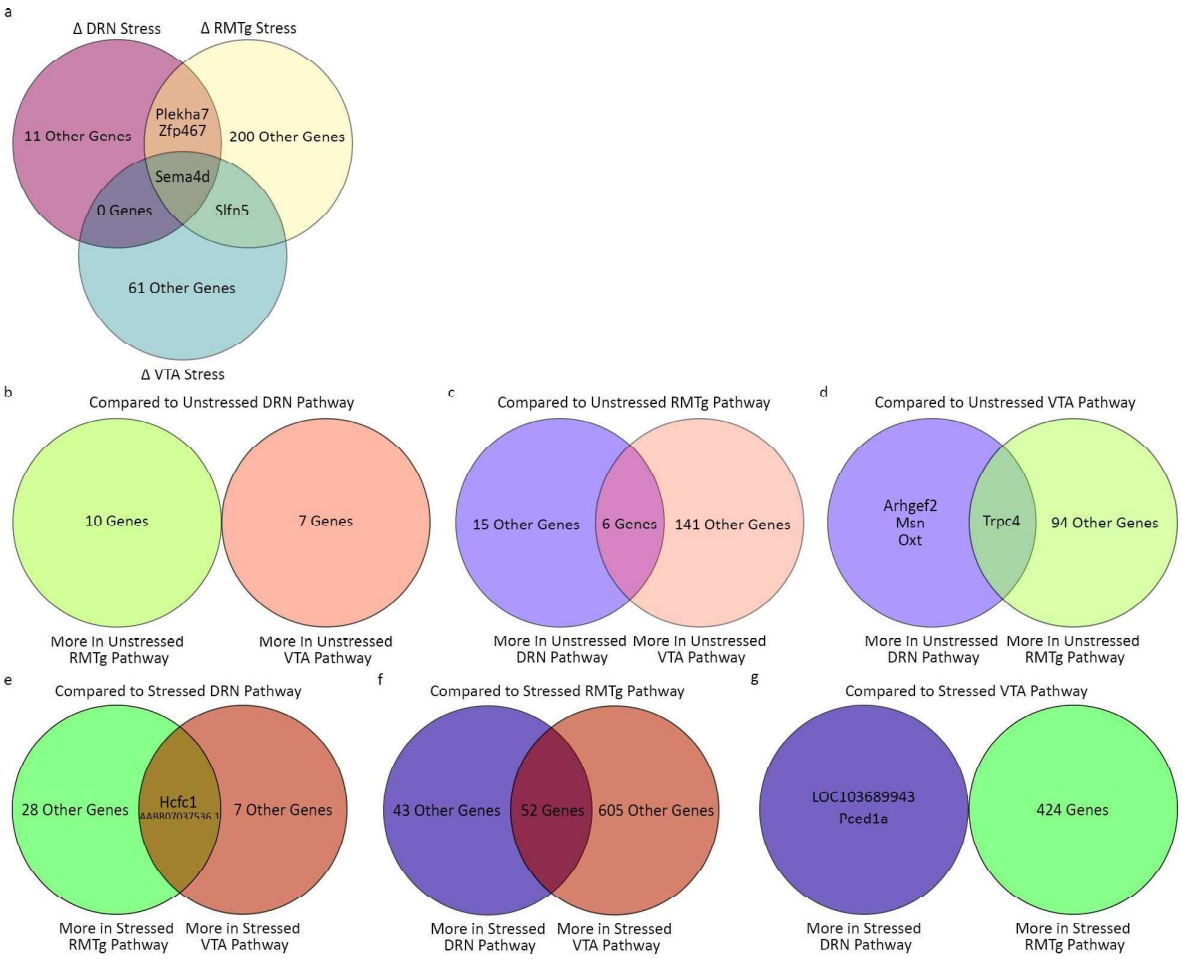

Figure 3: Venn diagrams of differentially expressed genes (q<0.1). a) The intersection of DEGs in stressed vs. unstressed neurons in each pathway were few; Sema4d was the only gene to be downregulated after stress in all pathways. b-d) Pairwise comparisons between RNA from the unstressed conditions revealed few differences between the pathways although the DRN and VTA pathways differed the least from each other and shared the most DEGs relative to RMTg. e-g) RNA in the RMTg-projecting neurons from stressed animals diverged from the other pathways. While the RNA from the DRN and VTA pathways of stressed animals were similar to one another, RNA in the RMTg-projecting neurons had ~4.5 fold more DEGs than in the comparisons from unstressed animals.

cases, 52 genes were more heavily expressed in both the stressed DRN and VTA pathways than in the stressed RMTg pathway (Figure 3f). Finally, when compared to the sVTA pathway, no genes were more heavily expressed in both the sDRN and sRMTg pathways (Figure 3g).

3.3 Stress Produced Opposite Patterns of Gene Set Enrichment in DRN and VTA Pathways as Compared to the RMTg Pathway

Next we used a curated gene set strategy to evaluate whether there were patterns of changes in sets of related genes using WebGestalt to perform Gene Set Enrichment Analysis (GSEA). The significantly enriched gene sets were similar across different databases and showed a clear pattern: in most cases stress led to a reduction in expression of a particular gene set within the DRN (sDRN vs usDRN) and VTA (sVTA vs usVTA) pathways, but an increase within RMTg (sRMTg vs usRMTg); in the few cases where this pattern was not replicated, stress induced changes in RMTg were always in the opposite direction than in VTA or DRN (Figure 4). While the function-defined gene sets shared this consistent pattern, gene sets relating to microRNA or transcription factor targets were not prominent nor shared across pathways and are not presented.

3.4 Stress Downregulated a PI3-Kinase Related Gene Network in the RMTg Pathway

Lastly, we performed Weighted Gene Co-expression Network Analysis (WGCNA), an unguided method for identifying modules of genes with correlated expression. WGCNA uses a special type of correlation matrix called a topological overlap matrix to represent the network connectedness of gene expression across all samples. This matrix was transformed into a hierarchical tree and clustered with the dynamic tree cut library for R [43]. WGCNA modules are randomly renamed using the “Crayola Color Palette” in order to combat attribution of meaning or importance to numbered

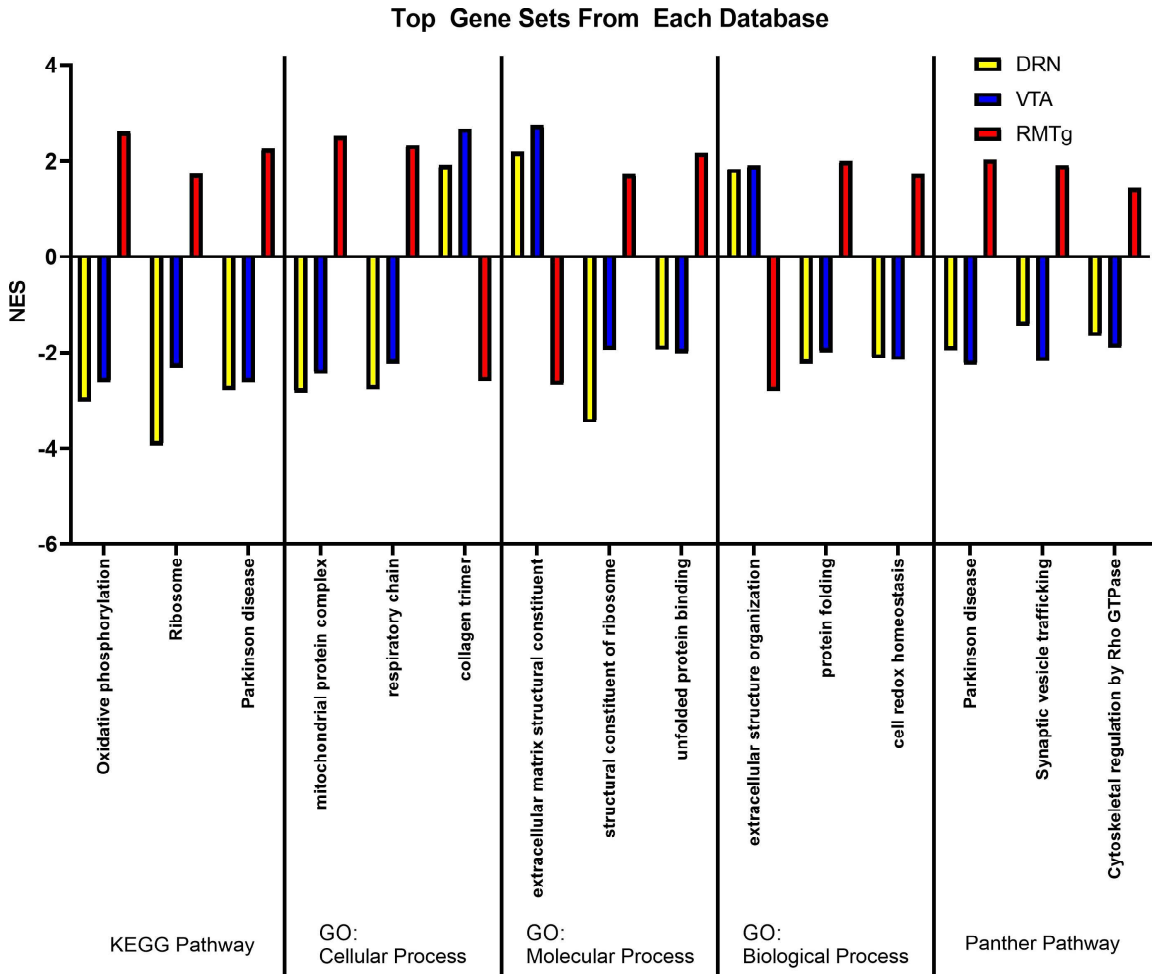

Figure 4: Gene set enrichment analysis. The average normalized enrichment scores (NES) for stressed vs. unstressed animalsfor each pathway of the three gene sets found in all three pairwise comparisonswith the largest differences are illustrated for each data base queried. Ofnote, in each gene set, the direction of RMTg changes (i.e. upregulation ordownregulation of DEGs) was in the opposite direction as for the DRN and VTApathways. Unlike other analyses in this paper, GSEA mostly detected gene sets thatwere upregulated by stress in the RMTg pathway. GO – Gene Ontology

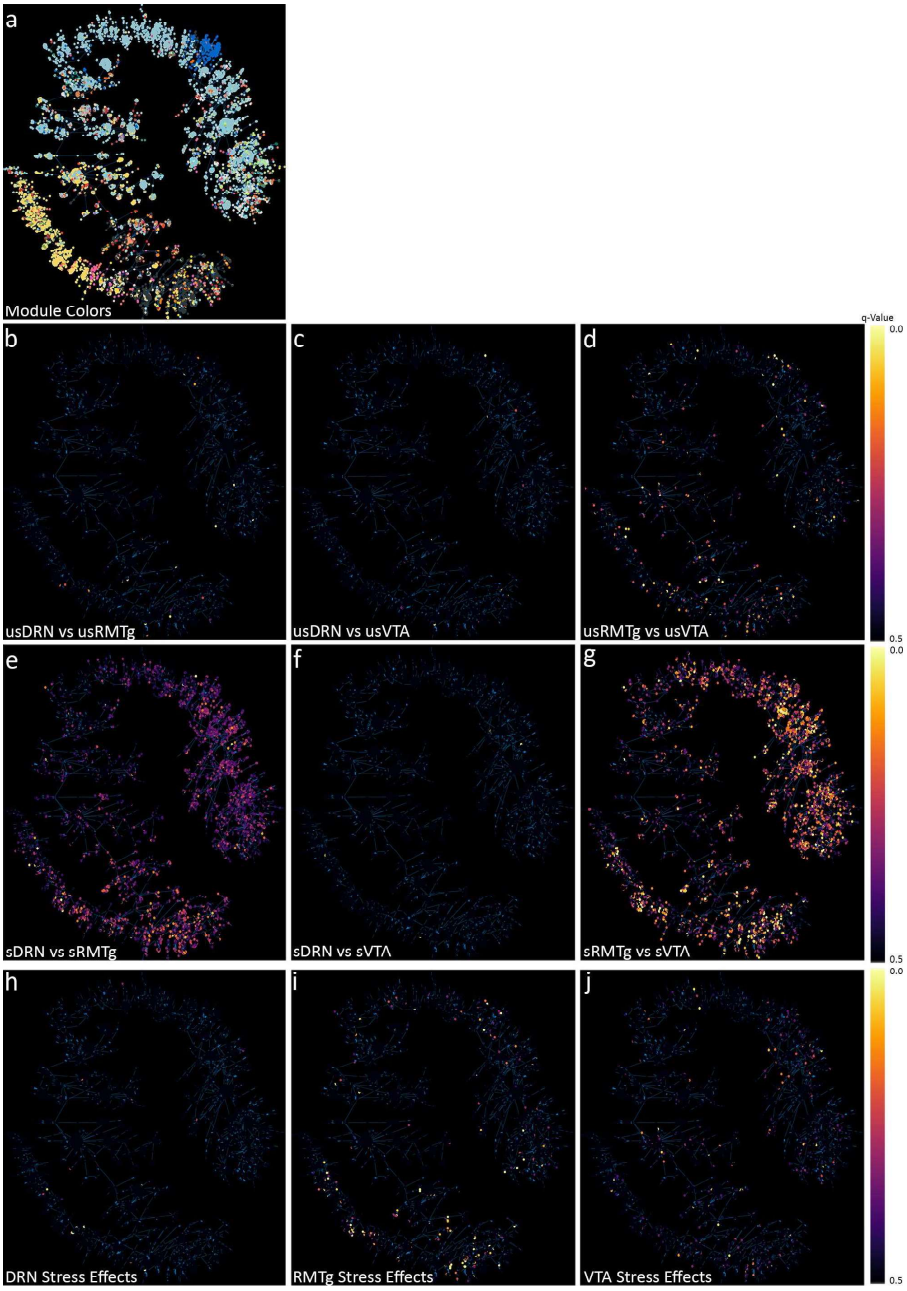

Figure 5: Minimum spanning trees of WGCNA results. a) Two-dimensional minimum spanning trees illustrate the 35 gene modules identified by weighted gene coexpression network analysis (WGCNA). Using the original DESeq2 analysis, the q-values for each individual gene is shown for pairwise comparisons of unstressed DRN to unstressed RMTg (b), unstressed DRN to unstressed VTA (c), and unstressed RMTg to unstressed VTA (d). There were relatively few changes apparent between the pathways in unstressed animals, but after stress, there were larger differences apparent in in the stressed DRN vs. stressed RMTg (e), stressed DRN vs. stressed VTA (f), and stressed RMTg vs. stressed VTA (g). The RMTg vs. VTA showed the most significant differences. (h-j) shows the pairwise comparisons for stressed vs. unstressed DRN (h), RMTg (i), and VTA (j).

modules. Initially, WGCNA identified 96 modules; however, many of the module eigengenes were highly correlated. Modules were merged down to 35 using hierarchical clustering with a tree cut height of 1.5. The module colors (Figure 5a) and q-scores for every gene for each of the nine pairwise comparisons are mapped onto minimum spanning trees in Figure 5. Notably, while the unstressed pathway comparisons (Figure 5b-d), and even the within-pathway stress comparisons (Figure 5h-j) have relatively few low q-values, the stressed DRN vs stressed RMTg (Figure 5e) and stressed RMTg vs stressed VTA (Figure 5g) contained many genes with low q-values as illustrated in the pseudocolor scale. Many of these DEGs map to the "Gold" module. Additionally, the distribution of Wald scores for each pair-wise comparison in each module are presented as violin plots in Figure 6. The Gold module stood out with an average Wald score $>\pm 2$ in multiple comparisons. The Gold module reached this threshold in the Stressed vs. Unstressed RMTg pathway (average Wald = -2.192,Figure 6b) and the Stressed RMTg vs. Stressed VTA pathway (average Wald = -2.317, not shown). Additionally, this module reached a less stringent threshold of $>\pm 1.5$ in the Stressed RMTg vs. Stressed DRN pathway comparison (average Wald = -1.584, not shown). Figure 7 depicts each gene in this module's importance within the network using a centrality metric (the more central genes have many strong bright lines); the genes most central to this module topologically are analogous to "hub" genes in other schemes. The centrality of individual genes in the Gold module correlated significantly with the Wald score in pairwise comparisons of differential expression for stressed vs. unstressed RMTg (Figure 7c), stressed RMTg vs stressed DRN (Figure 7d), and stressed RMTg vs stressed VTA (Figure 7e). Further, the Timberwolf, Turquoise Blue, and Silver modules reached a threshold of >1.5 in the Stressed DRN vs. Stressed RMTg and Stressed VTA vs. Stressed RMTg pathway comparisons (see

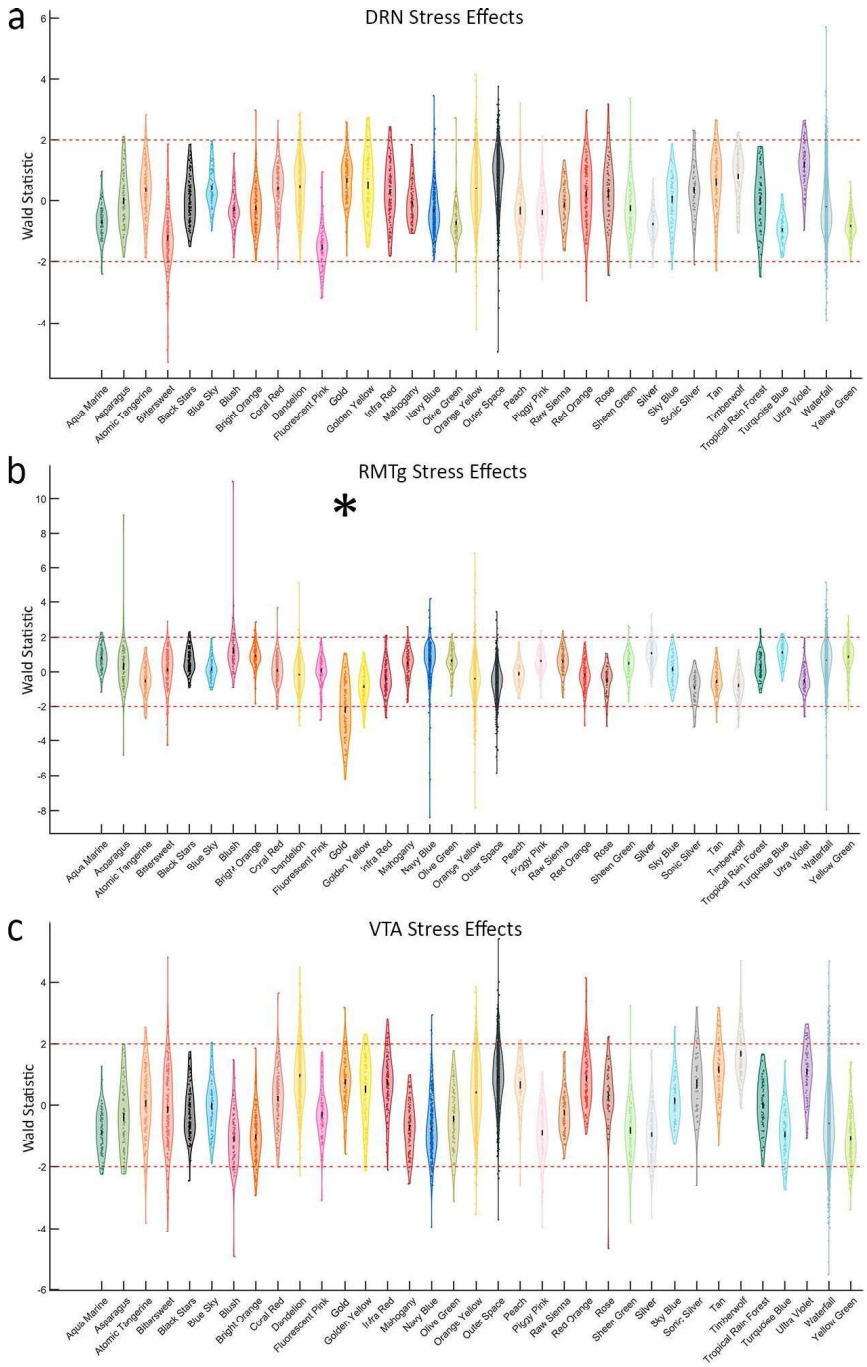

Figure 6: The Wald score for each gene within the 35 modules assigned by WGCNA. a) Stress effects in the DRN pathway. b) Stress effects in the RMTg pathway. The Gold module is downregulated with stress in the RMTg pathway (average Wald = -2.192) c) Stress effect in the VTA pathway.

Supplemental Code and Data). However, only the Gold and Silver modules demonstrated significant correlations between each gene's centrality in the module and that gene's Wald score. Interestingly, the Gold network genes tended to be decreased after stress in the RMTg pathway (i.e. downregulated) and were similarly downregulated in stressed RMTg compared to either the stressed DRN pathway or the stressed VTA pathway; we interpret this to mean that this gene module as a whole was downregulated in the stressed RMTg pathway.

We next performed an overrepresentation analysis to determine if the genes in the Gold module were associated with identified gene sets using WebGestalt. While there was significant overrepresentation of genes from several pathways, the regulation of PI3K signaling gene set was markedly overrepresented (enrichment ratio = 18.89; Figure 7f and Table 2).

This gene set included Kdr, Pld2, Plxnb1, Ptpn13, and Tek. Furthermore, these genes are downregulated in the stressed RMTg pathway compared to the unstressed RMTg, the stressed VTA or the stressed DRN pathways. Table 2 shows the Wald statistic and q score for each gene in this set for each comparison. Additionally, when investigating the top 25 most central genes in this network, 6 of them are regulated by the transcription factor ICSBP (IRF8) (enrichment ratio = 9.8, FDR=0.01) (Figure 7g). This gene set included Col4a1, Fryl, Rrbp1, Slc12a4, Tek, and Tnfrsf19. All specific genes mentioned in this article are located in Table 3.

3.5 *Validation of Downregulation of PI3-Kinase Related Genes in the Stressed RMTg Pathway*

In order to validate the RNAseq results, we repeated the stress procedure in a new cohort of rats that were first injected with AAV-DIO-RiboTag in LHb and CAV2-Cre into RMTg. RiboTag-purified RNA was prepared from RMTg-projecting LHb

Table 2: Phosphoinositide 3 kinase signaling genes in the Gold Network

Gene Symbol	Gene name	Relative to sRMTg Pathway					
		usRMTg		sDRN		sVTA	
		Wald	Q	Wald	Q	Wald	Q
Kdr	kinase insert domain receptor	4.829	<0.001	2.133	0.301	3.871	0.008
Pld2	phospholipase D2	2.096	0.543	2.577	0.234	2.569	0.121
Plxnb1	plexin B1	2.512	0.331	2.139	0.301	2.426	0.147
Ptpn13	protein tyrosine phosphatase, non-receptor type 13	3.339	0.068	2.532	0.237	3.060	0.052
Tek	TEK receptor tyrosine kinase	4.067	0.008	2.128	0.303	4.389	0.002

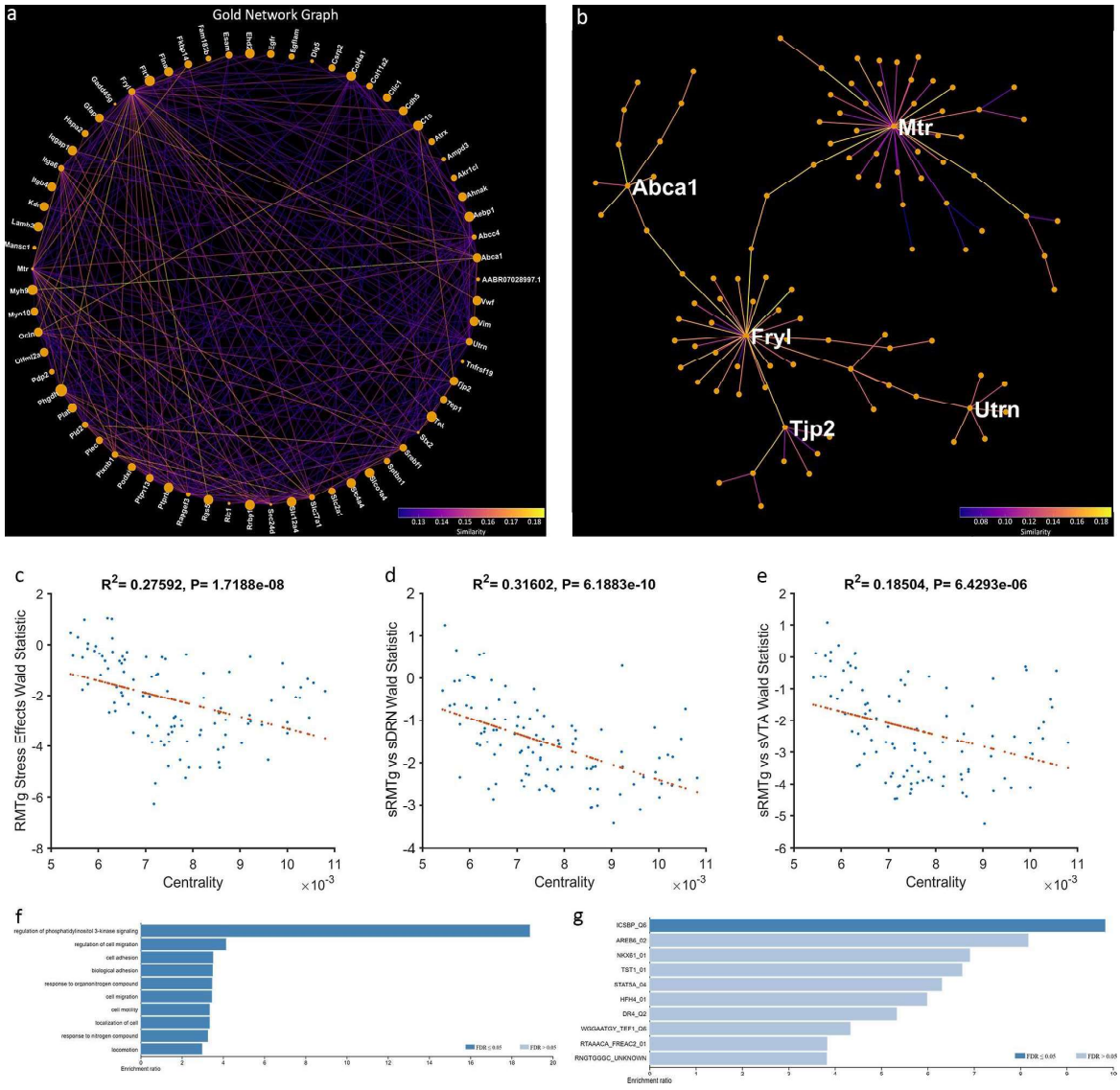

Figure 7: The Gold Network. a) Gold Gene Network projected onto a two-dimensional space using a circle layout. Line color represents pairwise gene expression similarity as calculated by WGCNA. Node size represents centrality to the network. b) Gold Network projected as a minimum spanning tree. The most central genes are labeled. c)Genes which are more downregulated with stress in the RMTg pathway are more central to the network (r^2=0.276, p<0.001). d) Genes which are less highly expressed in the stressed RMTg than the stressed DRN pathway are more central to the network (r^2=0.316, p<0.001). e) Genes which are less highly expressed in the stressed RMTg than the stressed VTA pathway are more central to the network (r^2=0.185, p<0.001). f) Overrepresentation analysis of GO: Biological Process of the entire network. g) Overrepresentation analysis of transcription factor targets for the 25 most central genes to the network.

Table 3: Genes named

Gene ID	Context
Sema4d	Consistently downregulated after stress across pathways
Plekha7	Upregulated after stress in DRN and RMTg pathways
Zfp467	Downregulated after stress in DRN and RMTg pathways
Slfn5	Downregulated after stress in RMTg and VTA pathways
Trpc4	Less expressed in usVTA than usDRN or usRMTg
Oxt	More expressed in usDRN than usVTA or usRMTg
Hcfc1	Less expressed in sDRN than sVTA or sRMTg
AABR07037536.1	Less expressed in sDRN than sVTA or sRMTg
Kdr	Highlighted in PI3K signaling pathway
Pld2	Highlighted in PI3K signaling pathway
Plxnb1	Highlighted in PI3K signaling pathway
Ptpn13	Highlighted in PI3K signaling pathway
Tek	Highlighted in PI3K signaling pathway and ICSBP transcription factor
Col4a1	Highlighted in ICSBP transcription factor
Fryl	Highlighted in ICSBP transcription factor
Rrbp1	Highlighted in ICSBP transcription factor
Slc12a4	Highlighted in ICSBP transcription factor
Tnfrsf19	Highlighted in ICSBP transcription factor

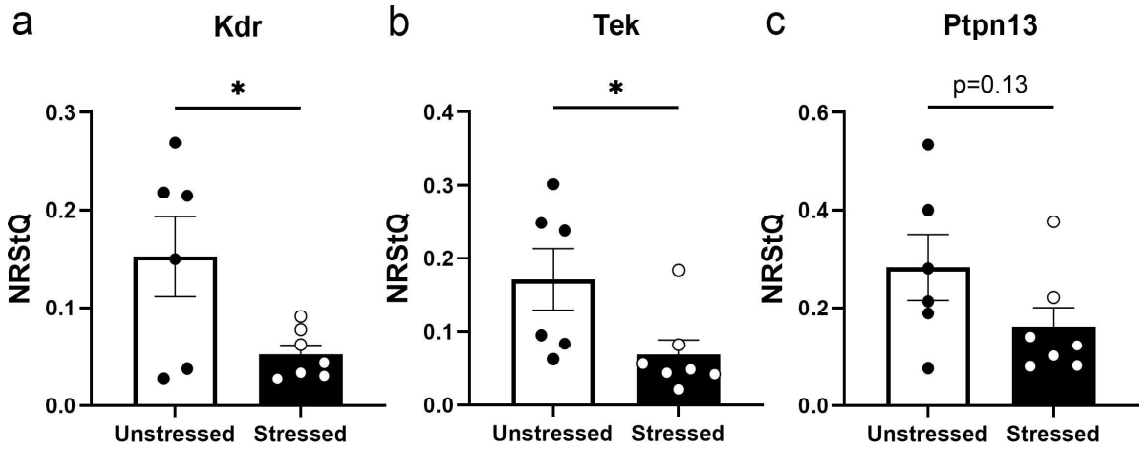

Figure 8: RTqPCR validates downregulation of PI3-Kinase related genes in RMTg-projecting LHb neurons. Based on the RNAseq analysis, we expressed RiboTag in the pathway from LHb to RMTg in a new cohort of control rats (n=6) and rats subjected to forced swim stress (n=7). RTqPCR of the ribosome-associated RNA showed that Kdr (a) and Tek (b) were significantly reduced after stress; there was a trend for stress to reduce Ptpn13 (c). *p<0.05.

neurons and used to quantify the expression level of three DEGs from the Gold network identified by WGCNA that are associated with PI3K signaling (Table 2). Kdr and Tek RNAs were significantly reduced in the ribosome-associated RNA from the sRMTg pathway compared to the usRMTg pathway ($t(11)=2.570$, $p=0.0260$; $t(11)=2.323$, $p=0.0404$, respectively; Figure 8) while there was a nonsignificant trend for Ptpn13 to be reduced ($t(11)=1.614$, $p=0.1348$). These changes replicated the results of the WGCNA analysis of the RNAseq data in a separate cohort of animals indicating that forced swim stress reduced the expression of several genes associated with PI3K signaling in RMTg-projecting LHb neurons.

4 Discussion

In this study we investigated the impact of stress on RNAs actively undergoing translation in LHb neurons comprising the three major output pathways to VTA, DRN,

and RMTg. We compared expression of individual genes between pathways and between unstressed and stressed conditions in a pairwise fashion. We found that GSEA and WGCNA revealed patterns in gene expression changes with stress that differed between these efferent LHb pathways. Whereas GSEA is based upon previously identified sets of functionally related genes, WGCNA uses an unbiased method of clustering genes into "modules" based on patterns of expression levels across the entire data set without assumptions about gene function. When we examined the average expression levels of all of the modules that were identified, just one repeatedly demonstrated significant differential expression between experimental groups. In most cases, the gene sets or modules were downregulated in RMTg-projecting LHb neurons after stress but upregulated in DRN- and VTA-projecting neurons after stress. When we compared the pathways to one another in a pairwise fashion in unstressed rats, there were relatively few differences in RNA expression; in particular, there were no dramatic phenotype-defining differences observed. A recent single cell RNAseq study in mice reached similar conclusions [33]. While some LHb neurons express neuropeptides and perhaps GABA, nearly every neuron in the LHb is glutamatergic [13, 45, 46]. Therefore, it is less surprising that the pathways are homogeneous at baseline and only change with stress. Our a priori hypothesis was that the neurons comprising these three pathways might be quite different because the pathways are highly segregated with few collaterals, but this was rejected; however, some differences between these pathways emerged following stress exposure.

Neurons projecting to different target regions are intermixed within subregions of the LHb yet have minimal collateralization between DRN, VTA, and RMTg. Given that the LHb neurons targeting these areas have similar phenotypes at baseline, perhaps the differences become apparent after stress because each pathway receives different

input information during stress. The LHb receives inputs from myriad sources throughout the brain. Perhaps, stress-sensitive inputs preferentially synapse onto neurons projecting to specific targets, and differential activation leads to changes in their subsequent gene expression. Indeed, a recent paper found that CaMKII-expressing neurons projecting from the entopeduncular nucleus tended to synapse onto LHb neurons projecting to the VTA; whereas, those from the lateral hypothalamus and VTA tended to synapse onto neurons projecting to the DRN [34].

We found that RMTg-projecting neurons changed the most following stress. This was unexpected since we previously found that the pathway to the DRN was the most involved in adaptations to forced swim immobility [4]. Chemogenetically inhibiting DRN-projecting neurons in between the first and second swim sessions decreased immobility and decreased perseverative seeking in the reward omission task. Conversely, activating these neurons increased perseverative seeking but did not further change immobility in the forced swim test. Inhibiting either of the other two pathways did not change behavior in any of the tests performed. Thus, we initially expected the pathway to the DRN to be the most affected by stress. One possible interpretation of these results is that inhibiting the LHb-RMTg pathway had no effect because the plasticity in this pathway already served to reduce its excitability, and inhibition with hM_4Di had no additional impact. Supporting this interpretation, Proulx and colleagues found that acute optogenetic stimulation of RMTg-projecting LHb neurons transiently increased immobility during a single FST session [47], suggesting that it indeed is not maximally activated during forced swim alone. It is interesting to consider that, if the pathway from LHb to RMTg becomes less excitable due to changes in gene expression following forced swim stress, perhaps this leads to a relative increased activation of VTA and DRN by LHb.

The circuitry of the LHb and its major targets, RMTg, DRN, and VTA, is complex. LHb stimulation generally decreases dopaminergic activity within the VTA; although there is also evidence of direct excitation of dopamine neurons [9]. Similarly, activation of the LHb has complex effects on the output of serotonin from raphe neurons; only high frequency stimulation increased serotonin release into striatum; this was further augmented by bicuculline injection into DRN [7]. Indeed, lesions of the habenula ablate the increase in serotonin in the DRN during and after stress [48]. LHb neurons project to both serotonergic and GABAergic neurons in DRN at roughly equal rates [14]. While direct projections to VTA or DRN may either activate monoaminergic or GABAergic neurons, the projection to RMTg innervates only GABAergic neurons which in turn inhibit VTA and DRN [49]. In this report we observed differential gene expression plasticity between neurons projecting to VTA and DRN on the one hand and RMTg on the other. Since the changes in RMTg-projecting neurons involved reduced expression of genes associated with excitability (such as in the PI3K signaling pathway), perhaps the overall balance of LHb stimulation of downstream GABAergic tone is reduced after repeated forced swim stress.

There is some diversity in the responses of LHb neurons to aversive stimuli. Both inescapable shock and reward omission increase firing in subpopulations of the LHb, exciting 30-50% of these neurons [50, 51]. Furthermore, roughly 10% of LHb neurons are actually inhibited by foot-shocks [52]. Further, RMTg-projecting LHb neurons have shown increased excitability 24 hours to 14 days after cocaine exposure, but VTA-projecting neurons did not [53, 54]. Thus, it is possible that the observed stress-induced reduction in the excitability of LHb projections to RMTg disinhibits the VTA and DRN monoaminergic outputs. On the contrary, activation of LHb-RMTg neurons optogenetically interferes with reward motivated behavior and reduces activity in the

FST [47]. Perhaps the pathway to the RMTg becomes less active following an inescapable stressor via an allostatic adaptation in neuronal excitability.

Cerniauskas, et al. (2019) [34] characterized the effect of chronic mild stress on LHb neurons projecting to either the VTA/RMTg or the DRN. They observed greater excitability in neurons projecting to the VTA/RMTg in mice with the greatest composite depression-like behaviors. No such pattern was observed in the pathway to the DRN. Further, chemogenetic activation of LHb-VTA/RMTg neurons produced a depression-like phenotype in stress-naïve mice. Conversely, DREADD-mediated inhibition of this pathway in stressed mice reduced their depression-like behaviors. Their data suggested that entopeduncular nucleus projections to LHb neurons that in turn project to VTA may be a critical functional circuit. Surgical targeting of VTA without hitting RMTg is difficult in mice, while these target areas can reliably be discriminated with retrograde strategies in rats [5, 41] [55], as we did in this study, so it is difficult to directly compare our results and theirs. Additionally, this study included pathway-specific scRNAseq investigating transcriptional differences between the LHb neurons projecting to the DRN and those to the VTA/RMTg as well as differences with the LHb-VTA/RMTg neurons from mice which displayed prolonged immobility in the Tail Suspension Test and those which did not. When comparing our data to theirs, a few caveats must be considered. The transcriptome and translatome represent distinct RNA pools and will inevitably be different. Additionally, Cerniauskas, et al. (2019) [34] probed the cells electrophysiologically prior to collection; whereas, we homogenized tissue and extracted actively translating ribosomes. Each of these methods may result in different artifacts within the data by altering transcription or translation. However, several of the gene expression changes between pathways were similar to changes we observed. While none of the more highly-

expressed genes in the DRN-projecting neurons, nor any genes which differed in relation to the tail suspension test criteria were differentially expressed in our study, several of the genes which they found that were more heavily expressed in the pathway to the VTA/RMTg approached significance in our data. Specifically, Grid2 and Sytl2 trended towards increased expression in the sRMTg versus sVTA comparison (q=0.126 and 0.18, respectively). Interestingly, both genes were more heavily expressed in the sRMTg pathway. While our GSEA results suggest that gene expression in these pathways diverge after stress, we focused on the unbiased topological analysis with WGCNA, which also indicated that the RMTg-projecting neurons diverged from the VTA- and DRN-projecting neurons. WGCNA clusters genes with no a priori knowledge of function; however, it is not uncommon for modules to have overrepresentations of biologically relevant sets of genes. This was exemplified by the Gold module, which had an overrepresentation of downregulated genes associated with PI3K signaling after stress, found both via GO: Biological Process and the KEGG database. In order to validate these results, we performed RTqPCR from ribosome-associated RNA isolated from the RMTg-projecting neurons in a new cohort of control and stressed rats. We measured the three differentially expressed PI3K-associated genes identified by WGCNA and confirmed the downregulation of Kdr and Tek while Ptpn13 exhibited a similar trend. We propose that this reduction in PI3K-associated genes may reduce excitability of RMTg-projecting LHb neurons. PI3K signaling regulates anxiety-like behavior, may be involved in the antidepressant effects of deep brain stimulation, and is implicated in the mood-stabilizing effects of lithium in post-mortem analyses of patients with major depressive disorder [56]. Phosphorylation of PI3K is implicated in the antidepressant effects of baicalin in a mouse model of depression [57]. We predict that downregulation of PI3K in the RMTg-projecting neurons after stress would be a

compensatory adaptation that reduces their excitability, thereby disinhibiting the monoaminergic neurons in the DRN and VTA. Since we examined RNA actively undergoing translation in this study, the impact of these changes on protein production might take additional time to manifest. Future studies should examine the role of PI3K signaling in this pathway on resilience after stress exposure.

5 Conclusions

In summary, RNA expression in the major efferent pathways from the LHb was more similar than anticipated at baseline; however, stress led to divergent patterns of gene expression. In particular, the RMTg-projecting neurons had a downregulation of PI3K signaling genes, which might lead to an altered balance of activity of these pathways during the response to stress.

6 Funding

This work was supported by MH106532 (JFN), NS099578 (MRL), and DA007278 (KRC).

Acknowledgements

MRL – Conceptualization, methodology, formal analysis, investigation, writing – original draft, visualization
KRC – methodology, software, visualization, writing – review & editing RM – methodology, software
AJL – conceptualization, methodology
JFN – Conceptualization, resources, supervision, funding acquisition, project administration, writing – review & editing

References

[1] L. M. Williams, Precision psychiatry: A neural circuit taxonomy for depression and anxiety, Lancet Psychiatry 3 (2016) 579–588. doi:10.1016/S2215-0366(15)00579-9.

[2] K. Brinschwitz, A. Dittgen, V. I. Madai, R. Lommel, S. Geisler, R. W. Veh, Glutamatergic axons from the lateral habenula mainly terminate on GABAergic neurons of the ventral midbrain, Neuroscience 168 (2) (2010) 463–476. doi:10.1016/j.neuroscience.2010.03.050.

[3] S. Geisler, M. Trimble, The Lateral Habenula: No Longer Neglected, CNS Spectrums 13 (6) (2008) 484–489. doi:10.1017/s1092852900016710.

[4] K. R. Coffey, R. G. Marx, E. K. Vo, S. G. Nair, J. F. Neumaier, Chemogenetic inhibition of lateral habenula projections to the dorsal raphe nucleus reduces passive coping and perseverative reward seeking in rats, Neuropsychopharmacology 45 (2020) 1115–1124. doi:10.1038/s41386-020-0616-0.

[5] L. Gonçalves, C. Sego, M. Metzger, Differential projections from the lateral habenula to the rostromedial tegmental nucleus and ventral tegmental area in the rat, The Journal of Comparative Neurology 520 (6) (2012) 1278–1300. doi:10.1002/cne.22787.

[6] R. Bernard, R. W. Veh, Individual neurons in the rat lateral habenular complex project mostly to the dopaminergic ventral tegmental area or to the serotonergic raphe nuclei, The Journal of Comparative Neurology 520 (11) (2012) 2545–2558. doi:10.1002/cne.23080.

[7] P. K. n, R. E. Strecker, E. Rosengren, A. B. rklund, Regulation of striatal serotonin release by the lateral habenula-dorsal raphe pathway in the rat as demonstrated by in vivo micro-dialysis: role of excitatory amino acids and GABA, Brain Research 492 (1-2) (1989) 187–202. doi:10.1016/0006-8993(89)90901-3.

[8] L. A. Quina, L. Tempest, L. Ng, J. A. Harris, S. Ferguson, T. C. Jhou, E. E. Turner, Efferent Pathways of the Mouse Lateral Habenula, Journal of Comparative Neurology 523 (1) (2015) 32–60. doi:10.1002/cne.23662.

[9] P. L. Brown, P. D. Shepard, Functional evidence for a direct excitatory projection from the lateral habenula to the ventral tegmental area in the rat, Journal of Neurophysiology 116 (3) (2016) 1161–1174. doi:10.1152/jn.00305.2016.

[10] S. Lammel, B. K. Lim, C. Ran, K. W. Huang, M. J. Betley, K. M. Tye, K. Deisseroth, R. C. Malenka, Input-specific control of reward and aversion in the ventral tegmental area, Nature 491 (7423) (2012) 212–217. doi:10.1038/nature11527.

[11] S. K. Ogawa, J. Y. Cohen, D. Hwang, N. Uchida, M. Watabe-Uchida, Organization of Monosynaptic Inputs to the Serotonin and Dopamine Neuromodulatory Systems, Cell Reports 8 (4) (2014) 1105–1118. doi:10.1016/j.celrep.2014.06.042.

[12] N. Omelchenko, R. Bell, S. R. Sesack, Lateral habenula projections to dopamine and GABA neurons in the rat ventral tegmental area, European Journal of Neuroscience 30 (7) (2009) 1239–1250. doi:10.1111/j.1460-9568.2009.06924.x.

[13] A. M. Stamatakis, G. D. Stuber, Activation of lateral habenula inputs to the

ventral midbrain promotes behavioral avoidance, Nature Neuroscience 15 (8) (2012) 1105–1107. doi:10.1038/nn.3145.
[14] B. Weissbourd, J. Ren, K. E. DeLoach, C. J. Guenthner, K. Miyamichi, L. Luo, Presynaptic Partners of Dorsal Raphe Serotonergic and GABAergic Neurons, Neuron 83 (3) (2014)645–662. doi:10.1016/j.neuron.2014.06.024.
[15] C. Gruber, A. Kahl, L. Lebenheim, A. Kowski, A. Dittgen, R. W. Veh, Dopaminergic pro-jections from the VTA substantially contribute to the mesohabenular pathway in the rat, Neuroscience Letters 427 (3) (2007) 165–170. doi:10.1016/j.neulet.2007.09.016.
[16] L. N. Han, L. Zhang, L. B. Li, Y. N. Sun, Y. Wang, L. Chen, Y. Guo, Y. M. Zhang, Q. J. Zhang, J. Liu, Activation of serotonin(2c) receptors in the lateral habenular nucleus increases the expression of depression-related behaviors in the hemiparkinsonian rat, Neuropharmacology 93 (2015) 68–79. doi:10.1016/j.neuropharm.2015.01.024.
[17] A. B. Kowski, R. W. Veh, T. Weiss, Dopaminergic activation excites rat lateral habenular neurons in vivo, Neuroscience 161 (4) (2009) 1154–1165. doi:10.1016/j.neuroscience.2009.04.026.
[18] Y.-Q. Li, M. Takada, Y. Shinonaga, N. Mizuno, The sites of origin of dopaminergic afferent fibers to the lateral habenular nucleus in the rat, The Journal of Comparative Neurology 333 (1) (1993) 118–133. doi:10.1002/cne.903330110.
[19] X. Shen, X. Ruan, H. Zhao, Stimulation of midbrain dopaminergic structures modifies firing rates of rat lateral habenula neurons, PLoS One 7 (2012). doi:10.1371/journal.pone.0034323.
[20] G. Xie, W. Zuo, L. Wu, W. Li, W. Wu, A. Bekker, J. H. Ye, Serotonin modulates glutamatergic transmission to neurons in the lateral habenula, Scientific Reports 6 (2016). doi:10.1038/srep23798.
[21] H. Zhang, K. Li, H. S. Chen, S. Q. Gao, Z. X. Xia, J. T. Zhang, F. Wang, J. G. Chen, Dorsal raphe projection inhibits the excitatory inputs on lateral habenula and alleviates depressive behaviors in rats, Brain Struct Funct 223 (2018) 2243–2258. doi:10.1007/s00429-018-1623-3.
[22] D. H. Root, A. F. Hoffman, C. H. Good, S. Zhang, E. Gigante, C. R. Lupica, M. Morales, Norepinephrine Activates Dopamine D4 Receptors in the Rat Lateral Habenula, Journal of Neuroscience 35 (8) (2015) 3460–3469. doi:10.1523/jneurosci.4525-13.2015.
[23] C. A. Browne, R. Hammack, I. Lucki, Dysregulation of the lateral habenula in major depressive disorder, Front Synaptic Neurosci 10 (2018). doi:10.3389/fnsyn.2018.00046.
[24] E. H. Lee, S. L. Huang, Role of lateral habenula in the regulation of exploratory behavior and its relationship to stress in rats, Behav Brain Res 30 (1988) 90169–90175. doi:10.1016/0166-4328(88)90169-6.
[25] D. Wirtshafter, K. E. Asin, M. R. Pitzer, Dopamine agonists and stress produce different patterns of Fos-like immunoreactivity in the lateral habenula, Brain Research 633 (1-2) (1994) 21–26. doi:10.1016/0006-8993(94)91517-2.
[26] Y. Ootsuka, M. Mohammed, Activation of the habenula complex evokes autonomic physiological responses similar to those associated with emotional

stress, Physiological Reports 3 (2015). doi:10.14814/phy2.12297.

[27] M. J. Gill, S. M. Ghee, S. M. Harper, R. E. See, Inactivation of the lateral habenula reduces anxiogenic behavior and cocaine seeking under conditions of heightened stress, Pharmacology Biochemistry and Behavior 111 (2013) 24–29. doi:10.1016/j.pbb.2013.08.002.

[28] X. F. Luo, B. L. Zhang, J. C. Li, Y. Y. Yang, Y. F. Sun, H. Zhao, Lateral habenula as a link between dopaminergic and serotonergic systems contributes to depressive symptoms in parkinson's disease, Brain Res Bull 110 (2015) 40–46. doi:10.1016/j.brainresbull.2014.11.006.

[29] Q. Zhang, J. J. Feng, S. Yang, X. F. Liu, J. C. Li, H. Zhao, Lateral habenula as a link between thyroid and serotoninergic system mediates depressive symptoms in hypothyroidism rats, Brain Res Bull 124 (2016) 198–205. doi:10.1016/j.brainresbull.2016.05.007.

[30] S. G. Nair, N. S. Strand, J. F. Neumaier, DREADDing the lateral habenula: A review of methodological approaches for studying lateral habenula function, Brain Research 1511 (2013) 93–101. doi:10.1016/j.brainres.2012.10.011.

[31] F. Wagner, L. French, R. W. Veh, Transcriptomic-anatomic analysis of the mouse habenula uncovers a high molecular heterogeneity among neurons in the lateral complex, while gene expression in the medial complex largely obeys subnuclear boundaries, Brain Struct Funct 221 (2016) 39–58. doi:10.1007/s00429-014-0891-9.

[32] Y. Hashikawa, K. Hashikawa, M. A. Rossi, M. L. Basiri, Y. Liu, N. L. Johnston, O. R. Ahmad, G. D. Stuber, Transcriptional and Spatial Resolution of Cell Types in the Mammalian Habenula, Neuron 106 (5) (2020) 743–758.e5. doi:10.1016/j.neuron.2020.03.011.

[33] M. L. Wallace, K. W. Huang, D. Hochbaum, M. Hyun, G. Radeljic, B. L. Sabatini, Anatomical and single-cell transcriptional profiling of the murine habenular complex, eLife 9 (2020). doi:10.7554/elife.51271.

[34] I. Cerniauskas, J. Winterer, J. W. de Jong, D. Lukacsovich, H. Yang, F. Khan, J. R. Peck, S. K. Obayashi, V. Lilascharoen, B. K. Lim, C. Földy, S. Lammel, Chronic Stress Induces Activity, Synaptic, and Transcriptional Remodeling of the Lateral Habenula Associated with Deficits in Motivated Behaviors, Neuron 104 (5) (2019) 899–915.e8. doi:10.1016/j.neuron.2019.09.005.

[35] E. Sanz, L. Yang, T. Su, D. R. Morris, G. S. McKnight, P. S. Amieux, Cell-type-specific isolation of ribosome-associated mRNA from complex tissues, Proceedings of the National Academy of Sciences 106 (33) (2009) 13939–13944. doi:10.1073/pnas.0907143106.

[36] A. J. Lesiak, K. Coffey, J. H. Cohen, K. J. Liang, C. Chavkin, J. F. Neumaier, Sequencing the serotonergic neuron translatome reveals a new role for Fkbp5 in stress, Molecular Psychiatry (2020). doi:10.1038/s41380-020-0750-4.

[37] K. R. Coffey, D. J. Barker, S. Ma, M. O. West, Building An Open-source Robotic Stereotaxic Instrument, Journal of Visualized Experiments (80) (2013). doi:10.3791/51006.

[38] M. S. Clark, T. J. Sexton, M. McClain, D. Root, R. Kohen, J. F. Neumaier, Overexpression of 5-HT1B Receptor in Dorsal Raphe Nucleus Using Herpes Simplex Virus Gene Transfer Increases Anxiety Behavior after Inescapable Stress, The Journal of Neuroscience 22 (11) (2002) 4550–4562. doi:10.1523/jneurosci.22-11-04550.2002.

[39] A. J. Lesiak, J. F. Neumaier, RiboTag: Not Lost in Translation,

Neuropsychopharmacology 41 (1) (2016) 374–376. doi:10.1038/npp.2015.262.
[40] A. J. Lesiak, M. Brodsky, J. F. Neumaier, RiboTag is a flexible tool for measuring the translational state of targeted cells in heterogeneous cell cultures, BioTechniques 58 (6) (2015) 308–317. doi:10.2144/000114299.
[41] K. R. Coffey, A. J. Lesiak, R. G. Marx, E. K. Vo, G. A. Garden, J. F. Neumaier, Ribotag-seq reveals a compensatory camp responsive gene network in striatal microglia induced by morphine withdrawal, BioRxiv (2020). doi:10.1101/2020.02.10.942953.
[42] Y. Liao, J. Wang, E. J. Jaehnig, Z. Shi, B. Zhang, WebGestalt 2019: gene set analysis toolkit with revamped UIs and APIs, Nucleic Acids Research 47 (W1) (2019) W199–W205. doi:10.1093/nar/gkz401.
[43] P. Langfelder, S. Horvath, WGCNA: an R package for weighted correlation network analysis, BMC Bioinformatics 9 (1) (2008). doi:10.1186/1471-2105-9-559.
[44] R: A language and environment for statistical computing, in: R Foundation for Statistical Computing, 2020.
[45] H. Aizawa, M. Kobayashi, S. Tanaka, T. Fukai, H. Okamoto, Molecular characterization of the subnuclei in rat habenula, The Journal of Comparative Neurology 520 (18) (2012) 4051–4066. doi:10.1002/cne.23167.
[46] W. Zuo, L. Wang, L. Chen, K. Krnjević, R. Fu, X. Feng, W. He, S. Kang, A. Shah, A. Bekker, J.-H. Ye, Ethanol potentiates both GABAergic and glutamatergic signaling in the lateral habenula, Neuropharmacology 113 (2017) 178–187. doi:10.1016/j.neuropharm.2016.09.026.
[47] C. D. Proulx, S. Aronson, D. Milivojevic, C. Molina, A. Loi, B. Monk, S. J. Shabel, R. Malinow, A neural pathway controlling motivation to exert effort, Proceedings of the National Academy of Sciences 115 (22) (2018) 5792–5797. doi:10.1073/pnas.1801837115.
[48] J. Amat, P. D. Sparks, P. Matus-Amat, J. Griggs, L. R. Watkins, S. F. Maier, The role of the habenular complex in the elevation of dorsal raphe nucleus serotonin and the changes in the behavioral responses produced by uncontrollable stress, Brain Research 917 (1) (2001) 118–126. doi:10.1016/s0006-8993(01)02934-1.
[49] Y. Yang, H. Wang, J. Hu, H. Hu, Lateral habenula in the pathophysiology of depression, Curr Opin Neurobiol 48 (2018) 90–96. doi:10.1016/j.conb.2017.10.024.
[50] S. Lecca, F. J. Meye, M. Trusel, A. Tchenio, J. Harris, M. K. Schwarz, D. Burdakov, F. Georges, M. Mameli, Aversive stimuli drive hypothalamus-to-habenula excitation to promote escape behavior, eLife 6 (2017). doi:10.7554/eLife.30697.
[51] S. J. Shabel, C. Wang, B. Monk, S. Aronson, R. Malinow, Stress transforms lateral habenula reward responses into punishment signals, Proceedings of the National Academy of Sciences 116 (25) (2019) 12488–12493. doi:10.1073/pnas.1903334116.
[52] M. Congiu, M. Trusel, M. Pistis, M. Mameli, S. Lecca, Opposite responses to aversive stimuli in lateral habenula neurons, European Journal of Neuroscience 50 (6) (2019) 2921–2930. doi:10.1111/ejn.14400.
[53] M. Maroteaux, M. Mameli, Cocaine Evokes Projection-Specific Synaptic

Plasticity of Lateral Habenula Neurons, Journal of Neuroscience 32 (36) (2012) 12641–12646. doi:10.1523/jneurosci.2405-12.2012.

[54] F. J. Meye, K. Valentinova, S. Lecca, L. Marion-Poll, M. J. Maroteaux, S. Musardo,

I. Moutkine, F. Gardoni, R. L. Huganir, F. Georges, M. Mameli, Cocaine-evoked negative symptoms require AMPA receptor trafficking in the lateral habenula, Nature Neuroscience 18 (3) (2015) 376–378. doi:10.1038/nn.3923.

[55] R. Fu, Q. Mei, W. Zuo, J. Li, D. Gregor, A. Bekker, J. Ye, Low-dose ethanol excites lateral habenula neurons projecting to vta, rmtg, and raphe, Int J Physiol Pathophysiol Pharmacol 9 (2017) 217–230.

[56] B. Voleti, R. S. Duman, The Roles of Neurotrophic Factor and Wnt Signaling in Depression, Clinical Pharmacology & Therapeutics 91 (2) (2012) 333–338. doi:10.1038/clpt.2011.296.

[57] L. T. Guo, S. Q. Wang, J. Su, L. X. Xu, Z. Y. Ji, R. Y. Zhang, Q. W. Zhao, Z. Q. Ma, X. Y. Deng, S. P. Ma, Baicalin ameliorates neuroinflammation-induced depressive-like behavior through inhibition of toll-like receptor 4 expression via the pi3k/akt/foxo1 pathway, J Neuroinflammation 16 (2019) 95–95. doi:10.1186/s12974-019-1474-8.

Supplemental Figures for Chapter 2: Stress induces divergent gene expression among lateral habenula efferent pathways

Marjorie R Levinstein[a,b], Kevin R Coffey[b], Russell G Marx[a,b], Atom J Lesiak[b,c], John F Neumaier[a,b,d]

[a]*Graduate Program in Neuroscience, University of Washington, Seattle, WA, USA*
[b]*Department of Psychiatry and Behavioral Sciences, University of Washington, Seattle, WA, USA*
[c]*Department of Genome Sciences, University of Washington, Seattle, WA, USA*
[d]*Department of Pharmacology, University of Washington, Seattle, WA, USA*

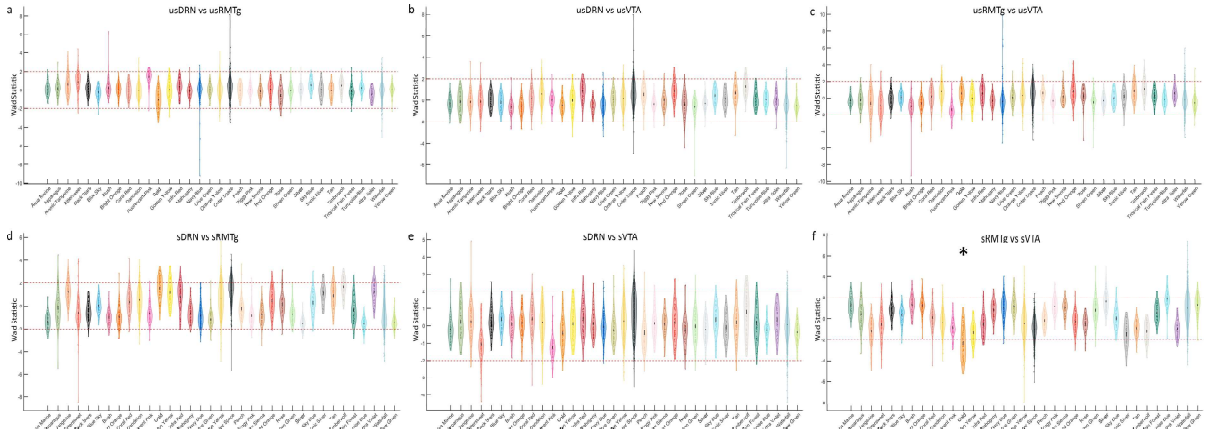

Supplemental Figure 1: The Wald score for each gene within the 35 modules assigned by WGCNA for remaining pairwise comparisons. a) Unstressed DRN pathway compared to Unstressed RMTg pathway. b) Unstressed DRN pathway compared to Unstressed VTA pathway. c) Unstressed RMTg pathway compared to Unstressed VTA pathway. d) Stressed DRN pathway compared to Stressed RMTg pathway. e) Stressed DRN pathway compared to Stressed VTA pathway. f) Stressed RMTg pathway compared to Stressed VTA pathway.

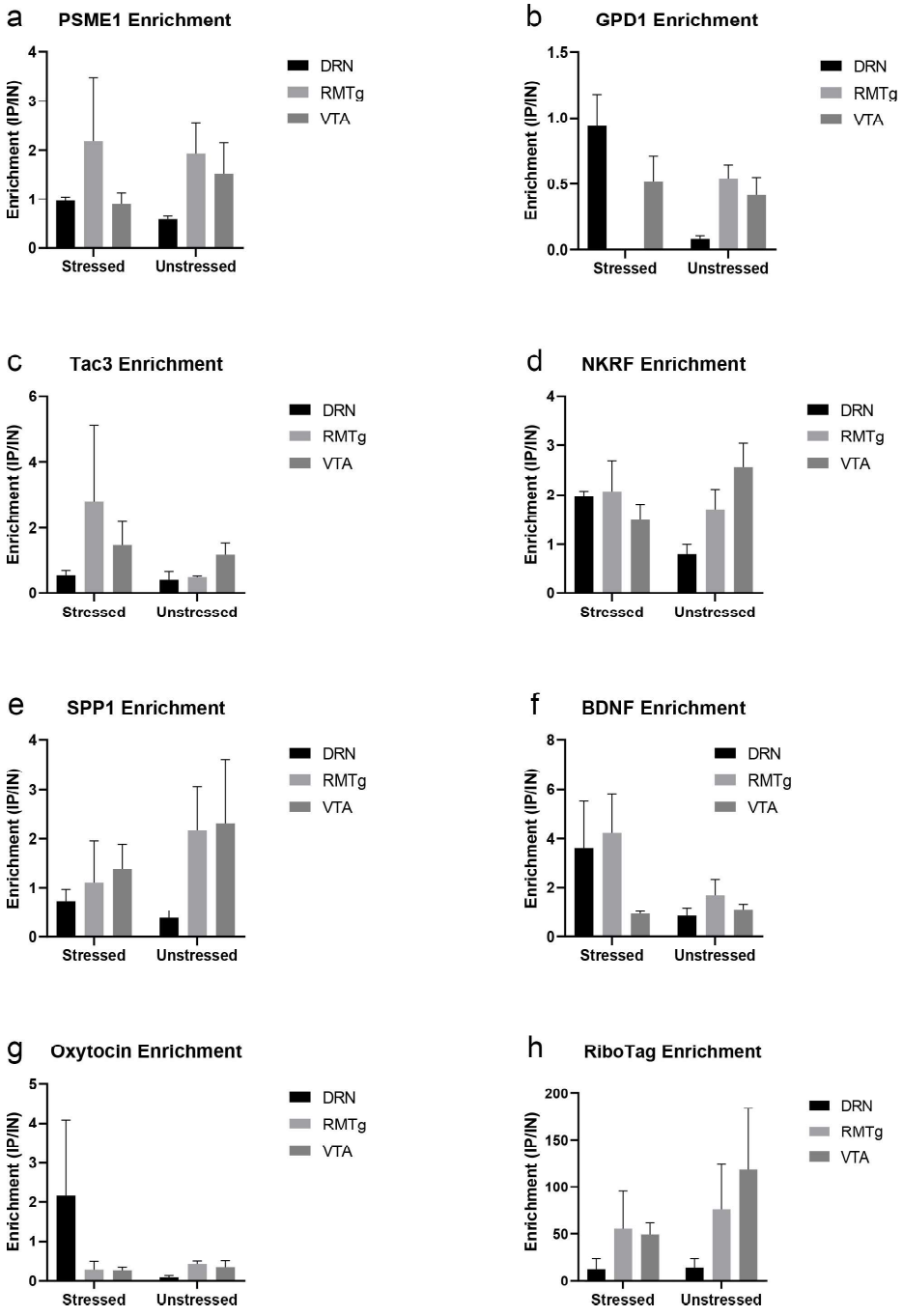

Supplemental Figure 2: RTqPCR validation of gene targets. a) Enrichment of PSME1 in each pathway. b) Enrichment of GPD1 in each pathway. c) Enrichment of Tac3 in each pathway. d) Enrichment of NKRF in each pathway. e) Enrichment of SPP1 in each pathway. f) Enrichment of BDNF in each pathway. g) Enrichment of Oxytocin in each pathway. h) Enrichment of RiboTag in each pathway.

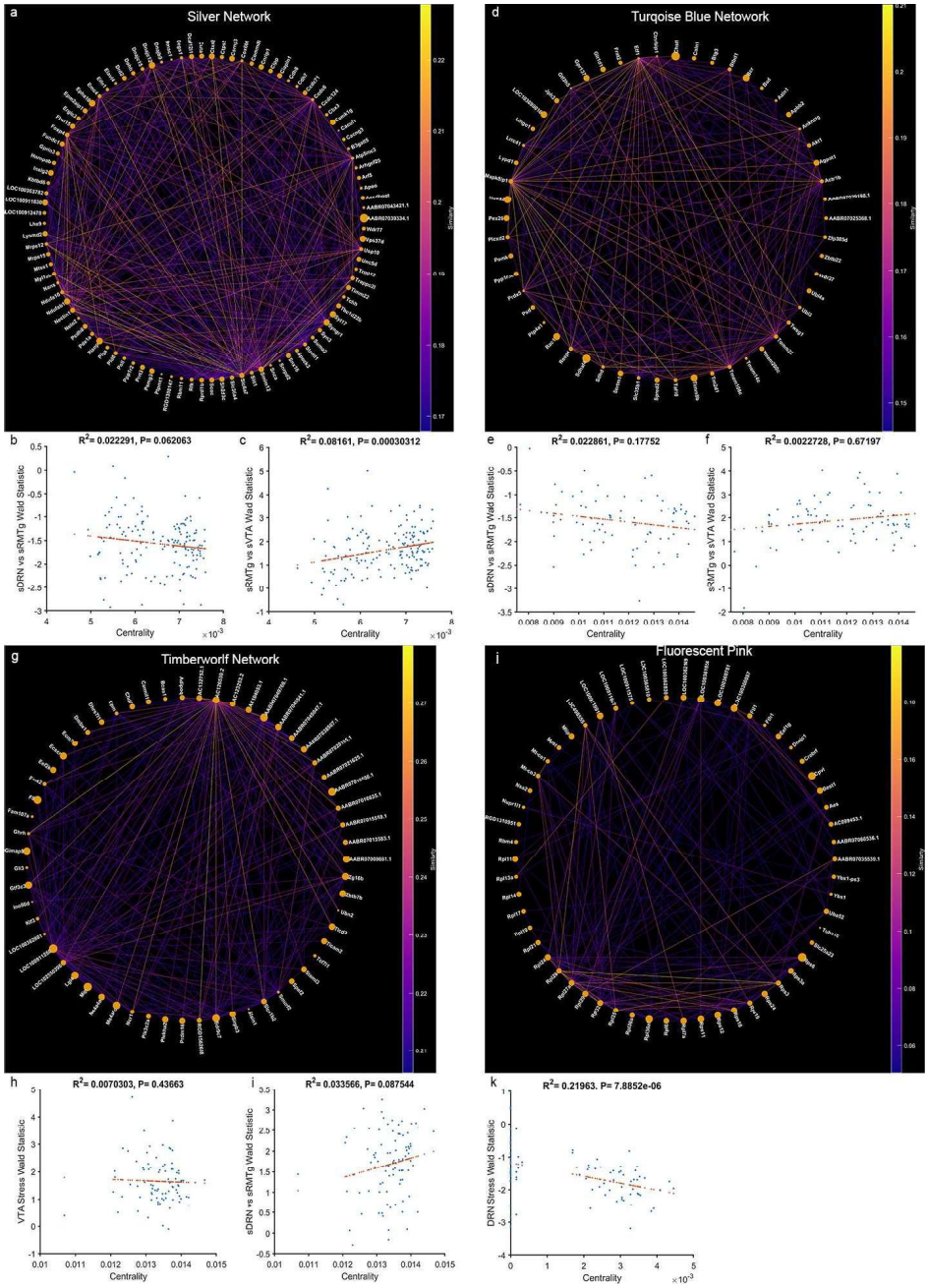

Supplemental Figure 3: Networks passing the 1.5 threshold. a) Silver network circular graph. b) Correlation of centrality of gene with the sDRN vs sRMTg Wald statistic for the Silver network. c) Correlation of centrality of gene with the sRMTg vs sVTA Wald statistic for the Silver network. d) Turquoise Blue network circular graph. e) Correlation of centrality of gene with the sDRN vs sRMTg Wald statistic for the Turquoise Blue network. f) Correlation of centrality of gene with the sRMTg vs sVTA Wald statistic for the Silver network. g) Timberwolf network circular graph. h) Correlation of centrality of gene with the VTA Stress Wald statistic for the Timberwolf network. i) Correlation of centrality of gene with the sDRN vs sRMTg Wald statistic for the Timberwolf network. j) Fluorescent Pink network circular graph. k) Correlation of centrality of gene with the DRN Stress Wald statistic for the Fluorescent Pink network.

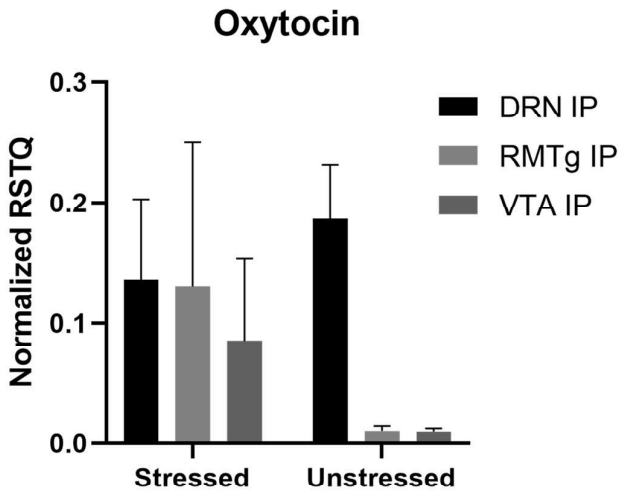

Supplemental Figure 4: Relative Starting Quantity for Oxytocin. Oxytocin expression in each pathway normalized to fourhousekeeping genes.

Chapter 3: PACAP-expressing neurons in the lateral habenula are a diverse neuronal set that diminish negative emotional valence

Marjorie R Levinstein[a,b], Zoë K Lewis[c], Alex Tsobanoudis[c], Koichi Hashikawa[d,e,f], Garret D Stuber[d,e,f], John F Neumaier[a,b,e,f]

[a]*Graduate Program in Neuroscience,*
[b]*Department of Psychiatry and Behavioral Sciences*
[c]*Department of Biology*
[d]*Department of Anesthesiology and Pain Medicine*
[e]*Center for Neurobiology of Addiction, Pain, and Emotion*
[f]*Department of Pharmacology*
University of Washington, Seattle, Washington, USA

Abstract

The lateral habenula (LHb) is a small nucleus which processes aversive information. While primarily glutamatergic, LHb neurons express numerous neuropeptides, such as pituitary adenylate cyclase-activating polypeptide (PACAP), which itself has been associated with anxiety and stress disorders. Using Cre-dependent viral vector expression, we characterized these neurons based on their anatomical projections and found that they projected to raphe and rostromedial tegmentum but not ventral tegmental area. Using RiboTag to capture ribosomal-associated RNA from these neurons and reanalysis of existing single cell RNA sequencing data, we did not identify a unique molecular phenotype that characterized these PACAP-expressing neurons in LHb.

In order to understand the function of these neurons, we chemogenetically excited PACAP-expressing neurons using virally-mediated gene transfer of DREADDs in PACAP-Cre mice and tested the mice using open field test, contextual fear conditioning, sucrose preference, novelty suppressed feeding, and conditioned place preference. We found that activating these neurons produce behaviors opposite to what is expected from the LHb as a whole – they decreased

anxiety-like and fear behavior and produced a conditioned place preference. In conclusion, PACAP-expressing neurons in LHb represents a unique population of cells that oppose the actions of the remainder of LHb neurons by being rewarding or diminishing the negative consequences of aversive events.

---

1. Introduction

The lateral habenula (LHb) is a small, bilateral epithalamic nucleus that borders the more diverse medial habenula, projects to a variety of targets, responds to aversive stimuli and promotes avoidances of future adverse events [1–4]. In general, stimulation of LHb neurons promotes passive avoidance [4, 5] while inhibiting the LHb, or its connections to DRN, VTA or RMTg, reduces anxiety- and depression-like behaviors [6–9]. Using virally mediated gene transfer of the inhibitory DREADD receptor, hM_4Di, we found that inhibiting LHb decreases passive coping in the forced swim test (FST), a measure of behavioral despair, in rats [10]. Furthermore, the LHb neurons projecting to the DRN appear to be responsible for this behavioral effect [11].

The LHb receives afferents from throughout forebrain and is thought to act as a key integrator of information about aversive events that shapes decisions regarding approach or avoidance of similar stimuli in the future. LHb outputs modulate dopaminergic and serotonergic function and is involved in updating outcome predictions that impact behavioral stability or flexibility [12]. Inactivation of the LHb causes trained rats to perform at a chance level in a tone-directed maze task, indicating the LHb's involvement in adaptive learning and decision making [13]. Lesions of the LHb significantly decreased a win-stay strategy but did not affect lose-shift strategy in a competitive choice task [14]. Additionally, the LHb has been found to be involved in fear learning and memory

[15]. Chemogenetic inhibition of rat LHb during conditioning reduced subsequent freezing to contextual cues, but increased freezing in response to discrete cues associated with an aversive stimulus (footshock) [15]. Thus, LHb has numerous impacts that can shift the pattern of conditioned responses and decision making in the face of potential aversive outcomes.

Physiological responses in the LHb are fairly heterogeneous. In the absence of threats, LHb neurons are relatively inactive, firing at roughly 5 Hz [16], but LHb bursts in response to aversive stimuli such as restraint stress [17–19]. Stress exposure activates LHb neurons intensely and induces c-Fos, a marker of neuronal activity [20], and chronic unpredictable stress increases firing rates [16]. However, different LHb neurons respond diversely to the same stimulus—about 30% of neurons in the LHb are activated by inescapable footshock [1], many do not respond at all and roughly 10% of neurons, mostly in the medial region of the LHb, are inhibited by footshock [17]. The basis for these distinctions in responses to stress are not yet understood.

Molecular diversity between LHb neurons has been identified in several ways. First, LHb neurons that project to three primary targets, dorsal raphe nucleus (DRN), ventral tegmental area (VTA), and rostromedial tegmental nucleus (RMTg) are highly segregated with minimal collateral branching [3, 21–25]. Using intersectional expression of RiboTag to immunopurify ribosome-associated mRNAs selectively from each of these pathways in rats, we identified only small differences between the neurons comprising these three pathways, suggesting that the regional target of LHb neurons is not defined by distinctions in neuronal phenotype [26]. LHb neurons are mostly glutamatergic, but numerous neuropeptides are also expressed in these neurons and these may be important in generating different patterns of output activity [27]. Recent gene

array and single cell RNA sequencing studies in mice identified several clusters of similar neurons within LHb, but these were not segregated into anatomical regions or pathways targeting distinct brain regions. Nevertheless, these modules of neurons with distinct patterns of gene expression may still have functional implications [28]. For example, a sparsely distributed population of neurons located in the rostromedial region of the LHb expresses pituitary adenylate cyclase-activating polypeptide (PACAP, encoded by the *Adycap1* gene), which is expressed in several brain regions and is particularly abundant in stress-associated nuclei [29, 30]. PACAP has been implicated in both stress and addiction [31, 32]. It regulates cellular signaling, protects from oxidative stress, and has organism-wide effects, such as activating the hypothalamic-pituitary-adrenal hormone system in response to stress [33] although previous studies have focused on other brain areas, such as the extended amygdala. Chronic stress increases PACAP expression in the bed nucleus of the stria terminalis, a brain region associated with anxiety [34]. Moreover, PACAP infusion increases freezing and other anxiety-like behaviors [35, 36]. A single nucleotide polymorphism of the cognate receptor for PACAP, *Adcyap1r1*, is associated with increased likelihood of developing posttraumatic stress disorder in adult women and female children [37, 38]. However, the effect of PACAP in LHb on stress-related behaviors has not been investigated.

Therefore, in this study, we examined PACAP neurons in LHb in greater detail using a combination of transgenic PACAP-promoter Cre mice injected with a viral vector carrying a floxed hM_3Dq DREADD receptor, allowing precise chemogenetic activation of PACAP neurons in LHb. We found that these neurons do not represent a distinct cluster of molecularly unique cells but chemogenetic activation of these neurons produced a paradoxical pattern of conditioned place

preference and reduced fear and anxiety-associated behaviors.

2. Materials and Methods

2.1 Animals

Adcyap1-2a-Cre recombinase (PACAP-Cre) transgenic mice (C57BL/6 background) [39] were bred to C57BL/6 wildtype mice creating PACAP-Cre and wildtype littermates. Litters were genotyped, and only transgenic mice were used except for 6 wildtype littermates that were used as negative controls for RiboTag expression; males and females were housed in separate cages. One hundred and eleven PACAP-Cre mice were placed in groups that were age matched with littermate controls. Mice ranged in size from 25 to 30 gm and were between 3 and 6 months old at the time of experiments. Mice were group housed and fed ad libitum. Experiments were performed in compliance with the Guide for the Care and Use of Laboratory Animals (NIH, 1985; Publication 865–23) and were approved by the Institutional Animal Care and Use Committee, University of Washington. Live decapitation was used for RiboTag RNA Isolation procedures, while paraformaldehyde (PFA) perfusion was conducted for immunohistochemistry.

2.2 Surgical Procedures

For stereotaxic surgeries, anesthesia was induced with 3% isoflurane/97% oxygen and maintained at 1% isoflurane during the surgical procedure. Using a custom robotic stereotaxic instrument [40], mice were injected with AAV8-DIO-hM$_3$Dq-2a-RiboTag (n=32), AAV8-DIO-hM$_3$Dq-mcherry (n=10), a 50/50 combination of AAV8-DIO-hM$_3$Dq-mcherry and AAV8-hSyn-DIO-RiboTag (n=13), AAV8-hSyn-DIO-RiboTag alone (n=44), or AAV1-DIO-Synaptophysin-GFP (n=3) into LHb. Blunt 28g needles were inserted bilaterally, terminating at

A/P -1.85, M/L ±0.35, and D/V −2.59, and 0.5 μl of the virus was injected at a rate of 0.2 μl/min. The needle was left *in situ* for 5 minutes post-injection then slowly withdrawn. After surgeries, mice were given meloxicam (0.5 mg/kg, s.c.) for analgesia and monitored daily for at least 3 days. Accuracy of injection coordinates was confirmed by RTqPCR detection of RiboTag and Cre RNAs from LHb homogenate; these injection volumes and coordinates were optimized to produce selective transduction of LHb neurons with minimal expression adjacent regions.

2.3 Plasmid and reagents

The hSyn-hM$_3$Dq-2A-RiboTag construct was generated using Gibson Assembly (NEB, Ipswich, MA) following PCR amplification of hM$_3$Dq sequence from pAAV-hSyn-DIO-hM$_3$D(Gq)-mCherry (Plasmid #44361, Addgene, Cambridge, MA); sequence fidelity was confirmed by sequencing. The 2A-skip sequence (ATNFSLLKQAGDVEENPGP) and RiboTag construct were PCR amplified from pcDNA3-hSyn-mRuby2-2A-RiboTag [41]. The flag sequence was (DYKDDDDK) was created using overlapping oligonucleotides. The final viral construct was sent to the Fred Hutchinson Cancer Research Center Co-Operative Center for Excellence in Hematology Vector Production Core and was packaged in an adeno-associated virus 8(AAV8) capsid. Clozapine-N-Oxide (CNO) was provided by the NIMH Chemical Synthesis Program.

2.4 Anterograde tracing

Three males PACAP-Cre mice were injected with AAV1-DIO-Synaptophysin-GFP and allowed to rest for 3 weeks for gene expression to develop. Mice were deeply anesthetized with Beuthanasia-D (diluted by 50% in saline, 4ml/kg *ip*, Merck Sharp & Dohme Corp) and perfused with ice cold physiological saline,

followed by 4% PFA in PBS. Brains were then extracted and stored in 4% PFA in PBS overnight, followed by cryoprotection in 30% sucrose. Brains were then sliced at 40 μm in preparation for immunohistochemistry. Slices were incubated in 4% BSA and 0.03% triton in PBS blocking solution for 1 h at room temperature. Rinses were performed between each step 3 × 15 min in PBS. Slices were incubated in primary antibodies diluted at 1:500 for chicken anti-GFP (ABCAM 13970) and slices which contained the DRN were also incubated in primary antibodies diluted at 1:500 for sheep anti-TPH2 (Millipore #2453653; Darmstadt, Germany) in blocking buffer overnight at 4 °C. For negative controls, primary antibodies were omitted from the incubation. Tissues were washed and then incubated in 5 μg/ml Alexa Fluor 488 anti-chicken (Thermo Fisher # A-11039; Waltham, MA), and DRN slices were also incubated with Alexa Fluor 568 anti-sheep (Thermo Fisher #A-21099; Waltham, MA).

2.5 Imaging

Dual-channel (GFP, excitation 450-490, emission 500-550; DAPI, excitation 335-383, emission 420-470) images were collected on a high-content fluorescent microscopy system (Zeiss Axio Imager M2, constant exposure settings for all experiments) using a 20x objective. All images were collected using Axiocam MRC camera.

2.6 Ribotag extraction

RiboTag-associated RNA extraction as previously described [26, 42, 43]. The LHb was extracted using a 3mm punch and homogenized in 1mL of supplemented homogenizing buffer [S-HB, 50 mM Tris-HCl, 100 mM KCl, 12 mM MgCl2, 1% NP40, 1 mM DTT, 1× Protease inhibitor cocktail (Sigma-Aldrich), 200 U/mL RNasin (Promega, Madison, WI), 100 μg/mL

cyclohexamide (Sigma-Aldrich), 1 mg/mL heparin (APP Pharmaceuticals, Lake Zurich, IL)]. Samples were centrifuged at 4°C at 11,934 × g for 10 min, and supernatant was collected, reserving 50 μL (10%) as an input fraction. Mouse monoclonal HA-specific antibody (2.5 μL) (HA.11, ascites fluid; Covance, Princeton, NJ) was added to the remaining supernatant, and RiboTag-IP fractions were rotated at 4°C for 4 h. Protein A/G magnetic beads (200 μL) (Pierce) were washed with Homogenizing Buffer (HB 50 mM Tris-HCl, 100 mM KCl, 12 mM MgCl2, 1% NP40) prior to addition to the RiboTag-IP fraction and were rotated at 4°C overnight. The next day, RiboTag-IP fractions were placed on DynaMag-2 magnet (Life Technologies), and the bead pellet was washed 3 times for 15 min with high salt buffer (HSB; 50 mM Tris, 300 mM KCl, 12 mM MgCl2, 1% NP40, 1 mM DTT, and 100μg/mL cyclohexamide) and placed on a rotator. After the final wash, HSB was removed and beads were re-suspended in 400 μL supplemented RLT buffer (10 μL β-mercaptoethanol/10 mL RLT Buffer) from the RNeasy Plus Micro Kit (Qiagen, Hilden, Germany) and vortexed vigorously. These samples were then placed back on the magnet and the RLT buffer was removed from the magnetic beads prior to RNA extraction. 350 μL supplemented RLT buffer was added to the Input Fraction prior to RNA extraction. RNA from the Input Fraction was extracted using Qiagen RNeasy Plus Mini kit (Qiagen, Hilden, Germany) and RNA from the RiboTag-IP fration was extracted using Qiagen RNeasy Plus Micro kit according to package directions. Input RNA was eluted with 40μl of water and RiboTag-IP RNA was eluted with 14-16μl of water. RNA concentration was measured using Quant-iT RiboGreen RNA Assay (ThermoFisher Cat. R11490, Waltham, MA).

2.7 RT-qPCR Analysis

The RNA was reverse transcribed to create cDNA libraries for qPCR using Superscript VILO Master Mix (ThermoFisher Cat. 11754050, Waltham, MA), and then cDNA libraries were diluted to a standard concentration before running the qPCR assay using Power Sybr Green on QuantStudio 7 Real-Time PCR System (Thermo Fisher). qPCR analysis was conducted using the standard curve method and normalized to four housekeeping genes (*Gapdh*, *Ppia*, *Hprt*, and *Actinb*). Normalized RSTQ data was analyzed using ANOVA with the Bonferroni post-hoc test. Neuronal activation and pulldown were determined using primers specific for cFos, RiboTag, and Cre recombinase. Genes of interest were determined from clusters determined by integrative expression matrices of scRNAseq data [28]. *Adcyap1* was most commonly expressed in LHb5 and LHb1 clusters. Clusters and *Adcyap1* expression are visualized using Uniform Manifold Approximation Projection (UMAP). The genes from these clusters with the most (*Lbhd2*, *Dlgap1*, and *Rgs4*) and least (*Id4*, *Sncg*, and *Nek7*) overlap of cells expressing *Adcyap1* were tested.

2.8 Behavioral experiments

2.8.1 Open field.

PACAP-Cre Mice that received an injection of AAV8-DIO-hM$_3$Dq-mcherry were given an injection of CNO (n=5) or vehicle (n=5) 30 minutes prior to placement in the open field chamber (50cmx50cm). The mice were allowed to freely explore the chamber while being video recorded for 20 minutes. Ninety minutes after the CNO or vehicle injection, mice were perfused and tissue treated as described below. Videos were scored using Ethovision.

2.8.2 Sucrose preference.

PACAP-Cre mice that received an injection of AAV8-DIO-hM$_3$Dq-2a-RiboTag (n=20) or AAV8-DIO-RiboTag (n=18) were placed in 2-bottle choice lickometer

chambers for 3 h and given free access to a bottle of water and a bottle of 2% sucrose solution to allow for habituation. The next day, mice received an injection of CNO or Vehicle 30 minutes prior to being placed back inside the two-bottle choice lickometer chambers for 3 h and given free access to a bottle of water and a bottle of 2% sucrose solution. Sucrose and water bottle sides were counterbalanced between animals, and licks were automatically counted.

2.8.3 Novelty suppressed feeding.

This procedure was performed as described [44, 45] in PACAP-Cre mice injected with either AAV8-DIO-hM$_3$Dq-2a-RiboTag (n=20) or AAV8-DIO-RiboTag (n=18). The testing chamber was a plastic box (50 × 50 × 20 cm), the floor of which was covered with approximately 2 cm of corncob bedding, with illumination of 1200 lux. 18 h before behavioral testing, all food was removed from the home cage. At the time of testing, a single pellet of food was placed on a white paper platform in the center of the box and secured with a rubber band. The mouse was placed in a corner of the box and a stopwatch was immediately started. The latency to eat (defined as the mouse sitting on its haunches and biting the pellet with the use of forepaws) was timed. Mice were in the testing arena for a total of 8 min. Immediately after the testing period, the mice were transferred to their home cages, and the amount of food consumed by the mouse in the next 5 min was measured. Each mouse was weighed before food deprivation and before testing to assess the percentage of body weight loss.

2.8.4 Contextual fear conditioning.

Behavior was performed three to four weeks after viral vector infusion (either AAV8-DIO-hM$_3$Dq-2a-RiboTag (n=32), or AAV8-DIO-hM$_3$Dq-mcherry + AAV8-DIO-RiboTag (n=13), or AAV8-DIO-RiboTag(n=44)). Acquisition of fear memory

was conducted in four identical chambers (21.6 × 17.8 × 12.7 cm; Med Associates) placed inside sound-attenuating boxes. Each chamber was made of two aluminum and two Plexiglas side walls. The floor consisted of 24 stainless steel rods which were wired to a scrambled shock generator. To add a context-specific odor, the chamber was cleaned with a 1% acetic acid solution between mice and a stainless-steel pan containing the same solution was placed under the grid floor [46]. For fear training, mice were placed in the middle of the test cage and allowed to acclimate for two minutes, then received three 1s, 0.6 mA footshocks at two-minute intervals. Following the third and final footshock, mice remained in the test cage for an additional minute before being returned to their home cage. After 24 h, mice were placed back in the test cage for a five-minute test session. Training and testing sessions were digitally recorded, and freezing was analyzed by reviewing the recorded sessions offline.

2.8.5 Conditioned place preference.

PACAP-Cre mice, with either AAV8-DIO-hM$_3$Dq-2a-RiboTag (n=11) or AAV8-DIO-hM$_3$Dq-mcherry + AAV8-DIO-RiboTag (n=13) for experimental mice and AAV8-DIO-RiboTag (n=25) for control mice were tested for preference or aversion to CNO in a two-chamber apparatus with distinct visual and tactile cues as described previously [47]. All conditioning and testing sessions lasted 30 min and were recorded on video for analysis in Ethovision version 3.0 (Noldus). On day 1 (pretest), mice freely explored each side of the apparatus. Total time on each side was calculated and mice were then conditioned with CNO (3 mg/kg) paired on either the preferred or not preferred side in a balanced (unbiased) manner. On days 2 and 3 (conditioning), mice were confined to one side with saline treatment and, >4 h later, confined to the other side starting five

minutes after CNO administration. On day 4, mice were allowed to freely explore each side of the apparatus and time spent on the drug-paired floor during the test was measured. Preference score was determined by subtracting time on the drug-paired compartment during posttest from time on the drug-paired compartment during pretest (post – pre).

3. Results

3.1 Fiber tracing

There are three dominant output pathways from LHB: to the DRN, VTA, and RMTg. Therefore, we injected three male PACAP-Cre mice with AAV1-DIO-Synaptophysin-GFP bilaterally into the LHb to evaluate the projection pattern for these neurons (Figure 1A). Anterograde tracing indicated that PACAP expressing LHb neurons project to the DRN (Figure 1B) and the RMTg (Figure 1C) but not to the VTA (Figure 1D).

3.2 Molecular characterization of PACAP neurons

Since PACAP-expressing neurons did not segregate into a single projection pathway, we next considered whether these neurons mapped onto a clustering scheme derived from single cell RNAseq (scRNAseq) from our recent report [28]. Using UMAP, we projected PACAP-positive neurons onto the existing clustering distribution. As shown in Figure 2A, most of the PACAP-positive neurons mapped to clusters LHb1 and LHb5, although there were some PACAP-positive neurons in the other clusters as well. We next injected AAV8-DIO-RiboTag virus into LHb of PACAP-cre mice so that we could retrieve ribosome-associated RNAs that were actively being translated by PACAP-expressing neurons. Using RTqPCR, we examined several RNA targets chosen for their relative enrichment or deenrichment in LHb1 and LHb5 neuron clusters as

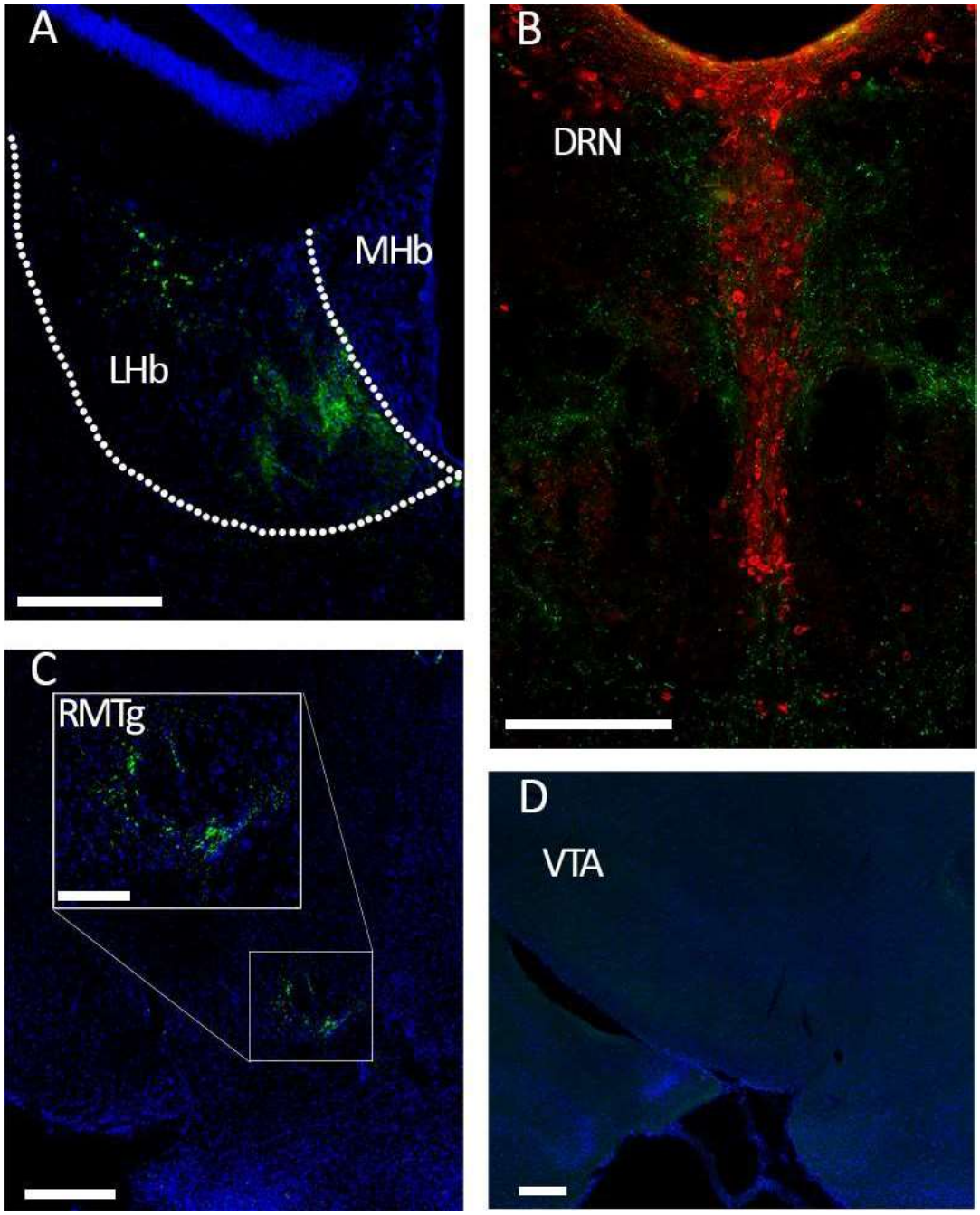

Figure 1: PACAP neurons in the LHb project to DRN and RMTg, but not VTA. AAV1-DIO-Synaptophysin-GFP was injected into LHb of PACAP-Cre mice to express GFP in terminals of infected neurons (green) (A). Sections containing the DRN (B) were co-stained for TPH2 (red). Synaptophysin terminals can be seen in both the raphe nuclei (especially the lateral aspects) and RMTg (C), but not the VTA (D). All scale bars represent 250μM except for the inset in (C) which represents 100μM.

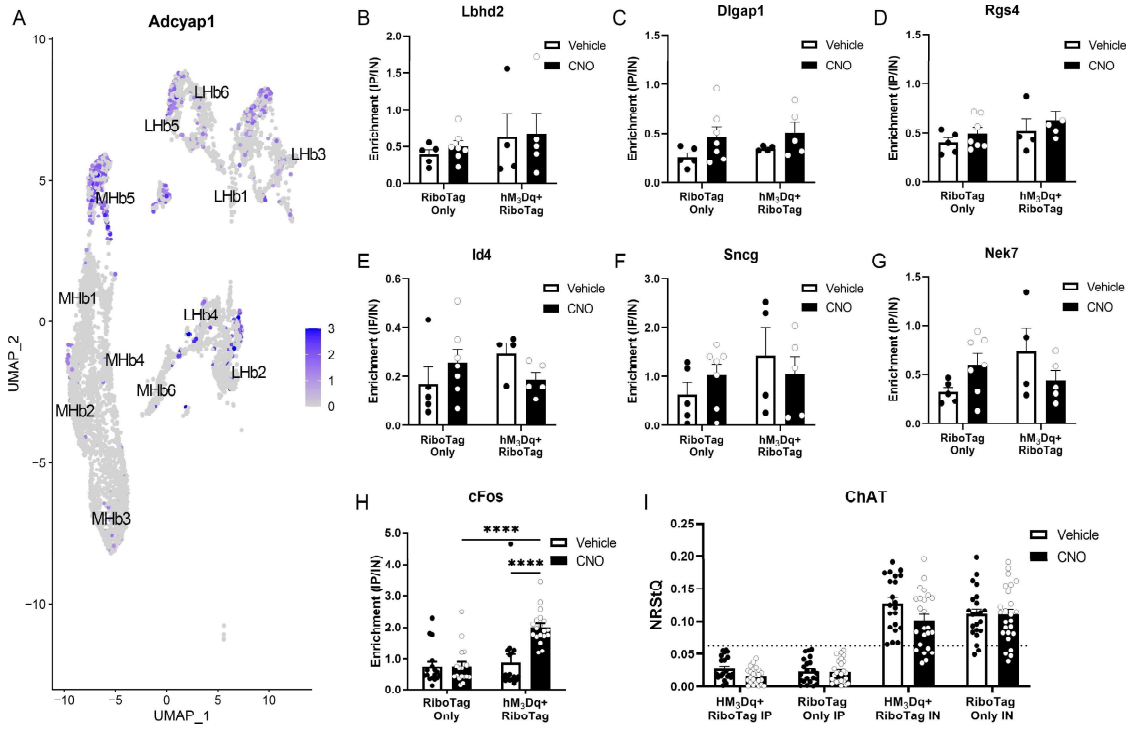

Figure 2: PACAP is expressed across multiple phenotypically clustered LHb neurons. (A) UMAP plot of PACAP expressing neurons (displayed in purple) shows that PACAP expression is distributed across the six clusters of LHb neurons defined by scRNAseq. Scale bar represents relative expression. By expressing RiboTag in LHb PACAP-Cre neurons, we examined severalgenes that were strongly associated with neurons that expressed PACAP in the scRNAseq dataset–Lbhd2(B), Dlgap1(C), and Rgs4 (D), although these were not uniquely enriched in PACAP-expressing neurons relative to the input RNA in the tissue punches. Genes that were predicted to be deenriched in PACAP neurons based on the scRNAseq data were also tested—Id4 (E), Sncg (F), and Nek7 (G)were also not enriched. In all of these cases we examined both PACAP-RiboTag-only mice and PACAP-hM3Dq mice after treatment with vehicle or CNO (3mg/kgip) the previous day and observed no significant effect of DREADD activation on gene expression or effect of CNO in mice lacking hM3Dq. However, CNO 50 minutes prior to sacrifice increased cFos expression dramatically in PACAP-hM3Dq mice but not PACAP-RiboTag only mice (H), indicating that both the Gq DREADD receptor and the RiboTag protein were functionally expressed in these neurons. ChAT expression was below the limit of our standard curve (dotted line) in the IP samples, but not their corresponding inputs (I).

compared to the other clusters (Figure 2B-G). None of these RNAs were especially enriched in RiboTag purified RNA from PACAP-Cre neurons as compared to the input RNA from the tissue punches; however, Id4 (Figure 2E) was actually deenriched relative to the input RNA, suggesting that it is less abundant in PACAP neurons in LHb. Thus, we conclude that PACAP-expressing neurons do not map tightly onto a specific phenotypic cluster of LHb neurons as defined by scRNASeq. Furthermore, stimulation of hM_3Dq with CNO the previous day did not alter the overall pattern of expression of these RNAs (Figure 2B-G). Since the MHb5 cluster also contains PACAP-expressing neurons, we tested whether choline acetyltransferase (ChAT) was detectable in the mice which we injected with RiboTag virus; ChAT RNA in the RiboTag IP samples was very low and below the lowest concentration on our standard curve (Figure 2I); this indicated that our injection procedures were well targeted and specific for LHb over MHb. Together, these results suggest that PACAP-expressing neurons in LHb are widely distributed and not restricted to a narrow cluster of neurons with a discrete phenotype, although they do not project to VTA.

3.3 Chemogenetic activation of LHb PACAP neurons

We tested the effects of activating hM3Dq, the Gq-coupled DREADD receptor [48, 49], when selectively expressed in LHb PACAP neurons. PACAP hM_3Dq mice were sacrificed 50 minutes after an injection of CNO, had significantly more cFos mRNA expression and enrichment than other groups (Interaction: $F_{1,67}=10.77$, $p=0.0016$; hM_3Dq CNO vs hM_3Dq Vehicle ($t(67)=4.697$, $p<0.0001$; vs RiboTag only CNO $t(67)=5.242$, $p<0.0001$; Figure 2H). In this and the behavioral chemogenetic experiments, sex differences were investigated by two-way ANOVA; none were found therefore males and females were combined and

analyzed together.

3.4 Behavioral testing after chemogenetic activation of LHb PACAP neurons

3.4.1 Open field

Mice which had hM_3Dq expressed in their LHb PACAP neurons (PACAP-hM_3Dq mice) had significantly more locomotion after treatment with CNO than those treated with vehicle ($t(8)=4.264$, $p=0.0027$; Figure 3A-C); they also spent significantly less time in the corners ($t(8)=2.433$, $p=0.0410$) after CNO (3mg/kg ip) as compared to vehicle (Figure 3D). There were no significant differences in locomotion, center or corner time between males and females.

3.4.2 Contextual fear conditioning

In the contextual fear conditioning test, when comparing males and females, there were no sex differences; therefore, the sexes were combined, and groups were analyzed together. On conditioning day, there were no differences with virus or treatment (Figure 3E). However, on test day, there was a significant Treatment x Virus interaction ($F_{1,78}=13.25$, $p=0.0005$) (Figure 3F). PACAP-hM_3Dq mice treated with CNO (3 mg/kg ip) froze significantly less than those treated with vehicle ($t(78)=4.366$, $p=0.0002$) or mice injected with AAV8-DIO-RiboTag (PACAP-RiboTag only mice) given CNO ($t(78)=3.234$, $p=0.0107$).

3.4.3 Conditioned place preference

PACAP-hM_3Dq mice had a stronger preference for CNO paired side than PACAP-RiboTag only mice $t(41)=3.7302$, $p=0.0006$ (Figure 4A). However, when performing a 2-way ANOVA including sex as a variable, there was a significant Sex x Virus interaction ($F_{1,44}=10.73$, $p=0.0148$). Male hM_3Dq mice had a higher preference score than Male RiboTag only mice ($t(44)=3.202$, $p=0.0152$); Male RiboTag only mice had lower preference scores than Female RiboTag only mice ($t(44)=3.182$,$p=0.0161$). Thus, it seems that the Male

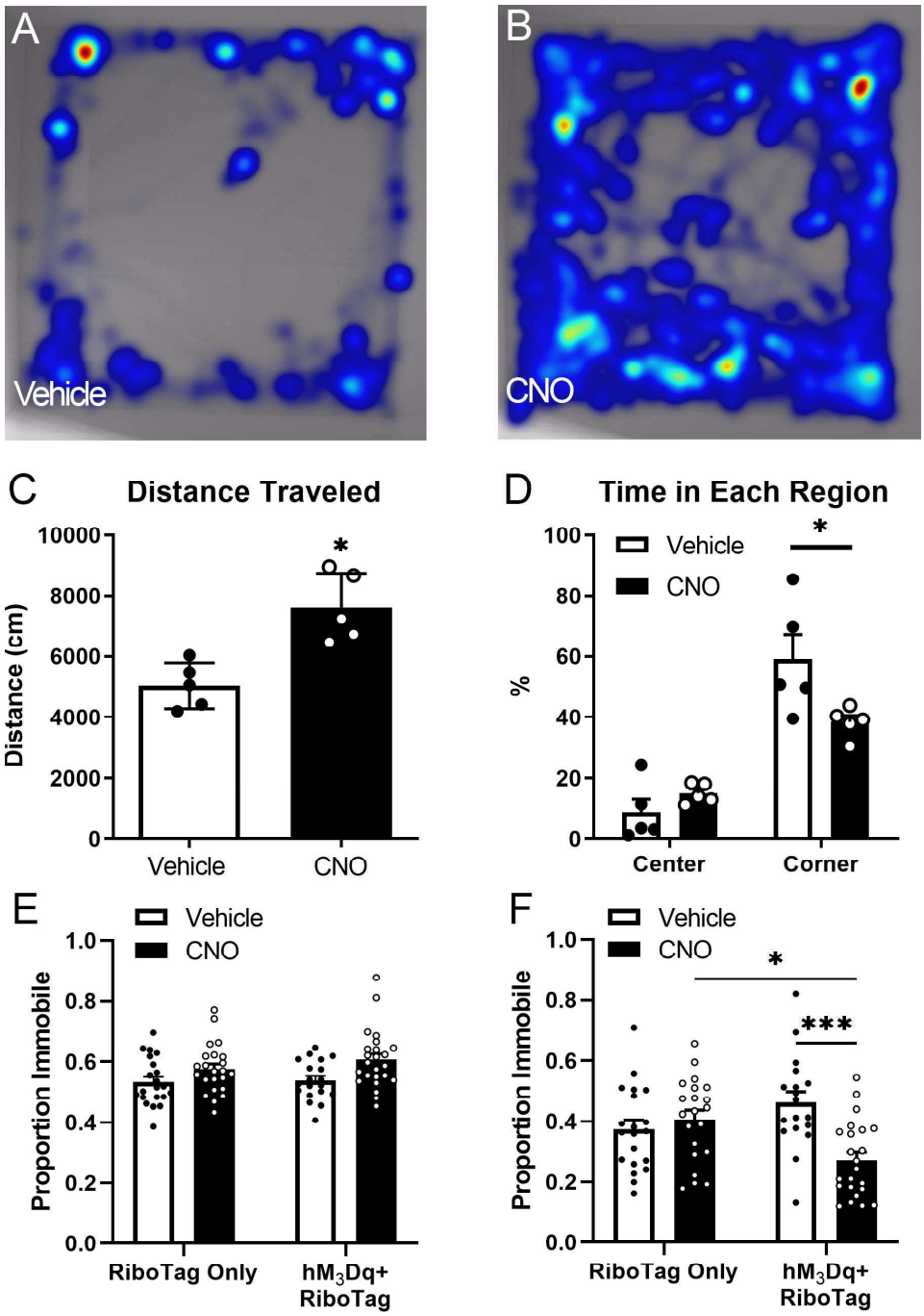

Figure 3: Activation of PACAP-expressing neurons in the LHb reduces anxiety and fear behaviors. Representative heatmaps of individual mouse position within the open field from PACAP-hM3Dq mice treated with vehicle (A) or CNO (3mg/kg ip) (B); the heatmap colors indicate time spent at a particular position ranging from blue (least) to red (most). Mice that were injected with CNO travelled a significantly greater distance (C) and spent less time in the corners (D). PACAP-hM3Dq mice and PACAP-RiboTag only mice treated with vehicle or CNO show similar levels of freezing during the conditioning session in contextual fear conditioning (E), but PACAP-hM3Dq mice showed reduced freezing in when given CNO compared to vehicle or PACAP-RiboTag only mice (F). *p<0.05, ***p<0.001

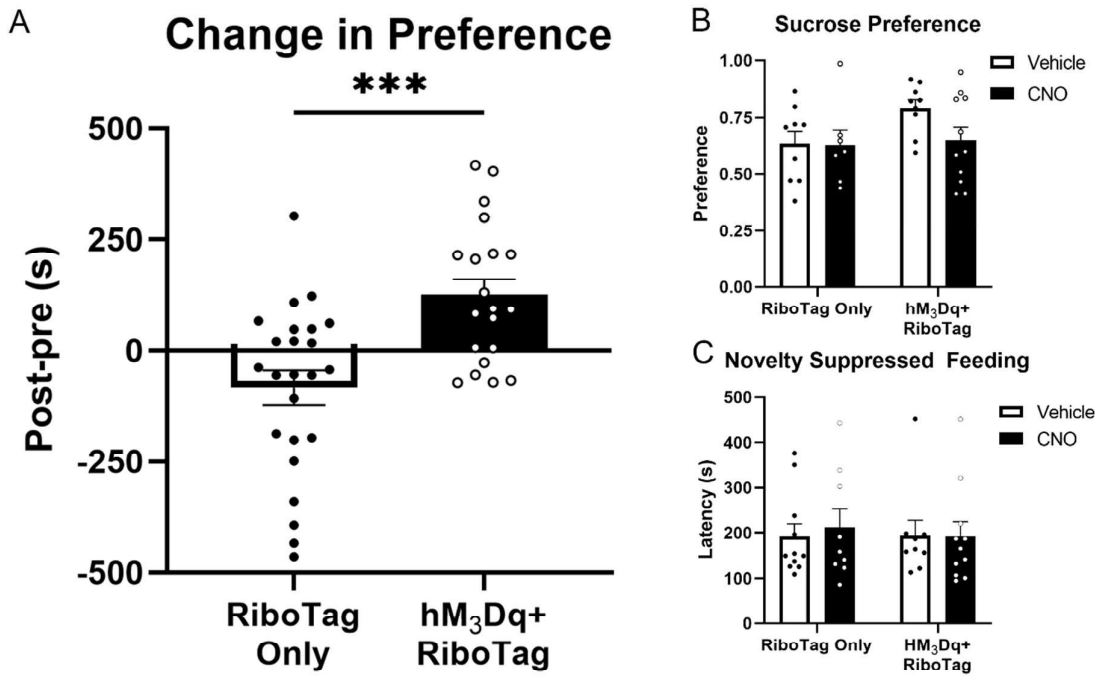

Figure 4: Activation of PACAP-expressing neurons in the LHb increases appetitive behavior but does not change hedonic state. PACAP-hM3Dq mice spent significantly more time in the CNO paired side than PACAP-RiboTag only mice, this is driven by male PACAP-RiboTag only mice (A). PACAP-hM3Dq mice or PACAP-RiboTag only mice did not differ in sucrose preference with or without CNO (B), or latency to eat in the novelty suppressed feeding test (C). *p<0.05

RiboTag Only mice are driving the total effect.

3.4.4 Sucrose preference and Novelty Suppressed Feeding

There were no differences between males and females in either of these behaviors, so sexes were combined and analyzed together. PACAP hM_3Dq or PACAP RiboTag only mice displayed no differences in sucrose preference with or without CNO (Figure 4B). Nor did they display any differences in latency to bite the pellet (Figure 4C) or homecage feeding (not shown) in the novelty suppressed feeding test.

4. Discussion

In this report we used viral vectors to express DREADD receptor and RiboTag conditionally in PACAP-Cre expressing neurons in LHb to investigate their role in the control of emotional behaviors. In these experiments we found that chemogenetic activation of LHb PACAP neurons increased locomotion, reduced anxiety-like behavior, reduced fear-learning, and may be modestly rewarding. These results are directly opposite of the published or predicted results for LHb neurons in general. However, activating these neurons did not affect neophobia in the novelty suppressed feeding test, nor did it affect hedonic valence as tested in the sucrose preference test. These results indicate these neurons may be behaving paradoxically compared to the LHb as a whole.

Recently, the LHb was found to be involved in fear memory [15]. Indeed, Durieux and colleagues (2020) [15] found that neurons in the rostral and medial LHb had increased cFos expression after fear conditioning compared to rats which remained in their homecage (rats exposed to tone and chambers also had increased cFos expression). Chemogenetic inhibition of the LHb prior to

conditioning altered conditioned fear later by reducing freezing to contextual cues but increasing freezing when the conditioned stimulus tone was presented in a new context. We found that activating LHb PACAP neurons during conditioning also decreased freezing when contextual cues were presented during the test session, which is consistent with these neurons playing a distinct role compared to LHb neurons in general.

In addition, we investigated the anatomical projections and genetic profile of PACAP-expressing neurons in LHb. We found that these neurons project to the raphe and RMTg, but not the VTA. Thus, these neurons are not specific to one pathway. Interestingly, our data indicate that PACAP-expressing LHb neurons tend to project mainly towards the lateral part of the dorsal raphe and the medial raphe nuclei where GABAergic interneurons reside; this suggests but does not prove that PACAP neurons in LHb can activate GABAergic interneurons in raphe and this might then inhibit serotonin neurons in turn.

We recently used scRNAseq in habenula and identified a number of clusters of LHb neurons based on their overall patterns of gene expression [28]. In that study, PACAP-expressing neurons were distributed across several clusters of LHb neurons, especially LHb5 and LHb1, suggesting that PACAP expression itself did not uniquely identify a specific subtype of LHb neurons. In the present study, using the reverse approach of examining RNA expression by PACAP-expressing neurons, we did not identify a unique molecular signature. Thus, PACAP expression does not seem to define these neurons as a unique molecular or anatomical set even though they do seem to have quite distinct effects on fear, anxiety, and approach behaviors.

PACAP-expressing neurons are found throughout the brain in both glutamatergic and GABAergic neurons [50]. This recent report examined the

colocalization of PACAP expression with glutamate or GABA markers. While PACAP was found in some GABAergic neurons, particularly in the cerebellum, the majority of PACAP-expressing neurons are glutamatergic indicating that these neurons primarily activate downstream targets [50]. Additionally, this report found that nearly all PACAP-expressing neurons and their neighbors also express PAC1, the primary receptor for PACAP, meaning that these neurons are using autocrine and paracrine mechanisms as well as projections to further away targets [50].

The LHb is surprisingly heterogeneous. While roughly one third of neurons in the LHb are activated by footshock, about 10% are actually inhibited [17]. Interestingly, these footshock-inhibited neurons had about twice the resting firing rate as footshock-activated neurons. While the vast majority of LHb neurons are glutamatergic, some produce GAD2 [51]. Interestingly, these neurons do not appear to package or excrete GABA. They also have a similar expression and projection pattern to the PACAP-expressing neurons.

PACAP has also been shown to disrupt fear memory. ICV administration of PACAP prior to conditioning decreased freezing in rats the next day and notably decreased cFos positive neurons in a variety of brain regions including the LHb [35]. Infusion of $PACAP_{6-38}$, a PAC1R antagonist, into the prefrontal cortex of rats decreased freezing to the tone cue, but not the context [52]. This effect was specific to female rats, and the mRNA expression levels of the receptor increased throughout the estrous cycle; however, PACAP mRNA levels did not change with estrous. In humans, a polymorphism of PAC1R increases the risk of PTSD and increases response to fear in the hippocampus and amygdala in women, but not men [38, 53].

Additionally, mice with constitutive knock out of PACAP had no morphine place preference after a single conditioning session, unlike their PACAP positive littermates; however, with two conditioning sessions, they had equal levels of preference [32]. Further, we found that activating these neurons was rewarding, producing a place preference on the CNO-paired side. Additional experiments should investigate whether inhibiting PACAP-expressing neurons in the LHb alters the rewarding properties of opioids.

Chemogenetic activation of these neurons produced a conditioned place preference but activating these neurons did not increase the reward associated with sucrose preference or reduce the latency to eat. It seems that while activating LHb PACAP neurons is rewarding, it does not change the hedonic valence of other rewards or the motivation to consume them. This may be due to a ceiling effect which could be examined using a lower percentage of sucrose. Additionally, chronically stressing the mice prior to activation of LHb PACAP neurons would be interesting to examine as chronic stress alters sucrose preference and novelty suppressed feeding [44, 54]. A caveat to note is that acute antidepressant effects are not observed in novelty suppressed feeding, and chronic treatment of classic antidepressants is needed to affect latency. However, anxiolytics do produce effects immediately in this test [44]. Thus, it may be of interest to activate LHb PACAP neurons chronically prior to testing novelty suppressed feeding.

5. Conclusion

In summary, LHb PACAP-expressing neurons are not definitive of a specific cluster of LHb neurons; however, they are unique in behavioral control. These neurons target the RMTg and lateral DRN, as well as the MRN. By targeting

these predominantly GABAergic regions, perhaps these neurons are diminishing circuit excitability, which may be responsible for the altered responses in behavior in comparison to whole LHb activation.

References

[1] S. Lecca, F. J. Meye, M. Trusel, A. Tchenio, J. Harris, M. K. Schwarz, D. Burdakov, F. Georges, M. Mameli, Aversive stimuli drive hypothalamus-to-habenula excitation to promote escape behavior, eLife 6 (2017). doi:10.7554/eLife.30697.

[2] V. M. K. Namboodiri, J. Rodriguez-Romaguera, G. D. Stuber, The habenula, Current Biology 26 (19) (2016) R873–R877. doi:10.1016/j.cub.2016.08.051.

[3] L. A. Quina, L. Tempest, L. Ng, J. A. Harris, S. Ferguson, T. C. Jhou, E. E. Turner, Efferent Pathways of the Mouse Lateral Habenula, Journal of Comparative Neurology 523 (1) (2015) 32–60. doi:10.1002/cne.23662.

[4] A. M. Stamatakis, G. D. Stuber, Activation of lateral habenula inputs to the ventral midbrain promotes behavioral avoidance, Nature Neuroscience 15 (8) (2012) 1105–1107. doi:10.1038/nn.3145.

[5] Y. Ootsuka, M. Mohammed, Activation of the habenula complex evokes autonomic physiological responses similar to those associated with emotional stress, Physiol Rep 3 (2015). doi:10.14814/phy2.12297.

[6] M. J. Gill, S. M. Ghee, S. M. Harper, R. E. See, Inactivation of the lateral habenula reduces anxiogenic behavior and cocaine seeking under conditions of heightened stress, Pharmacology Biochemistry and Behavior 111 (2013) 24–29. doi:10.1016/j.pbb.2013.08.002.

[7] X. F. Luo, B. L. Zhang, J. C. Li, Y. Y. Yang, Y. F. Sun, H. Zhao, Lateral habenula as a link between dopaminergic and serotonergic systems contributes to depressive symptoms in parkinson's disease, Brain Res Bull 110 (2015) 40–46.

[8] C. D. Proulx, S. Aronson, D. Milivojevic, C. Molina, A. Loi, B. Monk, S. J. Shabel, R. Malinow, A neural pathway controlling motivation to exert effort, Proceedings of the National Academy of Sciences 115 (22) (2018) 5792–5797. doi:10.1073/pnas.1801837115.

[9] Q. Zhang, J. J. Feng, S. Yang, X. F. Liu, J. C. Li, H. Zhao, Lateral habenula as a link between thyroid and serotoninergic system modiates depressive symptoms in hypothyroidism rats, Brain Res Bull 124 (2016) 198–205.

[10] S. G. Nair, N. S. Strand, J. F. Neumaier, DREADDing the lateral habenula: A review of methodological approaches for studying lateral habenula function, Brain Research 1511 (2013) 93–101. doi:10.1016/j.brainres.2012.10.011.
URL https://dx.doi.org/10.1016/j.brainres.2012.10.011

[11] K. R. Coffey, R. G. Marx, E. K. Vo, S. G. Nair, J. F. Neumaier, Chemogenetic inhibition of lateral habenula projections to the dorsal raphe nucleus reduces passive coping and perseverative reward seeking in rats, Neuropsychopharmacology (2020). doi:10.1038/s41386-020-0616-0.

[12] P. M. Baker, T. Jhou, B. Li, M. Matsumoto, S. J. Mizumori, M. Stephenson-Jones, A. Vicentic, The Lateral Habenula Circuitry: Reward Processing and Cognitive Control, The Journal of Neuroscience 36 (45) (2016) 11482–11488. doi:10.1523/jneurosci.2350-16.2016.

[13] S. J. Mizumori, P. M. Baker, The Lateral Habenula and Adaptive Behaviors, Trends in Neurosciences 40 (8) (2017) 481–493. doi:10.1016/j.tins.2017.06.001.

[14] R. Thapa, C. H. Donovan, S. A. Wong, R. J. Sutherland, A. J. Gruber, Lesions of lateral habenula attenuate win-stay but not lose-shift responses in a competitive choice task, Neuroscience Letters 692 (2019) 159–166. doi:10.1016/j.neulet.2018.10.056.

[15] L. Durieux, V. Mathis, K. Herbeaux, M. Muller, A. Barbelivien, C. Mathis, R. Schlichter, S. Hugel, M. Majchrzak, L. Lecourtier, Involvement of the lateral habenula in fear memory, Brain Structure and Function 225 (7) (2020) 2029–2044. doi:10.1007/s00429-020-02107-5.

[16] A. L. Berger, A. M. Henricks, J. M. Lugo, H. R. Wright, C. R. Warrick, M. A. Sticht,

M. Morena, I. Bonilla, S. A. Laredo, R. M. Craft, L. H. Parsons, P. R. Grandes, C. J. Hillard, M. N. Hill, R. J. McLaughlin, The Lateral Habenula Directs Coping Styles Under Conditions of Stress via Recruitment of the Endocannabinoid System, Biological Psychiatry 84 (8) (2018) 611–623. doi:10.1016/j.biopsych.2018.04.018.

[17] M. Congiu, M. Trusel, M. Pistis, M. Mameli, S. Lecca, Opposite responses to aversive stimuli in lateral habenula neurons, European Journal of Neuroscience 50 (6) (2019) 2921–2930. doi:10.1111/ejn.14400.

[18] H. Hu, Y. Cui, Y. Yang, Circuits and functions of the lateral habenula in health and in disease, Nat Rev Neurosci 21 (2020) 277–295.

[19] J. S. Seo, P. Zhong, A. Liu, Z. Yan, P. Greengard, Elevation of p11 in lateral habenula mediates depression-like behavior, Molecular Psychiatry 23 (5) (2018) 1113–1119. doi:10.1038/mp.2017.96.

[20] D. Wirtshafter, K. E. Asin, M. R. Pitzer, Dopamine agonists and stress produce different patterns of Fos-like immunoreactivity in the lateral habenula, Brain Research 633 (1-2) (1994) 21–26. doi:10.1016/0006-8993(94)91517-2.

[21] R. Bernard, R. W. Veh, Individual neurons in the rat lateral habenular complex project mostly to the dopaminergic ventral tegmental area or to the serotonergic raphe nuclei, The Journal of Comparative Neurology 520 (11) (2012) 2545–2558. doi:10.1002/cne.23080.

[22] S. Geisler, M. Trimble, The Lateral Habenula: No Longer Neglected, CNS Spectrums 13 (6) (2008) 484–489. doi:10.1017/s1092852900016710.

[23] L. Gonçalves, C. Sego, M. Metzger, Differential projections from the lateral habenula to the rostromedial tegmental nucleus and ventral tegmental area in the rat, The Journal of Comparative Neurology 520 (6) (2012) 1278–1300. doi:10.1002/cne.22787.

[24] P. K. n, R. E. Strecker, E. Rosengren, A. B. rklund, Regulation of striatal serotonin release by the lateral habenula-dorsal raphe pathway in the rat as demonstrated by in vivo microdialysis: role of excitatory amino acids and GABA, Brain Research 492 (1-2) (1989) 187–202. doi:10.1016/0006-8993(89)90901-3.

[25] K. Brinschwitz, A. Dittgen, V. I. Madai, R. Lommel, S. Geisler, R. W. Veh, Glutamatergic axons from the lateral habenula mainly terminate on GABAergic neurons of the ventral midbrain, Neuroscience 168 (2) (2010) 463–476. doi:10.1016/j.neuroscience.2010.03.050.

[26] M. R. Levinstein, K. R. Coffey, R. G. Marx, A. J. Lesiak, J. F. Neumaier, Stress induces divergent gene expression among lateral habenula efferent pathways, Neurobiology of Stress (2020) 100268–100268 doi:10.1016/j.ynstr.2020.100268.

[27] T. Christensen, L. Jensen, E. V. Bouzinova, O. Wiborg, Molecular Profiling of the Lat-eral Habenula in a Rat Model of Depression, PLoS ONE 8 (12) (2013) e80666–e80666. doi:10.1371/journal.pone.0080666.

[28] Y. Hashikawa, K. Hashikawa, M. A. Rossi, M. L. Basiri, Y. Liu, N. L. Johnston, O. R. Ahmad, G. D. Stuber, Transcriptional and Spatial Resolution of Cell Types in the Mammalian Habenula, Neuron 106 (5) (2020) 743–758.e5. doi:10.1016/j.neuron.2020.03.011.

[29] J. Hannibal, Pituitary adenylate cyclase-activating peptide in the rat central nervous system: An immunohistochemical and in situ hybridization study, The Journal of Comparative Neurology 453 (4) (2002) 389–417. doi:10.1002/cne.10418.

[30] F. Wagner, L. French, R. W. Veh, Transcriptomic-anatomic analysis of the mouse habenula uncovers a high molecular heterogeneity among neurons in the lateral complex, while gene expression in the medial complex largely obeys subnuclear boundaries, Brain Struct Funct 221 (2016) 39–58.

[31] H. Hashimoto, N. Shintani, M. Tanida, A. Hayata, R. Hashimoto, A. Baba, PACAP is Implicated in the Stress Axes, Current Pharmaceutical Design 17 (10) (2011) 985–989. doi:10.2174/138161211795589382.

[32] P. Marquez, D. Bebawy, V. Lelièvre, A.-C. Coûté, C. J. Evans, J. A. Waschek, K. Lutfy, The role of endogenous PACAP in motor stimulation and conditioned place preference induced by morphine in mice, Psychopharmacology 204 (3) (2009) 457–463. doi:10.1007/s00213-009-1476-9.

[33] N. Stroth, Y. Holighaus, D. Ait-Ali, L. E. Eiden, PACAP: a master regulator of neuroendocrine stress circuits and the cellular stress response, Annals of the New York Academy of Sciences 1220 (1) (2011) 49–59. doi:10.1111/j.1749-6632.2011.05904.x.

[34] S. E. Hammack, J. Cheung, K. M. Rhodes, K. C. Schutz, W. A. Falls, K. M. Braas, V. May, Chronic stress increases pituitary adenylate cyclase-activating peptide (PACAP) and brain-derived neurotrophic factor (BDNF) mRNA expression in the bed nucleus of the stria terminalis (BNST): Roles for PACAP in anxiety-like behavior, Psychoneuroendocrinology 34 (6) (2009) 833–843. doi:10.1016/j.psyneuen.2008.12.013.

[35] E. G. Meloni, A. Venkataraman, R. J. Donahue, W. A. Carlezon, Bi-directional effects of pituitary adenylate cyclase-activating polypeptide (PACAP) on fear-related behavior and c-Fos expression after fear conditioning in rats, Psychoneuroendocrinology 64 (2016) 12–21. doi:10.1016/j.psyneuen.2015.11.003.

[36] G. Telegdy, A. Adamik, Neurotransmitter-mediated anxiogenic action of PACAP-38 in rats, Behavioural Brain Research 281 (2015) 333–338. doi:10.1016/j.bbr.2014.12.039.

[37] T. Jovanovic, A. F. Stenson, N. Thompson, A. Clifford, A. Compton, S. Minton, S. J. F. van Rooij, J. S. Stevens, A. Lori, N. Nugent, C. F. Gillespie, B. Bradley, K. J. Ressler, Impact of ADCYAP1R1 genotype on longitudinal fear conditioning in children: interaction with trauma and sex, Neuropsychopharmacology 45 (10) (2020) 1603–1608. doi:10.1038/s41386-020-0748-2.

[38] K. J. Ressler, K. B. Mercer, B. Bradley, T. Jovanovic, A. Mahan, K. Kerley, S. D. Norrholm, V. Kilaru, A. K. Smith, A. J. Myers, M. Ramirez, A. Engel, S. E. Hammack, D. Toufexis, K. M. Braas, E. B. Binder, V. May, Post-traumatic stress disorder is associated with PACAP and the PAC1 receptor, Nature 470 (7335) (2011) 492–497. doi:10.1038/nature09856.

[39] J. A. Harris, K. E. Hirokawa, S. A. Sorensen, H. Gu, M. Mills, L. L. Ng, P. Bohn, M. Mortrud, B. Ouellette, J. Kidney, K. A. Smith, C. Dang, S. Sunkin, A. Bernard, S. W. Oh, L. Madisen, H. Zeng, Anatomical characterization of Cre driver mice for neural circuit mapping and manipulation, Frontiers in Neural Circuits 8 (2014) 76–76. doi:10.3389/fncir.2014.00076.

[40] K. R. Coffey, D. J. Barker, S. Ma, M. O. West, Building An Open-source Robotic Stereotaxic Instrument, Journal of Visualized Experiments (80) (2013). doi:10.3791/51006.

[41] A. J. Lesiak, M. Brodsky, J. F. Neumaier, RiboTag is a flexible tool for measuring the translational state of targeted cells in heterogeneous cell cultures, BioTechniques 58 (6) (2015) 308–317. doi:10.2144/000114299.

[42] A. J. Lesiak, J. F. Neumaier, RiboTag: Not Lost in Translation, Neuropsychopharmacology 41 (1) (2016) 374–376. doi:10.1038/npp.2015.262.

[43] A. J. Lesiak, K. Coffey, J. H. Cohen, K. J. Liang, C. Chavkin, J. F. Neumaier, Sequencing the serotonergic neuron translatome reveals a new role for Fkbp5 in stress, Molecular Psychiatry (2020). doi:10.1038/s41380-020-0750-4.

[44] B. A. Samuels, R. Hen, Mood and anxiety related phenotypes in mice: Characterization using behavioral tests, volume ii, Humana Press, Totowa, NJ, 2011.

[45] B. A. Samuels, C. Anacker, A. Hu, M. R. Levinstein, A. Pickenhagen, T. Tsetsenis,

N. Madroñal, Z. R. Donaldson, L. J. Drew, A. Dranovsky, C. T. Gross, K. F. Tanaka, R. Hen, 5-HT1A receptors on mature dentate gyrus granule cells are critical for the antidepressant response, Nature Neuroscience 18 (11) (2015) 1606–1616. doi:10.1038/nn.4116.

[46] Y. S. Jo, G. Heymann, L. S. Zweifel, Dopamine Neurons Reflect the Uncertainty in Fear Generalization, Neuron 100 (4) (2018) 916–925.e3. doi:10.1016/j.neuron.2018.09.028.

[47] A. D. Abraham, S. S. Schattauer, K. L. Reichard, J. H. Cohen, H. M. Fontaine, A. J. Song, S. D. Johnson, B. B. Land, C. Chavkin, Estrogen Regulation of GRK2 Inactivates Kappa Opioid Receptor Signaling Mediating Analgesia, But Not Aversion, The Journal of Neuroscience 38 (37) (2018) 8031–8043. doi:10.1523/jneurosci.0653-18.2018.

[48] B. N. Armbruster, X. Li, M. H. Pausch, S. Herlitze, B. L. Roth, Evolving

the lock to fit the key to create a family of G protein-coupled receptors potently activated by an inert ligand, Proceedings of the National Academy of Sciences 104 (12) (2007) 5163–5168. doi:10.1073/pnas.0700293104.

[49] S. M. Ferguson, P. E. M. Phillips, B. L. Roth, J. Wess, J. F. Neumaier, Direct-Pathway Striatal Neurons Regulate the Retention of Decision-Making Strategies, Journal of Neuroscience 33 (28) (2013) 11668–11676. doi:10.1523/jneurosci.4783-12.2013.

[50] L. Zhang, V. S. Hernández, C. R. Gerfen, S. Z. Jiang, L. Zavala, R. A. Barrio, L. E. Eiden, Behavioral role of pacap signaling reflects its selective distribution in glutamatergic and gabaergic neuronal subpopulations, bioRxiv (2020). doi:10.1101/2020.07.31.231795.

[51] L. A. Quina, A. Walker, G. Morton, V. Han, E. E. Turner, Gad2 expression defines a class of excitatory lateral habenula neurons in mice that project to the raphe and pontine tegmentum, eNeuro (2020). doi:10.1523/ENEURO.0527-19.2020.

[52] A. J. Kirry, M. R. Herbst, S. E. Poirier, M. M. Maskeri, A. C. Rothwell, R. C. Twining, M. R. Gilmartin, Pituitary adenylate cyclase-activating polypeptide (PACAP) signaling in the prefrontal cortex modulates cued fear learning, but not spatial working memory, in female rats, Neuropharmacology 133 (2018) 145–154. doi:10.1016/j.neuropharm.2018.01.010.

[53] J. S. Stevens, L. M. Almli, N. Fani, D. A. Gutman, B. Bradley, S. D. Norrholm, E. Reiser, T. D. Ely, R. Dhanani, E. M. Glover, T. Jovanovic, K. J. Ressler, PACAP receptor gene polymorphism impacts fear responses in the amygdala and hippocampus, Proceedings of the National Academy of Sciences 111 (8) (2014) 3158–3163. doi:10.1073/pnas.1318954111.

[54] M. Y. Liu, C. Y. Yin, L. J. Zhu, X. H. Zhu, C. Xu, C. X. Luo, H. Chen, D. Y. Zhu, Q. G. Zhou, Sucrose preference test for measurement of stress-induced anhedonia in mice, Nat Protoc 13 (2018) 1686–1698.

Chapter 4: Conclusions

Marjorie R Levinstein

1. Summary

Using a multitude of methods, I have investigated the diversity of neurons in the lateral habenula (LHb) using both anatomical projections and genetic markers. We used a mixture of molecular and behavioral tools in order to better understand this nucleus.

2. Genetic diversity of lateral habenula efferent pathways

In chapter 2, we investigated the impact of stress on RNAs actively undergoing translation in LHb neurons comprising three major output pathways to ventral tegmental area (VTA), dorsal raphe nucleus (DRN), and rostromedial tegmental nucleus (RMTg). We compared expression of individual genes between pathways and between unstressed and stressed conditions in a pairwise fashion. We found that gene set enrichment analysis (GSEA) and weighted gene co-expression network analysis (WGCNA) revealed patterns in gene expression changes with stress that differed between these efferent LHb pathways. Whereas GSEA is based upon previously identified sets of functionally related genes, WGCNA uses an unbiased method of clustering genes into “modules” based on patterns of expression levels across the entire data set without assumptions about gene function. When we examined the average expression levels of all of the modules that were identified, just one repeatedly demonstrated significant differential expression between experimental groups. In most cases, the gene sets

or modules were downregulated in RMTg-projecting LHb neurons after stress but upregulated in DRN- and VTA-projecting neurons after stress.

When we compared the pathways to one another in a pairwise fashion in unstressed rats, there were relatively few differences in RNA expression; in particular, there were no dramatic phenotype-defining differences observed. A recent single cell RNAseq study in mice reached similar conclusions [1]. While some LHb neurons express neuropeptides and perhaps GABA, nearly every neuron in the LHb is glutamatergic [2–4]. Therefore, it is less surprising that the pathways are homogeneous at baseline and only change with stress. Our a priori hypothesis was that the neurons comprising these three pathways might be quite different because the pathways have few collaterals among them, but this was rejected; however, some differences between these pathways emerged following stress exposure.

We found that RMTg-projecting neurons changed the most following stress. This was unexpected since we previously found that the pathway to the DRN was the most involved in adaptations to forced swim immobility [5]. Chemogenetically inhibiting DRN-projecting neurons in between the first and second swim sessions decreased immobility and decreased perseverative seeking in the reward omission task. Conversely, activating these neurons increased perseverative seeking but did not further change immobility in the forced swim test. Inhibiting either of the other two pathways did not change behavior in any of the tests performed. Thus, we initially expected the pathway to the DRN to be the most affected by stress. One possible interpretation of these results is that inhibiting the LHb-RMTg pathway had no effect because the plasticity in this pathway already served to reduce its excitability, and inhibition with hM_4Di had no additional impact. Supporting this interpretation, Proulx and colleagues

found that acute optogenetic stimulation of RMTg-projecting LHb neurons transiently increased immobility during a single FST session [6], suggesting that it indeed is not maximally activated during forced swim alone. It is interesting to consider that, if the pathway from LHb to RMTg becomes less excitable due to changes in gene expression following forced swim stress, perhaps this leads to a relative increased activation of VTA and DRN by LHb.

While our GSEA results suggest that gene expression in these pathways diverge after stress, we focused on the unbiased topological analysis with WGCNA, which also indicated that the RMTg-projecting neurons diverged from the VTA- and DRN-projecting neurons. WGCNA clusters genes with no a priori knowledge of function; however, it is not uncommon for modules to have overrepresentations of biologically relevant sets of genes. This was exemplified by the Gold module, which had an overrepresentation of downregulated genes associated with PI3K signaling after stress, found both via GO: Biological Process and the KEGG database. In order to validate these results, we performed RTqPCR from ribosome-associated RNA isolated from the RMTg-projecting neurons in a new cohort of control and stressed rats. We measured the three differentially expressed PI3K-associated genes identified by WGCNA and confirmed the downregulation of *Kdr* and *Tek* while *Ptpn13* exhibited a similar trend. We propose that this reduction in PI3K-associated genes may reduce excitability of RMTg-projecting LHb neurons. PI3K signaling regulates anxiety-like behavior, may be involved in the antidepressant effects of deep brain stimulation, and is implicated in the mood-stabilizing effects of lithium in post-mortem analyses of patients with major depressive disorder [7]. Phosphorylation of PI3K is implicated in the antidepressant effects of baicalin in a mouse model of depression [8]. We predict that downregulation of PI3K in the RMTg-

projecting neurons after stress would be a compensatory adaptation that reduces their excitability, thereby disinhibiting the monoaminergic neurons in the DRN and VTA. Since we examined RNA actively undergoing translation in this study, the impact of these changes on protein production might take additional time to manifest. Future studies should examine the role of PI3K signaling in this pathway on resilience after stress exposure.

3. The role of PACAP-expressing neurons in the LHb

In chapter 3, we used viral vectors to conditionally express DREADD receptor and RiboTag in PACAP-Cre expressing neurons in LHb to investigate the role of these neurons in the control of emotional behaviors. In these experiments we found that chemogenetic activation of LHb PACAP neurons increased locomotion, reduced anxiety-like behavior, reduced fear-learning, and may be modestly rewarding. These results are directly opposite of the published or predicted results for LHb neurons in general. However, activating these neurons did not affect neophobia in the novelty suppressed feeding test, nor did it affect hedonic valence as tested in the sucrose preference test. These results indicate these neurons may be behaving paradoxically to the LHb as a whole.

In addition, we investigated these neurons anatomical projections and genetic profile. We found that these neurons project to the raphe and RMTg, but not the VTA. Thus, these neurons are not specific to one pathway. Interestingly, it appears that PACAP-expressing LHb neurons tend to project more towards the lateral part of the dorsal raphe and the medial raphe nuclei. While it appears these LHb neurons play a unique role behaviorally, they do not map onto a specific cluster from our scRNAseq data [9]. These neurons are spread over multiple clusters, most prominently in LHb5 and LHb1, but they are also

somewhat present in all other LHb clusters. Thus, they are not defined by and they do not define a specific cluster.

Interestingly, mice with constitutive knock out of PACAP had no morphine place preference after a single conditioning session, unlike their PACAP positive littermates; however, with two conditioning sessions, they had equal levels of preference [10]. Further, we found that activating these neurons was rewarding, producing a place preference on the CNO-paired side. Additional experiments should investigate whether inhibiting PACAP-expressing neurons in the LHb prevents morphine place preference. Direct activation of these neurons produced a conditioned place preference but activating these neurons did not increase the reward associated with sucrose preference or reduce the latency to eat. It seems that while activating LHb PACAP neurons is rewarding, it does not change the hedonic valence of other rewards or the motivation to consume them. This may be due to a ceiling effect which could be examined using a lower percentage of sucrose. Additionally, chronically stressing the mice prior to activation of LHb PACAP neurons would be interesting to examine as chronic stress alters sucrose preference and novelty suppressed feeding [11, 12]. A caveat to note is that acute antidepressant effects are not observed in novelty suppressed feeding, and chronic treatment of classic antidepressants is needed to affect latency. However, anxiolytics do produce effects immediately in this test [12]. Thus, it may be of interest to chronically activate LHb PACAP neurons prior to testing novelty suppressed feeding.

PACAP-expressing neurons are found throughout the brain in both glutamatergic and GABAergic neurons [13]. This recent report examined the colocalization of PACAP expression with glutamate or GABA markers. While PACAP was found in some GABAergic neurons, particularly in the cerebellum,

the majority of PACAP-expressing neurons are glutamatergic indicating that these neurons primarily activate downstream targets [13]. Additionally, this report found that nearly all PACAP-expressing neurons and their neighbors also express PAC1, the primary receptor for PACAP, meaning that these neurons are using autocrine and paracrine mechanisms as well as projections to further away targets [13]. In summary, LHb PACAP neurons are definitive of a specific cluster of LHb neurons; however, they are unique in behavioral control.

4. Diversity within the LHb

Both of these projects aimed to understand the diversity of neurons within the LHb. The first profiled the output pathways with and without stress; the second examined the role of a subset of neurons in regard to anxiety, fear and appetitive behaviors. Neither of these approaches is sufficient to explain neuronal diversity of the nucleus. What other sources of differences might there be?

Neurons projecting to different target regions are intermixed within subregions of the LHb yet have minimal collateralization between DRN, VTA, and RMTg. Given that the LHb neurons targeting these areas have similar phenotypes at baseline, perhaps the differences become apparent after stress because each pathway receives different input information during stress. Inputs to the LHb arise from many places – the basal forebrain, medial pre- frontal cortex, the basal ganglia, hypothalamus, and olfactory bulbs [14]. Recent studies have shown that some of these inputs are projection- or cell-type specific. Neurons from the entopeduncular nucleus preferentially project onto neurons that project to the VTA [15]. Perhaps other inputs project onto neurons projecting to specific targets. The differences in incoming signal due to unique

inputs could lead to Perhaps, stress-sensitive inputs preferentially synapse onto neurons projecting to specific targets, and differential activation leads to changes in their subsequent gene expression. Indeed, a recent paper found that CaMKII-expressing neurons projecting from the entopeduncular nucleus tended to synapse onto LHb neurons projecting to the VTA; whereas, those from the lateral hypothalamus and VTA tended to synapse onto neurons projecting to the DRN [15].

The circuitry of the LHb and its major targets, RMTg, DRN, and VTA, is complex. LHb stimulation generally decreases dopaminergic activity within the VTA; although there is also evidence of direct excitation of dopamine neurons [16]. Similarly, activation of the LHb has complex effects on the output of serotonin from raphe neurons; only high frequency stimulation increased serotonin release into striatum; this was further augmented by bicuculline injection into DRN [17]. Indeed, lesions of the habenula ablate the increase in serotonin in the DRN during and after stress [18]. LHb neurons project to both serotonergic and GABAergic neurons in DRN at roughly equal rates [19]. While direct projections to VTA or DRN may either activate monoaminergic or GABAergic neurons, the projection to RMTg innervates only GABAergic neurons which in turn inhibit VTA and DRN [20].

There is some diversity in the responses of LHb neurons to aversive stimuli. Both inescapable shock and reward omission increase firing in subpopulations of the LHb, exciting 30-50% of these neurons [21, 22]. Furthermore, roughly 10% of LHb neurons are actually inhibited by footshocks [23]. Interestingly, these footshock-inhibited neurons had about twice the resting firing rate as footshock-activated neurons. While the vast majority of LHb neurons are glutamatergic, some produce GAD2 [24]. Interestingly, these neurons do not appear to package

or excrete GABA. They also have a similar expression and projection pattern to the PACAP-expressing neurons.

Further, RMTg-projecting LHb neurons have shown increased excitability 24 hours to 14 days after cocaine exposure, but VTA-projecting neurons did not [25, 26]. Thus, it is possible that the observed stress-induced reduction in the excitability of LHb projections to RMTg disinhibits the VTA and DRN monoaminergic outputs. On the contrary, activation of LHb-RMTg neurons optogenetically interferes with reward motivated behavior and reduces activity in the FST [6]. Perhaps the pathway to the RMTg becomes less active following an inescapable stressor via an allostatic adaptation in neuronal excitability. In chapter 2 we observed differential gene expression plasticity between neurons projecting to VTA and DRN on the one hand and RMTg on the other. Since the changes in RMTg-projecting neurons involved reduced expression of genes associated with excitability (such as in the PI3K signaling pathway), perhaps the overall balance of LHb stimulation of downstream GABAergic tone is reduced after repeated forced swim stress.

Recently, the LHb was found to be involved in fear memory [27]. Indeed, Durieux andcolleagues (2020) [27] found that the neurons in the rostral and medial LHb had increased cFos expression after fear conditioning compared to rats which remained in their homecage (rats exposed to tone and chambers also had increased cFos expression). When they chemogenetically inhibited the LHb prior to conditioning, the rats showed less freezing to the context, but more freezing to the CS tone when tested later. We found that activating LHb PACAP neurons during conditioning also decreased freezing in context. PACAP has also been shown to disrupt fear memory. ICV administration of PACAP prior to conditioning decreased freezing in rats the next day and notably decreased cFos

positive neurons in a variety of brain regions including the LHb [28]. Infusion of $PACAP_{6-38}$, a PAC1R antagonist, into the prefrontal cortex of rats decreased freezing to the tone cue, but not the context [29]. This effect was specific to female rats, and the mRNA expression levels of the receptor increased throughout the estrous cycle; however, PACAP mRNA levels did not change with estrous. In humans, a polymorphism of PAC1R increases the risk of PTSD and increases response to fear in the hippocampus and amygdala in women, but not men [30, 31].

Additional diversity of responses may be due to the heterogeneity of cell types within the nucleus. A multitude of neuropeptides are expressed within the LHb, mostly as a mosaic [32]. While it does not seem that these neuropeptides are projection- specific, the cell-types to which they correspond may provide varying information to their targets. Although the neurons expressing PACAP do not appear to correspond to a unique molecular cell-type, perhaps other markers will.

5. Future directions

While we elucidated some of the mysteries of the LHb, many still remain. The pathway- specific RiboTag RNAseq data indicate that LHb neurons projecting to the RMTg experience a change in plasticity which may decrease in activity following stress. The most obvious follow-up experiment would be to examine the activity of these neurons during or after stress.

The PACAP neurons pose other questions. While we activated these neurons in this study, inactivating these neurons would also be interesting. Would chemogenetically inhibiting LHb PACAP neurons exacerbate anxiety-like behavior? Additionally, we examined neurons which express PACAP, but we do

not know whether the effects seen are due to PACAP transmission. We could employ a few different methods to address this question. For example, we could combine a CRISPR viral construct targeting PACAP with hM_3Dq in the LHb and activate the DREADD during the behaviors tested here. If the behavioral results remain the same, then PACAP transmission is not necessary for these results, but if the behavior is altered, then PACAP transmission is likely needed to reduce anxiety or to be rewarding. Though we investigated the projections from these neurons and found that they predominantly project to the raphe and somewhat to the RMTg, it would also be interesting to understand what projects onto these neurons. We could use a Cre-inducible pseudorabies virus expressing GFP which would retrogradely label the neurons projecting specifically to the PACAP neurons in the LHb.

References

[1] M. L. Wallace, K. W. Huang, D. Hochbaum, M. Hyun, G. Radeljic, B. L. Sabatini, Anatomical and single-cell transcriptional profiling of the murine habenular complex, eLife 9 (2020). doi:10.7554/elife.51271.

[2] H. Aizawa, M. Kobayashi, S. Tanaka, T. Fukai, H. Okamoto, Molecular characterization of the subnuclei in rat habenula, The Journal of Comparative Neurology 520 (18) (2012) 4051–4066. doi:10.1002/cne.23167.

[3] A. M. Stamatakis, G. D. Stuber, Activation of lateral habenula inputs to the ventral midbrain promotes behavioral avoidance, Nature Neuroscience 15 (8) (2012) 1105–1107. doi:10.1038/nn.3145.

[4] W. Zuo, L. Wang, L. Chen, K. Krnjević, R. Fu, X. Feng, W. He, S. Kang, A. Shah, A. Bekker, J.-H. Ye, Ethanol potentiates both GABAergic and glutamatergic signaling in the lateral habenula, Neuropharmacology 113 (2017) 178–187. doi:10.1016/j.neuropharm.2016.09.026.

[5] K. R. Coffey, R. G. Marx, E. K. Vo, S. G. Nair, J. F. Neumaier, Chemogenetic inhibition of lateral habenula projections to the dorsal raphe nucleus reduces passive coping and perseverative reward seeking in rats, Neuropsychopharmacology (2020). doi:10.1038/s41386-020-0616-0.

[6] C. D. Proulx, S. Aronson, D. Milivojevic, C. Molina, A. Loi, B. Monk, S. J. Shabel, R. Malinow, A neural pathway controlling motivation to exert effort, Proceedings of the National Academy of Sciences 115 (22) (2018) 5792–5797. doi:10.1073/pnas.1801837115.

[7] B. Voleti, R. S. Duman, The Roles of Neurotrophic Factor and Wnt Signaling in Depression, Clinical Pharmacology & Therapeutics 91 (2) (2012) 333–338. doi:10.1038/clpt.2011.296.

[8] L. T. Guo, S. Q. Wang, J. Su, L. X. Xu, Z. Y. Ji, R. Y. Zhang, Q. W. Zhao, Z. Q. Ma, X. Y. Deng, S. P. Ma, Baicalin ameliorates neuroinflammation-induced depressive-like behavior through inhibition of toll-like receptor 4 expression via the pi3k/akt/foxo1 pathway, J Neuroinflammation 16 (2019) 95–95.

[9] Y. Hashikawa, K. Hashikawa, M. A. Rossi, M. L. Basiri, Y. Liu, N. L. Johnston, O. R. Ahmad, G. D. Stuber, Transcriptional and Spatial Resolution of Cell Types in the Mammalian Habenula, Neuron 106 (5) (2020) 743–758. e5. doi:10.1016/j.neuron.2020.03.011.

[10] P. Marquez, D. Bebawy, V. Lelièvre, A.-C. Coûté, C. J. Evans, J. A. Waschek, K. Lutfy, The role of endogenous PACAP in motor stimulation and conditioned place preference induced by morphine in mice, Psychopharmacology 204 (3) (2009) 457–463. doi:10.1007/s00213-009-1476- 9.

[11] M. Y. Liu, C. Y. Yin, L. J. Zhu, X. H. Zhu, C. Xu, C. X. Luo, H. Chen, D. Y. Zhu, Q. G. Zhou, Sucrose preference test for measurement of stress-induced anhedonia in mice, Nat Protoc 13 (2018) 1686–1698.

[12] B. A. Samuels, R. Hen, Mood and anxiety related phenotypes in mice: Characterization using behavioral tests, volume ii, Humana Press, Totowa, NJ, 2011.

[13] L. Zhang, V. S. Hernández, C. R. Gerfen, S. Z. Jiang, L. Zavala, R. A. Barrio, L.

E. Eiden, Behavioral role of pacap signaling reflects its selective distribution in glutamatergic and gabaergic neuronal subpopulations, bioRxiv (2020).

[14] V. M. K. Namboodiri, J. Rodriguez-Romaguera, G. D. Stuber, The habenula, Current Biology 26 (19) (2016) R873–R877. doi:10.1016/j.cub.2016.08.051.

[15] I. Cerniauskas, J. Winterer, J. W. de Jong, D. Lukacsovich, H. Yang, F. Khan, J. R. Peck, S. K. Obayashi, V. Lilascharoen, B. K. Lim, C. Földy, S. Lammel, Chronic Stress Induces Activity, Synaptic, and Transcriptional Remodeling of the Lateral Habenula Associated with Deficits in Motivated Behaviors, Neuron 104 (5) (2019) 899–915.e8. doi:10.1016/j.neuron.2019.09.005.

[16] P. L. Brown, P. D. Shepard, Functional evidence for a direct excitatory projection from the lateral habenula to the ventral tegmental area in the rat, Journal of Neurophysiology 116 (3) (2016) 1161–1174. doi:10.1152/jn.00305.2016.

[17] P. K. n, R. E. Strecker, E. Rosengren, A. B. rklund, Regulation of striatal serotonin release by the lateral habenula-dorsal raphe pathway in the rat as demonstrated by in vivo microdialysis: role of excitatory amino acids and GABA, Brain Research 492 (1-2) (1989) 187–202. doi:10.1016/0006-8993(89)90901-3.

[18] J. Amat, P. D. Sparks, P. Matus-Amat, J. Griggs, L. R. Watkins, S. F. Maier, The role of the habenular complex in the elevation of dorsal raphe nucleus serotonin and the changes in the behavioral responses produced by uncontrollable stress, Brain Research 917 (1) (2001) 118–126. doi:10.1016/s0006-8993(01)02934-1.

[19] B. Weissbourd, J. Ren, K. E. DeLoach, C. J. Guenthner, K. Miyamichi, L. Luo, Presynaptic Partners of Dorsal Raphe Serotonergic and GABAergic Neurons, Neuron 83 (3) (2014) 645– 662. doi:10.1016/j.neuron.2014.06.024.

[20] Y. Yang, H. Wang, J. Hu, H. Hu, Lateral habenula in the pathophysiology of depression, Curr Opin Neurobiol 48 (2018) 90–96.

[21] S. Lecca, F. J. Meye, M. Trusel, A. Tchenio, J. Harris, M. K. Schwarz, D. Burdakov, F. Georges, M. Mameli, Aversive stimuli drive hypothalamus-to-habenula excitation to promote escape behavior, eLife 6 (2017). doi:10.7554/eLife.30697.

[22] S. J. Shabel, C. Wang, B. Monk, S. Aronson, R. Malinow, Stress transforms lateral habenula reward responses into punishment signals, Proceedings of the National Academy of Sciences 116 (25) (2019) 12488–12493. doi:10.1073/pnas.1903334116.

[23] M. Congiu, M. Trusel, M. Pistis, M. Mameli, S. Lecca, Opposite responses to aversive stimuli in lateral habenula neurons, European Journal of Neuroscience 50 (6) (2019) 2921–2930. doi:10.1111/ejn.14400.

[24] L. A. Quina, A. Walker, G. Morton, V. Han, E. E. Turner, Gad2 expression defines a class of excitatory lateral habenula neurons in mice that project to the raphe and pontine tegmentum, eNeuro (2020). doi:10.1523/ENEURO.0527-19.2020.

[25] M. Maroteaux, M. Mameli, Cocaine Evokes Projection-Specific Synaptic Plasticity of Lateral Habenula Neurons, Journal of Neuroscience 32 (36)

(2012) 12641–12646. doi:10.1523/jneurosci.2405-12.2012.

[26] F. J. Meye, K. Valentinova, S. Lecca, L. Marion-Poll, M. J. Maroteaux, S. Musardo, I. Moutkine, F. Gardoni, R. L. Huganir, F. Georges, M. Mameli, Cocaine-evoked negative symptoms require AMPA receptor trafficking in the lateral habenula, Nature Neuroscience 18 (3) (2015) 376–378. doi:10.1038/nn.3923.

[27] L. Durieux, V. Mathis, K. Herbeaux, M. Muller, A. Barbelivien, C. Mathis, R. Schlichter, S. Hugel, M. Majchrzak, L. Lecourtier, Involvement of the lateral habenula in fear memory, Brain Structure and Function 225 (7) (2020) 2029–2044. doi:10.1007/s00429-020-02107-5.

[28] E. G. Meloni, A. Venkataraman, R. J. Donahue, W. A. Carlezon, Bi-directional effects of pituitary adenylate cyclase-activating polypeptide (PACAP) on fear-related behavior and c-Fos expression after fear conditioning in rats, Psychoneuroendocrinology 64 (2016) 12–21. doi:10.1016/j.psyneuen.2015.11.003.

[29] A. J. Kirry, M. R. Herbst, S. E. Poirier, M. M. Maskeri, A. C. Rothwell, R. C. Twining, M. R. Gilmartin, Pituitary adenylate cyclase-activating polypeptide (PACAP) signaling in the prefrontal cortex modulates cued fear learning, but not spatial working memory, in female rats, Neuropharmacology 133 (2018) 145–154. doi:10.1016/j.neuropharm.2018.01.010.

[30] K. J. Ressler, K. B. Mercer, B. Bradley, T. Jovanovic, A. Mahan, K. Kerley, S. D. Norrholm, V. Kilaru, A. K. Smith, A. J. Myers, M. Ramirez, A. Engel, S. E. Hammack, D. Toufexis, K. M. Braas, E. B. Binder, V. May, Post-traumatic stress disorder is associated with PACAP and the PAC1 receptor, Nature 470 (7335) (2011) 492–497. doi:10.1038/nature09856.

[31] J. S. Stevens, L. M. Almli, N. Fani, D. A. Gutman, B. Bradley, S. D. Norrholm, E. Reiser, T. D. Ely, R. Dhanani, E. M. Glover, T. Jovanovic, K. J. Ressler, PACAP receptor gene polymorphism impacts fear responses in the amygdala and hippocampus, Proceedings of the National Academy of Sciences 111 (8) (2014) 3158–3163. doi:10.1073/pnas.1318954111.

[32] S. M. Sunkin, L. Ng, C. Lau, T. Dolbeare, T. L. Gilbert, C. L. Thompson, M. Hawrylycz, C. Dang, Allen Brain Atlas: an integrated spatio-temporal portal for exploring the central nervous system. Nucleic Acids Research 41 (D1) (2012) D996-D1008. doi:10.1093/nar/gks1042.